

**Some pages of this thesis may have been removed for copyright restrictions.**

If you have discovered material in AURA which is unlawful e.g. breaches copyright, (either yours or that of a third party) or any other law, including but not limited to those relating to patent, trademark, confidentiality, data protection, obscenity, defamation, libel, then please read our [Takedown Policy](#) and [contact the service](#) immediately

# THE CATIONIC RING-OPENING POLYMERIZATION OF CYCLIC ETHERS

A thesis submitted for the degree of Doctor of Philosophy

October 1995

(SUMMARY)

Frédéric Pierre GOUARDÈRES

Doctor of Philosophy

The Gel permeation chromatography studies showed that the molecular weight distribution of the samples of polyoxetanes was bimodal. This was in agreement with previous work establishing that the cyclic monomer is found to react in a more reactive than any of the other cyclic oligomers. However the molecular weight distribution of the copolymer made from oxetane and THF or from oxetane and propylene oxide could not be explained. These observations could be explained by a change in the mechanism of growing and transfer in the cationic polymerization.

In addition crown ethers like dibenzo-18-crown-6 and crown ether with a nitrogen atom were believed to stabilize the propagating end and prevent the termination reaction. This was supported by the results of the GPC studies.

THE UNIVERSITY OF ASTON IN BIRMINGHAM

October 1995

This copy of the thesis has been supplied on condition that anyone who consults it is understood to recognise that its copyright rests with its author and that no quotation from the thesis and no information derived from it may be published without proper acknowledgement

THE UNIVERSITY OF ASTON IN BIRMINGHAM

**THE CATIONIC RING OPENING POLYMERIZATION OF CYCLIC ETHERS**

**Frédéric Pierre GOUARDÈRES**

A thesis submitted for the degree of Doctor of Philosophy

October 1995

**SUMMARY**

The kinetics and mechanisms of ring opening polymerization and copolymerization of different cyclic ethers were studied using mainly a cationic system of initiation,  $\text{BF}_3\text{OEt}_2$ /ethanediol. The cyclic ethers reacted differently showing that ring strain and basicity are the main driving forces in cationic ring opening polymerization.

In most cases it was found that the degree of polymerization is controlled kinetically via terminations with the counterion and the monomers, and that the contribution of each type of reaction to the overall termination differs markedly.

The Gel permeation chromatography studies showed that the molecular weight distribution of the samples of polyoxetanes were bimodal. This was in accordance with previous work establishing that the cyclic tetramer is found in much higher proportions than any of the other cyclic oligomers. However the molecular weight distribution of the copolymers made from oxetane and THF or from oxetane and oxepane were shown to be unimodal. These observations could be explained by a change in the structure of the growing end involved in the cationic polymerization.

In addition crown ethers like dibenzo-crown-6 and compounds such as veratrole are believed to stabilise the propagating end and promote the formation of living polymers from oxetane.

**KEY WORDS:**

**OXETANE, POLYETHERS, CYCLIC OLIGOMERS,  
BACK-BITING, LIVING POLYMERIZATION**



## ACKNOWLEDGEMENTS

I would sincerely like to thank my supervisor, Dr Allan J. Amass for his friendship, guidance and constant support during the course of this three years' work.

I would like to convey my thanks to my co-supervisor Prof. Brian Tighe.

My thanks are also extended to Drs Eamon Colclough and Hemant Desai of the Defence Research Agency for their scientific advice during our numerous meetings.

Special thanks to my friends and colleagues of labs 208/209.

A special mention to the technical staff namely Dr Mike Perry, Steve Ludlow, Denise Ingram and Mike Oughton.

Finally I would like to thank Vicky for her patience and support during the "writing up" period.

## LIST OF CONTENTS

<b><u>CHAPTER 1 - Introduction</u></b>	<b>13</b>
1.1. General introduction	13
1.2. Cationic Polymerization	14
1.3. Ring opening Polymerization	15
1.3.1. Factors affecting the ring opening polymerization of cyclic ethers	15
1.3.1.1 Ring strain of the monomer	16
1.3.1.2. Basicity of the monomer	17
1.3.2. Type of initiation	18
1.3.2.1. Group A: - Superacids type initiators	18
1.3.2.2. Group B: - Lewis acids initiators	19
1.3.2.3. Group C: - Oxonium ions salts	20
1.3.2.4. Group D: - Photoinitiators	20
1.4. Mechanism of the ring opening polymerization of oxetane	21
1.4.1 Active Chain End Mechanism (A.C.E.)	22
1.4.1.1. Initiation	23
1.4.1.2. Propagation	24
1.4.1.3. Termination	24
1.4.2. The Activated Monomer Mechanism (AMM)	25
1.5. Formation of cyclic oligomers	27
1.5.1. Back-biting process	27
1.5.2. The Jacobson Stockmayer model	30
1.5.3. Discussion	31
1.6. Cationic copolymerization of cyclic ethers	31
1.7. Living polymerization	34
1.7.1. "Living" polymers concept	34
1.7.2. Characterization of "living polymers"	35
1.7.3. Living cationic polymerization	35
1.7.4. Immortal polymerization	38
1.8. Applications of polyethers	42
1.8.1. Liquid crystals polymers	42
1.8.2. Energetic materials	43
1.8.3. Scope of this project	44

<b>CHAPTER 2 - Experimental techniques</b>	<b>45</b>
2.1 High vacuum techniques	45
2.1.1 The Vacuum line	45
2.1.2 Freeze - thaw degassing of solvents	47
2.1.3 Flasks	47
2.1.4 Trap to trap distillation	47
2.2. Treatment of glassware	50
2.3.Manipulation techniques	50
2.3.1 Inert gas techniques	50
2.3.2 Glove box techniques	51
2.4. Preparation and purification of materials	52
2.4.1 Monomers	52
2.4.1.1.Oxetane	52
2.4.1.2.3,3-Dimethyloxetane	53
2.4.1.3.Tetrahydrofuran (THF)	53
2.4.1.4.Oxepane	53
2.4.1.5.Epichlorohydrin	53
2.4.1.6.Propylene oxide	53
2.4.1.7.Cyclohexene oxide	54
2.4.2.Catalysts	54
2.4.2.1.Boron trifluoride etherate	54
2.4.2.2.Ethenediol	54
2.4.2.3.Tetrafluoroboric acid - diethyl ether complex 85 %	54
2.4.2.4.Triflic acid	54
2.4.3.Solvents	55
2.4.3.1.Dichloromethane	55
2.4.3.2.THF (gpc solvent)	56
2.4.4.Drying agents	56
2.4.4.1.Sodium metal	56
2.4.4.2.Benzophenone	56
2.4.4.3.Calcium hydride	56
2.4.4.4.Sodium sulphate	56
2.4.5.Other chemicals	57
2.4.5.1.Veratrole	57
2.4.5.2.Dibenzo-18-crown-6	57
2.4.5.3.12-crown-4, 15-crown-5, 18-crown-6	57
2.5.Polymerization techniques	58
2.5.1.Calorimetric Techniques	58
2.5.2 Discussion	58
2.6.Analytical techniques	60
2.6.1.Gel Permeation Chromatography	60
2.6.1.1.Experimental	61
2.6.1.2.Calibration of the GPC column	62
2.6.1.3.Calculations of average molecular weights	63

2.6.2. Nuclear magnetic resonance spectroscopy (NMR)	65
<b>CHAPTER 3 - Cationic homopolymerization of cyclic ethers</b>	<b>66</b>
3.1 The cationic ring opening polymerization of oxetane	66
3.1.1. Introduction	66
3.1.2. Effect of the molar ratio BF <sub>3</sub> OEt <sub>2</sub> :ethanediol on the rate of polymerization and on average molecular weights	66
3.1.3. Effect of the concentration of oxetane	70
3.1.4. Effect of the concentration of catalyst on the rate of polymerization and on the average molecular weights	73
3.1.3. Molecular weight distribution (MWD) in homopolymerization of oxetane.	75
3.1.3.1. Effect of added salts on the MWD	76
3.2. Homopolymerization of 3,3-dimethyloxetane DMOX	79
3.2.1. Introduction	79
3.2.2. Kinetic studies	79
3.2.3. Homopolymerization of 3,3-dimethyloxetane and the formation of cyclic oligomers	82
3.3. Homopolymerization of tetrahydrofuran	85
3.3.1. Introduction	85
3.3.2. Kinetic and GPC studies	85
3.4. Homopolymerization of oxepane	86
<b>CHAPTER 4 - Copolymerizations of oxetane and other cyclic ethers</b>	<b>87</b>
4.1. Copolymerization of oxetane and tetrahydrofuran (OX:THF)	87
4.1.1. Introduction	87
4.1.2. Procedure	87
4.1.3. Kinetic studies	87
4.1.4. Molecular weight studies	89
4.1.5. Copolymer composition study	94
4.2. Copolymerization of oxetane and oxepane (OX:OXE)	96
4.2.1. Introduction	96
4.2.2. Kinetic study	96
4.2.3. Molecular weight studies	97
4.2.4. Copolymer composition	100
4.3. Copolymerizations and cyclooligomerization.	101
4.4. Copolymerization oxetane and 3,3-dimethyloxetane. (OX:DMOX)	106
4.5. Terpolymerizations between oxetane and other cyclic ethers	109



<b><u>CHAPTER 5 - Living Polymerizations</u></b>	112
5.1.Introduction	112
5.2.Use of crown-ethers	112
5.2.1.Effect of the addition of crown-ethers on the homopolymerization of oxetane	113
5.3.Use of Veratrole	115
5.3.1.Effect of Veratrole on the homopolymerization of oxetane	115
5.3.2.Effect of the concentration of oxetane on the molecular weight	118
5.3.3.Effect of veratrole on the homopolymerization of 3,3-dimethyloxetane	120
5.4.Pseudo-living copolymerizations of cyclic ethers	122
5.4.1.Copolymerizations of oxetane : THF and oxetane : oxepane	122
5.4.2.Copolymerizations with DMOX and other cyclic ethers	123
<b><u>CHAPTER 6 - Conclusion and Further work</u></b>	125
6.1.Kinetic studies	125
6.2.Molecular weight distribution	126
6.3.Pseudo-living polymerizations	127
<b><u>REFERENCES</u></b>	129
<b><u>APPENDIX 1</u></b>	138
Figure 1.a. <sup>1</sup> H NMR spectrum of polyoxetane	139
Figure 1.b. <sup>13</sup> C NMR spectrum of polyoxetane	140
Figure 1.c. <sup>1</sup> H NMR spectrum of copolymer OX:THF (feed 1:1)	141
Figure 1.d. <sup>1</sup> H NMR spectrum of copolymer OX:OXp (feed 1:1)	142
Figure 1.e. <sup>1</sup> H NMR spectrum of polyDMOX	143
Figure 1.f. <sup>1</sup> H NMR spectrum of the copolymer OX:DMOX (feed ratio 1:1)	144
Figure 1.g. <sup>13</sup> C NMR spectrum of the copolymer OX:DMOX (feed ratio 1:1)	145
Figure 1.h. <sup>1</sup> H NMR spectrum of the copolymer OX:DMOX (feed ratio 2:1)	146
Figure 1.i. <sup>13</sup> C NMR spectrum of the copolymer OX:DMOX (feed ratio 2:1)	147
Figure 1.j. <sup>1</sup> H NMR spectrum of the copolymer OX:DMOX (feed ratio 3:1)	148
Figure 1.k. <sup>13</sup> C NMR spectrum of the copolymer OX:DMOX (feed ratio 3:1)	149
<b><u>APPENDIX 2</u></b>	150
Figure 2.a. COSY 2D NMR spectrum of polyDMOX	151
Figure 2.b. GPC chromatogram of polyDMOX	152
<b><u>APPENDIX 3</u></b>	153
Figure 3.a. GPC chromatogram of Polyoxetane with 18-crown-6	154
Figure 3.b. GPC chromatogram of Polyoxetane with dibenzo-18-crown-6	155
Figure 3.c. GPC chromatogram of Polyoxetane with veratrole - MWD control	156

## LIST OF FIGURES

Figure 1.3.1.	Propagation via oxonium ion	16
Figure 1.3.2.	Ring strain ( $/ \text{kJ mol.}^{-1}$ ) of cyclic ethers	16
Figure 1.3.3.	Order of basicity	17
Figure 1.3.4.	Initiation of THF with $\text{CF}_3\text{SO}_3\text{H}$	18
Figure 1.3.5.	Formation of the secondary oxonium ion	19
Figure 1.3.6.	The use of a "promotor" molecule for the initiation of BCMO	20
Figure 1.3.7.	Initiation of THF with trialkyloxonium salt	20
Figure 1.3.8.	Photoinitiators for the polymerization of difunctional cyclic ethers	21
Figure 1.4.1.	Cationic initiation of oxetane	22
Figure 1.4.2.	Propagation step of the propagation of oxetane	23
Figure 1.4.3.	Chain transfer to the polymer	24
Figure 1.4.4.	Chain transfer with the co-catalyst	24
Figure 1.4.5.	Combination with anionic fragment derived from the counter ion	25
Figure 1.4.6.	The activated monomer mechanism	25
Figure 1.4.7.	Comparison of the AMM and ACE mechanisms	26
Figure 1.5.1.	Crown-ethers and their "cavity size"	27
Figure 1.5.2.	Tetramers of a) oxetane and b) 3,3-dimethyloxetane	28
Figure 1.5.3.	Formation of the tetramer by back-biting process	29
Figure 1.6.1.	The Mayo-Lewis equations	32
Figure 1.7.1.	Living polymerization of styrene	34
Figure 1.7.2.	Synthesis scheme of triblock copolymers	36
Figure 1.7.3.	Polymerization of AMMO with BSB/AgSbF <sub>6</sub> initiator system	37
Figure 1.7.4.	Transformation of the end groups	37
Figure 1.7.5.	Intramolecular aggregation of polyethers through the ionic end groups	38
Figure 1.7.6.	Tertiary amine end group of living polyTHF	38
Figure 1.7.7.	Coordinate anionic mechanism of immortal polymerization of ethylene oxide	39
Figure 1.7.8.	(5,10,15,20-tetraphenylporphinato) aluminium chloride (TPP) AlCl	40
Figure 1.7.9.	Immortal polymerization of propylene oxide	40
Figure 1.7.10.	Mechanism of the polymerization of oxetane using (TPP)AlCl	41
Figure 1.8.1.	Main chain and side chain liquid crystal polymers	43
Figure 1.8.2.	Oxetane derivatives monomers	44
Figure 2.1.	The vacuum line	46
Figure 2.2.	Vacuum line distillation	48
Figure 2.3.a.	Monomer drying flask	49
Figure 2.3.b.	Monomer solution storage flask	49
Figure 2.4.	The argon line	51
Figure 2.5.	Distillation apparatus used for the purification of dichloromethane	55
Figure 2.6.	The calorimeter	59
Figure 2.7.	A typical thermogram	60
Figure 2.8.	The Gel Permeation Chromatography	61
Figure 2.9.	GPC calibration curve (PolyTHF)	62
Figure 2.10.	A typical GPC trace	63
Figure 3.1.	Effect of the initiator system ratio on the rate of polymerization $T_{\text{initial}} = 35 \text{ }^\circ\text{C}$ , $[\text{OX}]_{\text{initial}} = 2\text{M}$	67
Figure 3.2.	Effect of the initiator system ratio on $\overline{Mn}$	68
Figure 3.3.	Dependence of $1/R_p$ on the $[\text{OH}]_{\text{ex}}$	70

Figure 3.4.	Dependence of rate of polymerization on [OX]	72
Figure 3.5.	Dependence of $\overline{Mn}$ and $\overline{Mw}$ on [OX]	72
Figure 3.6.	Dependence of the rate on [BF <sub>3</sub> OEt <sub>2</sub> ]	74
Figure 3.7.	Dependence of $\overline{Mn}$ on 1/[BF <sub>3</sub> OEt <sub>2</sub> ]	76
Figure 3.8.	A typical GPC chromatogram of polyoxetane - Bimodal distribution	77
Figure 3.9.	GPC chromatogram of polyoxetane with LiCl	78
Figure 3.10.	Lithium ion complexation of the polymer chain and the tetramer	78
Figure 3.11.	Effect of initiator concentration on the rate of polymerization	80
Figure 3.12.	Effect of initiator concentration on $\overline{Mn}$ , $\overline{Mw}$	80
Figure 3.13.	Dependence of $\overline{Mn}$ on 1/[BF <sub>3</sub> OEt <sub>2</sub> ]	81
Figure 3.14.	Areas of the <sup>1</sup> H NMR spectrum of polyDMOX showing side peaks a) O-CH <sub>2</sub> - (3.05-3.20 ppm) b) CH <sub>3</sub> - (0.8-1.1 ppm)	82
Figure 3.15.	Areas of the <sup>1</sup> H NMR spectrum of polyDMOX after separation from the oligomers a) O-CH <sub>2</sub> - (3.10-3.20 ppm) b) CH <sub>3</sub> - (0.80-1.10 ppm)	83
Figure 3.16.	Cyclic tetramer of DMOX	84
Figure 3.17.	Hydroxyl end group of PolyDMOX	84
Figure 4.1.	Copolymerization Oxetane and THF	
	Dependence of the catalyst concentration on the rate/[ox]	89
Figure 4.2.	Copolymerization OX:THF, Dependence of $\overline{Mn}$ on [BF <sub>3</sub> OEt <sub>2</sub> ]	90
Figure 4.3.	Dependence of 10 <sup>4</sup> / $\overline{Mn}$ on [BF <sub>3</sub> OEt <sub>2</sub> ]	91
Figure 4.4.	Dependence of 10 <sup>4</sup> / $\overline{Mn}$ on [THF]	93
Figure 4.5.	Copolymerization OX:THF (feed ratio 1:1), Percentage of the monomers units in the copolymer.	95
Figure 4.6.	Copolymerization OX:OXP, Dependence of the Rate on [BF <sub>3</sub> OEt <sub>2</sub> ]	97
Figure 4.7.	Copolymerization OX:OXP, Dependence of $\overline{Mn}$ and $\overline{Mw}$ on [BF <sub>3</sub> OEt <sub>2</sub> ]	98
Figure 4.8.	Dependence of 10 <sup>4</sup> / $\overline{Mn}$ on [OXP] and [THF]	100
Figure 4.9.	Copolymerization OX:OXP (feed ratio 1:1), Percentage of the monomers units in the copolymer.	101
Figure 4.10.	Typical GPC chromatograms of a) polyoxetane b) copolymer oxetane and thf c) copolymer oxetane and oxepane.	102
Figure 4.11.	Possible structure of the propagating end in a) homopolymerization of OX and b) copolymerization OX:THF	105
Figure 4.12.	Composition of the terpolymers	111
Figure 5.1.	Crown-ethers added to the feed as complexing agents	113
Figure 5.2.	Molecule of Veratrole	115
Figure 5.3.	Thermogram and procedure of the homopolymerization of oxetane with veratrole	116
Figure 5.4.	Variation of $\overline{Mn}$ after addition of fractions of fresh monomer	117
Figure 5.5.	Stabilisation of the propagating end	117
Figure 5.6.	Homopolymerization of oxetane with veratrole, Effect of [OX] on $\overline{Mn}$ calculated and $\overline{Mn}$ observed	119
Figure 5.7.	Homopolymerization of DMOX with veratrole, Effect of [DMOX] on $\overline{Mn}$	121

## LIST OF TABLES

Table 1.1	Cationic polymerization of styrene in media of varying dielectric constant $\epsilon$	14
Table 1.3.1.	Basicities of some cyclic ethers	17
Table 1.5.1	Formation of cyclic oligomers in the polymerization of oxetane at 70 °C.	28
Table 3.1.	Effect of the molar ratio $\text{BF}_3\text{OEt}_2:\text{OH}$ on the rate of polymerization, $\overline{M}_n$ , $\overline{M}_w$ and Pd	67
Table 3.2.	Homopolymerization of oxetane, effect of $[\text{OX}]$ on the rate, $\overline{M}_n$ , $\overline{M}_w$ and Pd	71
Table 3.3.	Effect of $[\text{BF}_3\text{OEt}_2]$ on $\overline{M}_n$ and $\overline{M}_w$ and on the rate of polymerization	73
Table 3.4.	Homopolymerization of DMOX, effect of $[\text{DMOX}]$ on the rate, $\overline{M}_n$ , $\overline{M}_w$ and Pd	79
Table 3.5.	Homopolymerization of THF with $\text{CF}_3\text{SO}_3\text{H}$	85
Table 4.1.	Copolymerization OX:THF, initial conditions and rate observed.	88
Table 4.2.	Copolymerization OX : THF, Molecular weight studies	90
Table 4.3	Copolymerization OX:THF, Dependence of $\overline{M}_n$ and $\overline{M}_w$ , Pd on the OX:THF ratio	92
Table 4.4.	Copolymerization OX:OXP, Initial conditions and rate observed	96
Table 4.5	Copolymerization OX:OXP, Molecular weight studies	97
Table 4.6.	Copolymerization OX:OXP, Dependence of $\overline{M}_n$ and $\overline{M}_w$ , Pd on the concentration of OXP	99
Table 4.7.	Comparison of homopolymerization and copolymerization characteristics	103
Table 4.8.	Copolymerization OX:DMOX, Effect of the feed molar ratio on the average molecular weights and on the copolymer composition.	107
Table 4.9.	Terpolymerizations, GPC analysis and polymer composition	110
Table 5.1.	Effect of crown ether addition on the homopolymerization of oxetane	114
Table 5.2.	Homopolymerization of oxetane with Veratrole Effect of the variation of $[\text{OX}]$ on $\overline{M}_n$ , $\overline{M}_w$ and Pd.	119
Table 5.3.	Homopolymerization of DMOX with Veratrole Effect of the variation of $[\text{DMOX}]$ on $\overline{M}_n$ , and Pd.	120
Table 5.4.	Copolymerizations OX:THF and OX:OXP with dibenzo 18-crown-6 (db18c6) and veratrole (VTL)	122
Table 5.5.	Copolymerizations DMOX:THF, DMOX:OXP and DMOX:OX with dibenzo 18-crown-6 (db18c6) and veratrole (VTL)	124

## LIST OF SCHEMES

Scheme 1.1.	Ionisation producing carbonium ions	14
Scheme 2.1.	Sodium and benzophenone drying procedure	52
Scheme 3.1.	Termination involving the gegenion	75
Scheme 3.2.	Equilibrium between the different forms of crown-ether	77
Scheme 5.1.	Transesterification between the propagating end and the polymer chain	118

## CHAPTER 1

### INTRODUCTION

#### 1.1. General introduction

Since the pioneering work of Wurtz on the oligomerization of ethylene oxide published in 1863, investigations on the synthesis and the possible use of polyethers have been studied more or less consistently in the time<sup>1</sup>. The progress of the petrochemical industry, enabling the production of ethylene oxide and propylene oxide, has allowed chemists to imagine new compounds and new routes of polymer synthesis.

Opening rings to make polymers was reported by Levene in 1927 and Staudinger in 1929. Meerwein in 1937 polymerized tetrahydrofuran when at the same time polymer science gave birth to new organic synthetic materials which have transformed the industry in a similar revolution that occurred a century ago with metallurgy.

Polyethers made by ring opening polymerization have been studied for the last thirty years. Their intrinsic properties have led to a relatively wide range of applications from the manufacture of elastomers and foams to the more specific design of liquid-crystals or energetic materials.

In 1929, W.H. Carothers, the future inventor of Nylon, sub-divided synthetic polymers into two main groups so that a distinction could be made between polymers prepared by stepwise reaction of monomers and those formed by chain reactions. These he called:

- Condensation polymers, which involves elimination of small molecules such as water or carbon dioxide during the reaction.
- Addition polymers, where no such loss occurs during the polymerization.

It was soon found that this type of classification was too restrictive and the first group was renamed step-growth polymerization including the synthesis of polyurethanes which occurs without elimination of a small molecule.

To the second group were added ionic polymerizations, including ring opening processes. These types occur via three distinct stages, first an active site is created on the monomer

by the action of an initiator, then a chain growth reaction by propagation of the active centre, and eventually the termination stage

Ionic initiated polymerizations, where the active site is a stabilised anion or cation, largely depend on the nature of the monomer and its substituents. Cationic initiation is limited to monomers with electron donating groups which help to stabilise the growing positive charge. As these ions are associated with a counter-ion, the choice of the reaction solvent is of great importance, for a successful propagation step.

## 1.2. Cationic Polymerization

The term ionic polymerization is in most case ambiguous, it depends on the polarity of the medium used for the reaction. The reactivity of the active site needed for the chain growth step can be affected by the position and type of the counter ion. By varying the dielectric constant ( $\epsilon$ ) of the solvent a large change in the kinetics of polymerization can be obtained<sup>2</sup> as shown in table 1.1 for a perchloric acid initiated polymerization of styrene in several media.

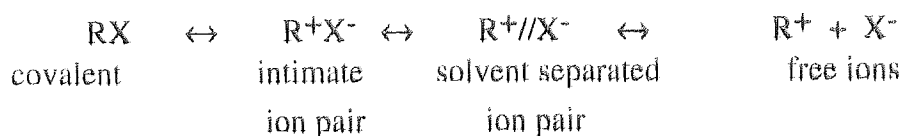
**Table 1.1 Cationic polymerization of styrene in media of varying dielectric constant  $\epsilon$**

Solvent	$\epsilon$	$k_p/\text{dm}^{-3}\cdot\text{mol}^{-1}\cdot\text{s}^{-1}$
$\text{CCl}_4$	2.3	0.0012
$\text{CCl}_4+\text{CH}_2\text{Cl}_2$ (40/60)	5.2	0.40
$\text{CCl}_4+\text{CH}_2\text{Cl}_2$ (20/80)	7.0	3.20

Initiator  $\text{HClO}_4$

The various stages of the ionisation producing carbonium ions can be represented in scheme 1.1 followed:

### Scheme 1.1 Ionisation producing carbonium ions



Increasing the polarity of the solvent affects the distance between ions. Free ions propagate faster than tight ion pairs consequently an increase in  $k_p$  is observed with increase in  $\epsilon$  and the result is an increase in the polymer chain length.

The same result was observed by changing the solvent on the cationic polymerization of cyclic ethers such as THF<sup>3-5</sup> or oxepane<sup>6,7</sup>. In the polymerization of THF using  $\text{CH}_3\text{NO}_2$  it was found that the propagation rate constants of various macroion pairs are independent of the structure of the anion<sup>3,8</sup>.

### 1.3. Ring opening Polymerization

Ring opening polymerization has become increasingly important to large segments of the chemical and polymer industries<sup>9</sup>. The synthesis of polyesters using lactones as monomer, polymerization of  $\epsilon$ -caprolactam to give Nylon-6, metathesis polymerization of cyclopentene, and polymerization of miscellaneous heterocyclic compounds such as epoxides, acetals, cyclic amines, cyclic sulphides are various examples of the scope of ring opening polymerizations<sup>10,11</sup>. In addition, there has been a considerable interest in inorganic or partially inorganic polymers such as polysiloxanes<sup>12</sup> or polyphosphazenes<sup>13</sup> synthesised from cyclic monomers. Biodegradable and biocompatible polymers made from ring opening polymerization of phosphorus or sulphur containing cyclic esters<sup>14,15</sup> have been studied for use in drug delivery systems.

The mechanism of ring opening polymerization is governed by different thermodynamic or kinetic factors.

#### **1.3.1. Factors affecting the ring opening polymerization of cyclic ethers**

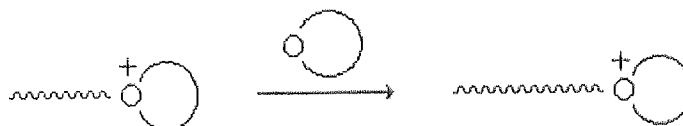
The tendency toward polymerization of a cyclic monomer depends upon the existence and the extent of ring strain, the initiator being used, and the reactivity of any substituent group within the ring.



### 1.3.1.1. Ring strain of the monomer

In the cationic polymerization of cyclic ethers, a cyclic tertiary oxonium ion is proposed as the propagating species.

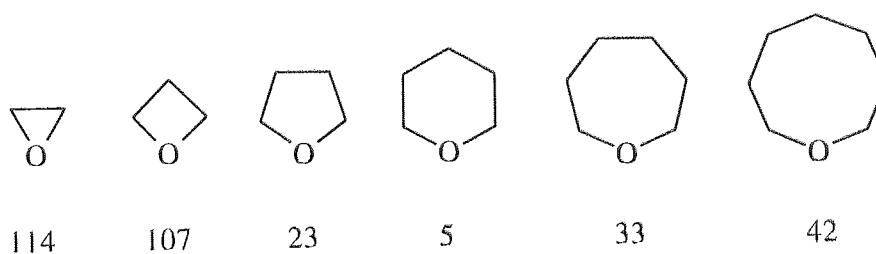
**Figure 1.3.1. Propagation via oxonium ion**



The tendency for a cyclic monomer to undergo ring opening polymerization is greatly dependent on the ring size and the principal driving force in small rings is to relieve this strain. Ring strain is a thermodynamic factor which is caused by the presence of bond angle distortions, conformational strain, and non-bonded interactions between hydrogen atoms in the eclipsed conformation<sup>16,17</sup>.

The ring strain energies of some common cyclic ethers are presented in figure 1.3.2.

**Figure 1.3.2. Ring strain (/ kJ mol.<sup>-1</sup>) of cyclic ethers**



The less stable cyclic ether produces, in general, a more strained and therefore a more reactive oxonium ion. From the above values, the most stable oxonium ion is derived from tetrahydropyran, the six membered ring, a compound that does not polymerize. The strainless chair conformation, in which it is similar to cyclohexane provides a thermodynamic stability for this monomer. Although the homopolymerization of tetrahydropyran has not been reported, it has been known to undergo copolymerization

with other reactive monomers<sup>18</sup>. Under appropriate conditions the polymerization of tetrahydrofuran proceeds without appreciable chain transfer or termination, indicating that the propagation proceeds via a stable oxonium species. The driving force of the polymerization of four membered rings is probably the angle ring strain. The unsubstituted rings containing less than five or more than six atoms are invariably polymerizable.

### 1.3.1.2. Basicity of the monomer

The basicity of the monomer is also an important factor controlling its reactivity. It is reported that the basicity of a monomer plays an important role in the initiation step, when the monomer is facing the acid type initiator.

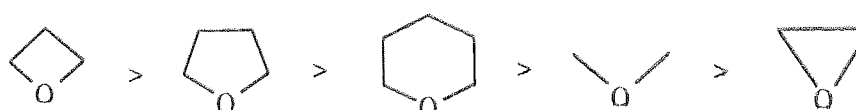
Relative basicities of deuterated cyclic ethers have been determined by several infrared spectroscopic methods<sup>19,20</sup>, recording the shift values of the characteristic stretching bands. Table 1.3.1. shows a few of the results obtained from the investigation.

**Table 1.3.1. Basicities of some cyclic ethers**

Cyclic Ether	pKa
oxetane	3.13
THF	5.00
Tetrahydropyran	5.42
Propylene oxide	6.94
Epichlorohydrin	8.84

The order of basicity of cyclic ethers is as follows (figure 1.3.3.)

**Figure 1.3.3. Order of basicity**



In cationic polymerization, the basicity of the monomer strongly affects the modes of the reactions of growing species, since various nucleophiles other than the monomer, which may cause chain growth to compete with various side reactions, are also present in the present in the reaction system. Such nucleophiles are the linear ether group in the polymer chain end and the counter-anion at the growing end. The basicity of the monomer is also of importance in the cationic copolymerization of cyclic ethers.

Important factors affect the basicity of a cyclic ether, methyl substitution onto the ring increases the positive inductive effect whereas chloromethyl substitution decreases the basicity<sup>21,22</sup>. The ring size affects the basicity in various ways: a decrease in the angle, involving a heteroatom associated with a decrease in the ring size, results in less steric hindrance to interaction; changes in its valence angle result in a variation of the electron density on the heteroatom.

### 1.3.2. Type of initiation

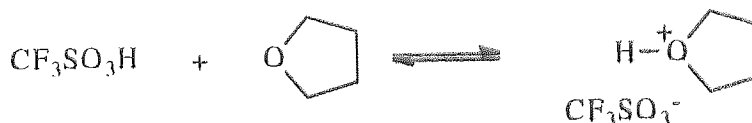
Initiation of the cationic polymerization of cyclic ethers can be accomplished in many ways. The ether group is characteristically basic in a Lewis sense and the implication of this is that ring opening polymerization of cyclic ethers is initiated by cationic species. The epoxides are the exception to this generalisation, as they can be polymerized by both anionic and cationic initiators.

Different types of initiators are of interest and are described below:

#### 1.3.2.1. Group A: - Superacids type initiators

Superacids such as concentrated sulphuric and fluorosulphuric acids initiate the polymerization of THF via the formation and the propagation of oxonium ions<sup>23,24</sup>. Figure 1.3.4. shows the initiation of tetrahydrofuran with trifluoromethane sulfonic acid

**Figure 1.3.4. Initiation of THF with  $\text{CF}_3\text{SO}_3\text{H}$**

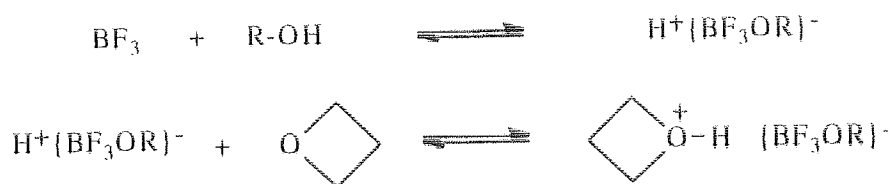


### 1.3.2.2. Group B: - Lewis acids initiators

Lewis acids  $\text{BF}_3$ ,  $\text{BF}_3 \cdot \text{OEt}_2$ ,  $\text{SnCl}_4$ ,  $\text{SbCl}_5$ ,  $\text{AlCl}_3$ ,  $\text{FeCl}_3$ ,  $\text{PF}_5$  have been used extensively for the homopolymerization of oxetanes<sup>25-30</sup>. Using  $\text{BF}_3$  for the polymerization of oxetane, traces of water react as a cocatalyst. Other cocatalysts can be used ( $\text{ROH}$ ,  $\text{MeCO}_2\text{H}$ ,  $\text{HBr}$ ,  $\text{Cl}_3\text{CO}_2\text{H}$ , etc) as a source of this proton. The use of a cocatalyst is necessary because polymerization does not occur without it.

The action of this type of initiator is the protonation of the oxygen atom creating a secondary oxonium ion.(figure 1.3.5.)

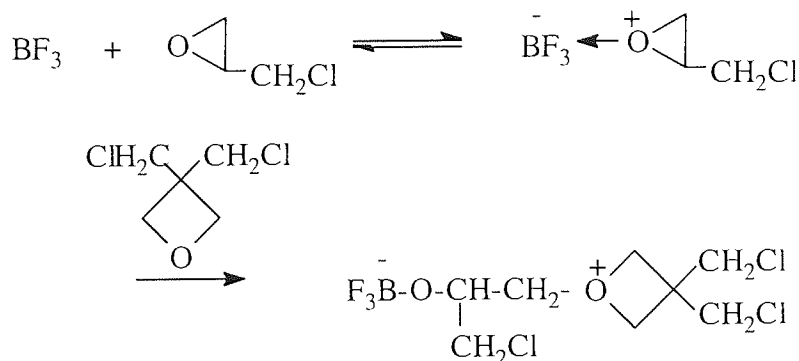
**Figure 1.3.5. Formation of the secondary oxonium ion**



In addition a combination of a Lewis acid, a cocatalyst, and a reactive ether (promotor) can initiate the polymerization of less reactive ethers<sup>31-34</sup>. The promotor is generally a cyclic ether, usually an epoxide, having a higher ring opening activity towards the Lewis acid compared with the monomer itself.

The interaction of the promotor and the Lewis acid provides the initiating oxonium ion. An example of this type of polymerization includes the initiation of bischloromethyl oxetane (BCMO) in either the presence of  $\text{BF}_3$ ,  $\text{AlCl}_3$  or  $\text{SnCl}_4$  with promotor molecules such as epichlorohydrin<sup>32</sup> or propylene oxide. This is illustrated in figure 1.3.6.

**Figure 1.3.6. The use of a "promotor" molecule for the initiation of BCMO**



### 1.3.2.3. Group C: - Oxonium ions salts

Oxonium ions salts,  $\text{R}_3\text{O}^+\text{A}^-$ , where  $\text{A}^-$  is a complex metal halide ( $\text{MtX}_{n+1}^-$ ), are of interest. With triethyloxonium salts, the initiation reaction is the simple alkylation of the monomer<sup>23</sup>, as shown in figure 1.3.7. The first addition reaction was studied for the polymerization of tetrahydrofuran.

**Figure 1.3.7. Initiation of THF with trialkyloxonium salt**



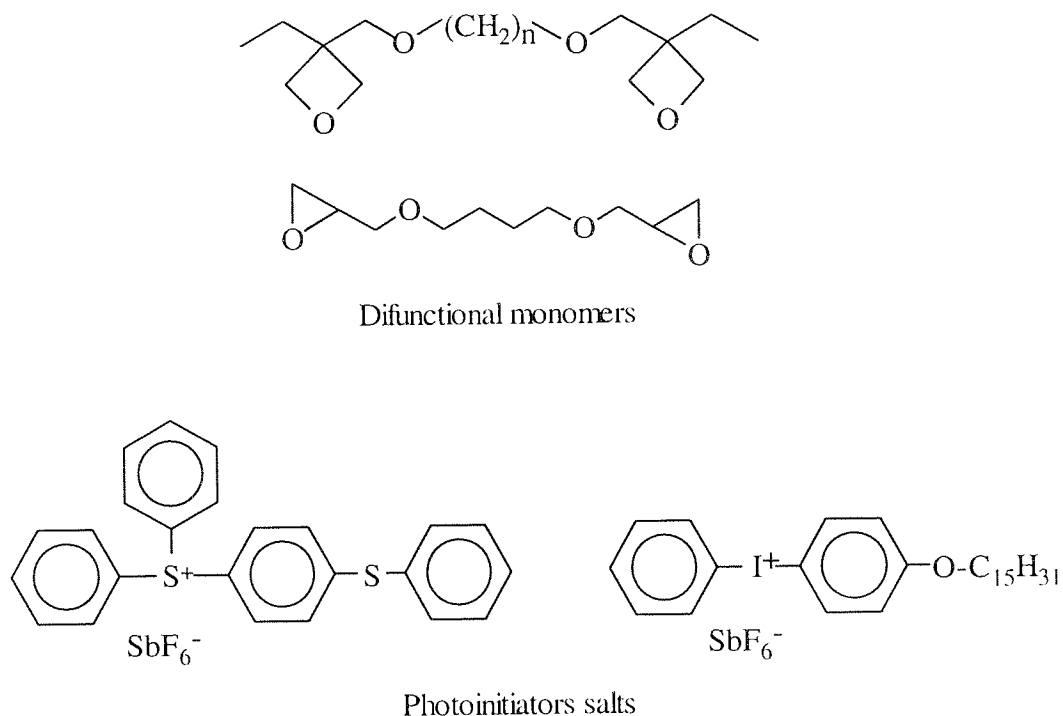
### 1.3.2.4. Group D: - Photoinitiators

In recent years, photoinitiated cationic polymerization, also called UV curing, has become an important technique. Many different types of monomer and oligomers, including vinyl ethers and epoxide compounds, have been polymerized using this technique<sup>35-39</sup>.

Crivello reported the polymerization of difunctional oxetanes<sup>38</sup> using phenylsulfonium or phenyliodonium salts. These salts decompose upon UV and visible light irradiation to form cations ready for initiation. The rates of polymerization of the various monomers were measured by recording their gel times, the shorter the gel time the more reactive

the monomer in cationic UV curing. The results show that these difunctional oxetane monomers are more reactive than epoxides with similar structures.(figure 1.3.8.)

**Figure 1.3.8. Photoinitiators for the polymerization of difunctional cyclic ethers**



## 1.4. Mechanism of the ring opening polymerization of oxetane

### 1.4.1 Active Chain End Mechanism (A.C.E.)

This section will discuss the cationic polymerization mechanism of oxetane, though it must be emphasised that the general principles apply to other cyclic ethers as well.

The cationic polymerization of oxetane, first recorded by Farthing<sup>27</sup> in 1955, gave linear polymer of high molecular weight. Rose<sup>28</sup> extended Farthing's work and reported that cationic polymerization would not occur under absolutely anhydrous conditions when  $\text{BF}_3$  is used as an initiator. Water was the essential co-catalyst. Furthermore he

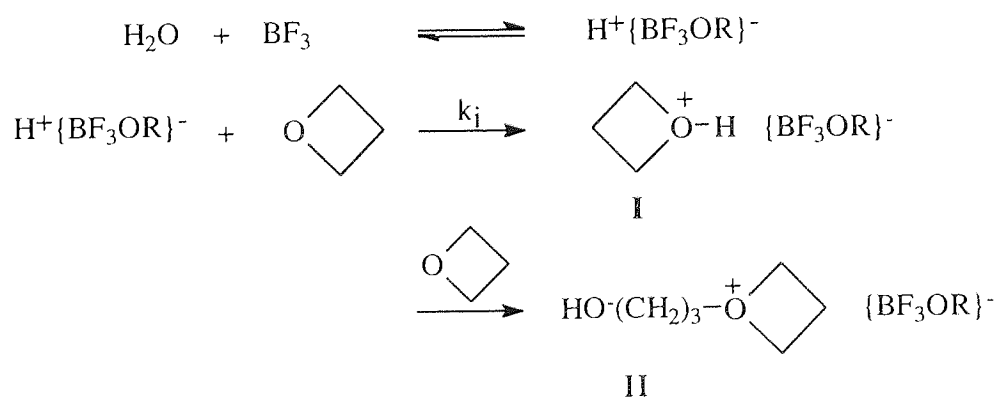
observed the rate of polymerization of oxetane initiated by  $\text{BF}_3$  was proportional to the amount of water added.

Kinetic chain polymerizations are characterised by three main stages, initiation, propagation and termination. Rose proposed the following mechanism for the polymerization of oxetane, based upon a detailed investigation of the kinetics of the  $\text{BF}_3$  catalysed system. This mechanism is called the active chain end (ACE) mechanism because the active site appears at the end of the polymer chain and the attacking nucleophile is the uncharged monomer.

#### 1.4.1.1. Initiation

Figure 1.4.1. shows the initiation step for the polymerization of oxetane. The complex role of water as a co-catalyst required the postulation of a two-step initiation process. The complex formed between  $\text{BF}_3$  and water, proceeds to initiate the reaction by acting as a protonic acid. Protonation of the oxygen atom in the ring results in the formation of a secondary oxonium ion (**I**), which a second monomer molecule then attacks at one of the  $\alpha$ -carbons to create the propagating end(**II**). The secondary oxonium ion (**I**), which exists as an ion pair, is much less active than the tertiary oxonium ion (**II**).

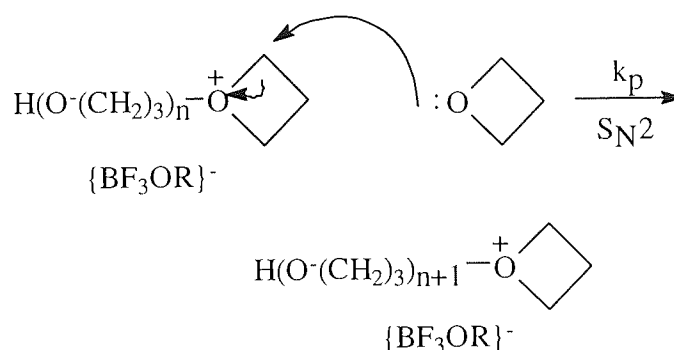
**Figure 1.4.1. Cationic initiation of oxetane**



### 1.4.1.2. Propagation

The chain propagates by a nucleophilic attack of the oxygen atom of the monomer on the  $\alpha$  - carbon of the propagating tertiary oxonium ion. The propagation step is thought to occur by an  $S_N2$  type mechanism.  $\{BF_3OH\}^-$ , the counter ion presumed to be formed in initiation, maintains its integrity during propagation. It should be noted however that similar inorganic complexes are known to be unstable. Under the reaction conditions,  $\{BF_3OH\}^-$  may disproportionate or it may react further with  $BF_3$  to give  $BF_4^-$ .

**Figure 1.4.2. Propagation step of the propagation of oxetane**



### 1.4.1.3. Termination

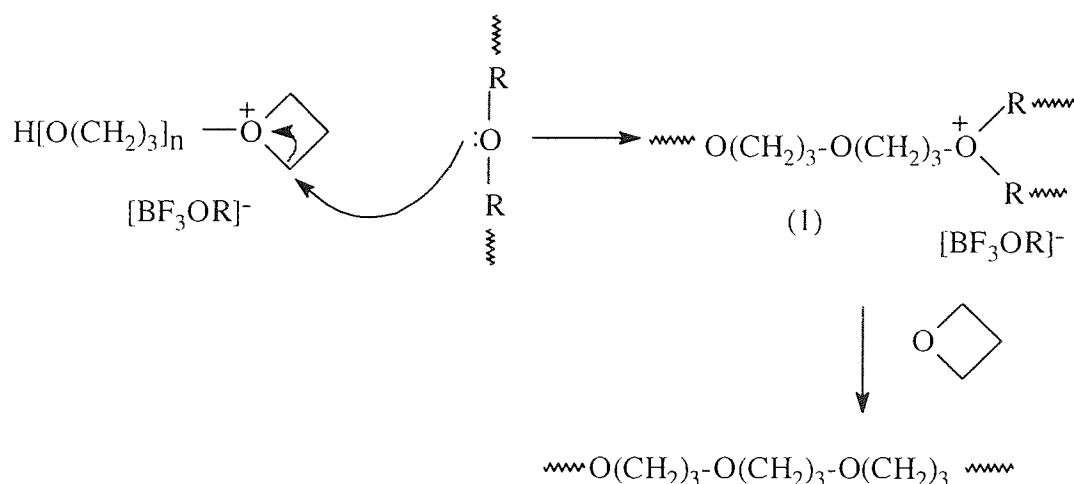
Some cationic polymerizations of cyclic ethers have stable propagating species that do not terminate and which are characteristic of living polymers.

In other cases termination exists and can occur by an array of different reactions.

Chain transfer to the polymer is one possible way by which the propagating chain may be terminated. This involves alkyl exchange between the propagating oxonium ion and the ether linkage of the polymer chain. Such reactions result in the formation of open chain tertiary oxonium ions of lesser reactivity. Figure 1.4.3. describes the chain transfer reaction to the polymer.



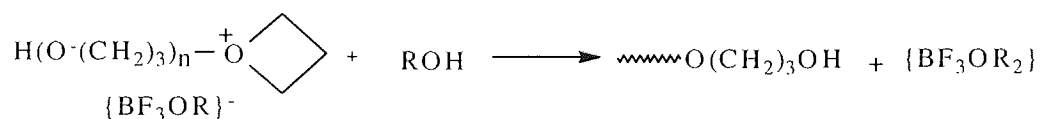
**Figure 1.4.3. Chain transfer to the polymer**



The greater the extent of polymer formed during the course of the polymerization, the greater is the probability of this transfer reaction occurring. On deactivation of the open chain tertiary oxonium ion (1), one of the carbon oxygen is cleaved. This results in a statistical redistribution of the chain lengths in the system and results in an increase in the polydispersity index.

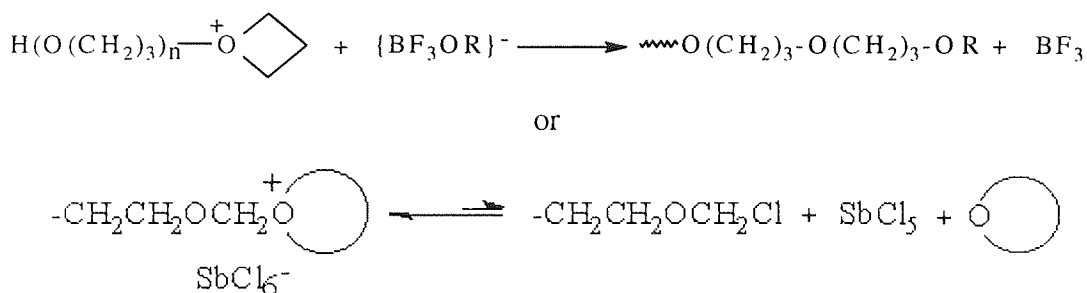
Figure 1.4.4. shows the mode of termination by chain transfer with the co-catalyst.

**Figure 1.4.4. Chain transfer with the co-catalyst**



The propagating oxonium ion may also be terminated by combination with either the counter-ion itself or an anionic fragment derived from the counter ion, resulting from anion splitting.

**Figure 1.4.5. Combination with anionic fragment derived from the counter ion**

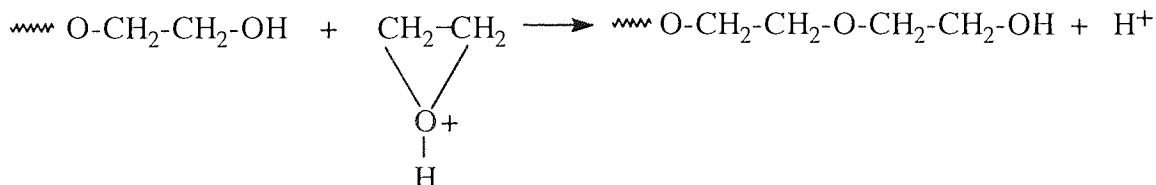


The tendency of an anion to transfer is different for various counter ions and depends on the stability of the counter ion. Counter ions such as  $\text{SbF}_6^-$  and  $\text{PF}_6^-$  have little tendency to bring about termination, whereas anions derived from aluminium have greater transfer tendencies, because in this case the counterion is from a weaker acid.

#### 1.4.2. The Activated Monomer Mechanism (AMM)

Under certain experimental conditions, particularly when addition of the monomer was slow, the polyethers obtained by the polymerization of oxiranes exhibited a narrow molecular weight distribution and the molecular weight increased with conversion. Penczek<sup>44</sup> explained this observation by proposing a mechanism for the cationic ring-opening polymerization of epoxides. The mechanism known as the Activated Monomer Mechanism (AMM) and shown in figure 1.4.6, consists of the step-by-step addition of a protonated monomer to the growing chain, which has a terminal nucleophilic hydroxyl group.

**Figure 1.4.6. The activated monomer mechanism**

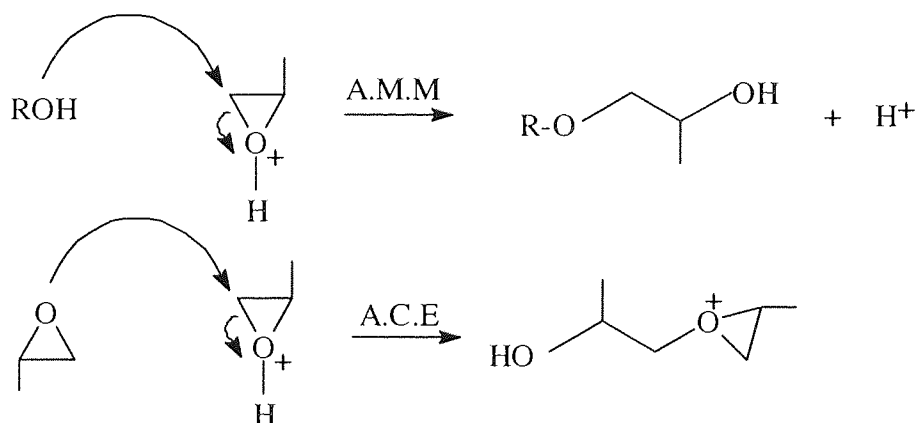


It is important that by its very nature AMM leads to a reduction in back-biting and consequent formation of cyclic oligomers.

Penczek considered the initiation of polymerization of an oxirane, catalysed by an alcohol in the presence of a protonic acid, to take place by the mechanism shown in figure 1.4.7. Superficially these polymerizations of oxirane would appear to be under identical conditions but this is not the case. The conventional ACE mechanism would apply if the protonic acid catalyst were added to a solution of oxirane. In this case the added alcohol would act as a transfer agent during the course of the polymerization.

In the AMM polymerizations, monomer is admitted slowly into the reaction solution so that at any instant its concentration is only of the order of that of the initiator. The proton from the acid catalyst preferentially protonates the monomer, as would be the case in the ACE mechanism. However because the concentration of the monomer is so low the only nucleophile present, capable of attacking the hydroxonium compound, is the alcohol.

**Figure 1.4.7. Comparison of the AMM and ACE mechanisms**



Because there is a difference in the structures of the chain ends, the ACE mechanism leads to approximately 40% of cyclic tetramer formed by either back-biting or by chain transfer, whilst with AMM tetramer formation is less than 1% when slow addition of the monomer takes place. Side reactions that do appear are the direct result of some ACE propagation which is an inherited property of AMM.

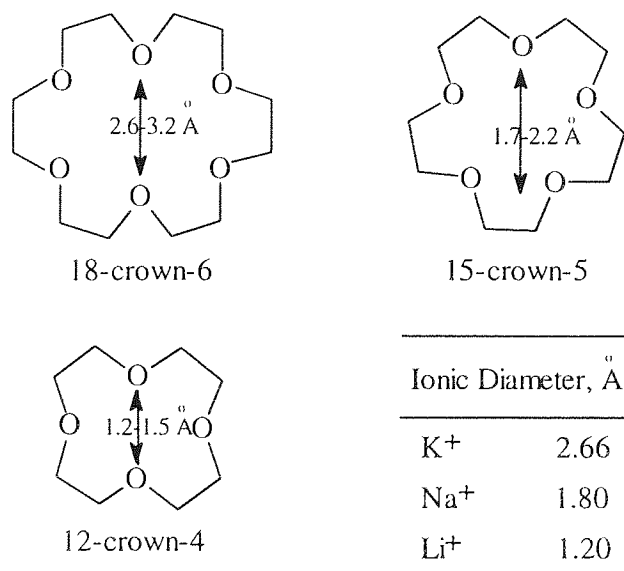
## 1.5. Formation of cyclic oligomers

Formation of cyclic oligomers in the polymerization of the heterocyclic monomers is a phenomenon very often encountered. Macrocycles have been observed in the cationic polymerization of cyclic ethers<sup>45-51</sup>, acetals<sup>52,53</sup>, siloxanes<sup>54,55</sup>.

### 1.5.1. Back-biting process

The polymerization of cyclic ethers frequently gives not only polymer but also cyclic oligomers. The polymers are the desired products but since the discovery of the usefulness of crown ethers, interest in cyclic oligomers has increased greatly<sup>56-64</sup>. Macrocyclic polyethers behave as highly selective complexing agents for cations especially alkali metal ions and have potential significance in analysis and separation of various ions. Crown ethers are cyclic oligomers of cyclic ethers, and are named in the form of x-crown-y, where x is the total number of atoms in the ring and y is the number of oxygens. 18-crown-6 shows a high affinity for  $K^+$ , 15-crown-5 for  $Na^+$ , and 12-crown-4 for  $Li^+$ . Measurements of molecular models of these three molecules reveals that the "cavity size", is in each case a good match for the ionic diameter of the cation most strongly bound by the molecule (figure 1.5.1.).

**Figure 1.5.1. Crown-ethers and their "cavity size"**



Aiming at the polymer Rose<sup>27</sup> observed that, using  $\text{BF}_3$  and water as a catalyst system, and working at  $50^\circ\text{C}$ , up to 40% of the product was a cyclic tetramer (16-crown-4). In later work aiming at the synthesis of cyclic oligomers, Dreyfuss and Dreyfuss<sup>51</sup> reported that only trimer and tetramer were found with no higher cyclic oligomers. The tetramer was predominant for polymerization initiated by triethyloxonium tetrafluoroborate, whereas trimer was more important, if the polymerization was initiated by ethyl trifluoromethanesulfonate (table 1.5.1.). This tendency is enhanced by changing the solvent from 1,2-dichloroethane to benzene.

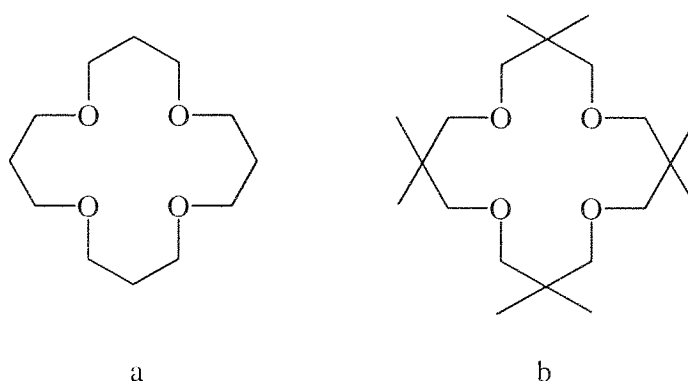
**Table 1.5.1 Formation of cyclic oligomers in the polymerization of oxetane at  $70^\circ\text{C}$ .**

Counter anion	Solvent	Trimer/Tetramer <sup>*</sup>
$\text{BF}_4^-$	$\text{ClCH}_2\text{CH}_2\text{Cl}$	0.5
$\text{CF}_3\text{SO}_3^-$	$\text{ClCH}_2\text{CH}_2\text{Cl}$	1.83
$\text{BF}_4^-$	$\text{C}_6\text{H}_6$	0.18
$\text{CF}_3\text{SO}_3^-$	$\text{C}_6\text{H}_6$	3.50

<sup>\*</sup>Intensity ratio of GLC peaks for trimer and tetramer

Concerning the homopolymerization of 3,3-dimethyloxetane, tetramer was found to be the most predominant cyclic oligomer<sup>64</sup> but in contrast, higher oligomers were also found to be present in small quantities in oxetane homopolymerization.

**Figure 1.5.2. Tetramers of a) oxetane and b) 3,3-dimethyloxetane**

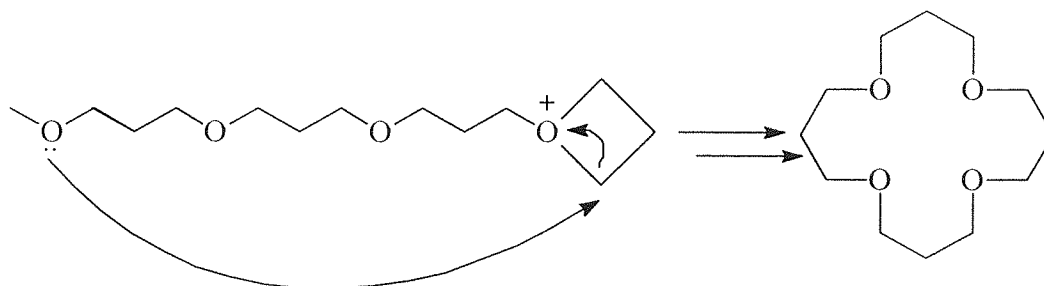


It is thought that the tetramers (figure 1.5.2.) and other cyclic oligomers are not formed from the degradation of the polymer but concurrently with the polymer, and that once

formed, the products do not change. As soon as the monomer is completely consumed the oligomer formation ceases.

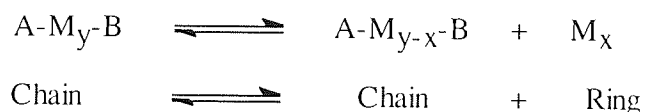
This stability of the tetramer is due to conformational restrictions and its formation can be attributed to the fact that in the preferred conformation of the polymer chain the third oxygen atom is placed in the best position to perform an intramolecular  $S_N2$  reaction. This mechanism of formation is called a back-biting reaction (figure 1.5.3)

**Figure 1.5.3. Formation of the tetramer by back-biting process**



### 1.5.2. The Jacobson Stockmayer model

A theory was developed to describe the dependence of the equilibrium concentration of macrocyclics on the ring size<sup>65</sup>. The model developed by Jacobson and Stockmayer states that above the equilibrium concentration for polymer formation, the relative concentrations of the oligomers are independent of the initial concentrations of the monomer and the catalyst; only a slight dependency on the temperature is observed, and above the equilibrium concentration of monomer, the polymer/oligomer ratio increases with increasing concentration of monomer. The equilibrium between open chain polymer and each cyclic oligomer ( $M_x$ ) may be summarised as:



The equilibrium constant  $K_x$  for the formation of the oligomer ( $M_x$ ) may be written as

$$K_x = \frac{[\text{A-M}_{y-x}\text{-B}][\text{M}_x]}{[\text{A-M}_y\text{-B}]}$$

The distribution of cyclic structures has been shown to obey to the relationship that demonstrates ring - chain equilibrium. In such cases:

$$[\text{M}_x] = K_x X^{-5/2}$$

where X is correlated to the ring size of the macrocycle, and equals 2 for a dimer, 3 for a trimer, etc.

Plots of  $\ln[\text{M}_x]$  against  $\ln X$  for a series of different ring-size cyclic monomers should give linear relationships with gradients of -2.5. The intercepts of such plots also show the predicted dependence on the ring size. Many systems obey this type of independence but it should be noted that the concentrations of certain oligomers, particularly tetramers, appear to deviate from predicted behaviour in the polymerization of cyclic ethers such as oxetane.

### 1.5.3. Discussion

The presence of cyclic oligomers can be detected in a GPC profile of a polymer sample. They are eluted according to their size, and so they can be identified. NMR spectroscopy is also a useful technique for the determination of the ring structure<sup>66</sup>. The chemical shifts of the protons and carbons of cyclic oligomers are slightly different from the corresponding chemical shifts for the atoms in a polymeric chain.

## 1.6. Cationic copolymerization of cyclic ethers

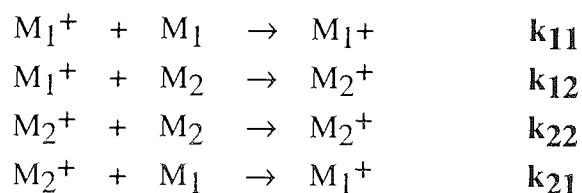
Copolymerizations between pairs of cyclic structure have been studied<sup>10,16</sup>. Numerous reports have been published on the copolymerization of cyclic ethers, mainly with cationic initiators. These are concerned with the kinetics of the reaction, the relative reactivities of the comonomers. In general, the basicity and the ring strain are the main factors which govern the reactivity of the cyclic ethers. Copolymerizations have been achieved between closely related types of monomers such as cyclic ethers and cyclic acetals or lactones<sup>67,68</sup>. Copolymerizations involving oxiranes have been widely reported.

The tendency of a cyclic ether to undergo a copolymerization is not related to its ability to homopolymerize. A few cyclic ethers have been found to be significantly more reactive in copolymerization reactions than they are in homopolymerizations. For other monomers the opposite has been found.

The copolymer composition has been determined by assuming that the reactivity of the propagating chain is dependent only on the nature of the growing end, and independent of the chain composition. The copolymerization reaction of two monomers  $M_1$  and  $M_2$ , results in the formation of two propagating centres. One of which has  $M_1$  at the propagating end and the other with  $M_2$ . The consequence of this is that there are four possible propagation steps. The kinetics of copolymerization of cyclic ethers are described by the Mayo-Lewis equations<sup>10</sup> (figure 1.6.1.).



### Figure 1.6.1. The Mayo-Lewis equations



Propagation proceeding by the addition of the same type of monomer is known as homo-propagation, whereas propagation by the addition of the other monomer is referred to as cross-propagation.

The monomer reactivity ratios are defined as:

$$r_1 = k_{11}/k_{12} \qquad r_2 = k_{22}/k_{21}$$

The rate of consumption of  $M_1$  from the initial reaction mixture is then:

$$-d[M_1]/dt = k_{11} [M_1] [M_1^+] + k_{21} [M_1] [M_2^+] \quad (1)$$

and  $M_2$  by

$$-d[M_2]/dt = k_{22} [M_2] [M_2^+] + k_{12} [M_2] [M_1^+] \quad (2)$$

The copolymer equation can be obtained by dividing (1) by (2) and assuming that

$$k_{21} [M_2^+] [M_1] = k_{12} [M_1^+] [M_2]$$

for steady-state conditions, so that

$$d[M_1]/d[M_2] = ([M_1]/[M_2]) \{ (r_1[M_1] + [M_2]) / ([M_1] + r_2[M_2]) \}$$

The monomer reactivity ratios and the copolymer composition equations are independent of many reaction parameters, such as differences in the rates of initiation and termination and the absence or presence of inhibitors or transfer agents.

Depending on the values of the monomer reactivity ratios, the following copolymers result from polymerization.

$r_1 = r_2 = 1$	Random copolymer
$r_1 = r_2 \approx 0$	Alternating copolymer
$r_1 > 1, r_2 > 1$	Block copolymer
$r_1 > 1, r_2 < 1$ or $r_1 < 1, r_2 > 1$	Copolymer rich in one monomer

The rate constants for the four propagation reactions are said to depend on the reactivity of the propagating end and the nucleophilicity of the attacking monomer.

As the reactivity of cyclic ethers is partly related to the basicity, then the nucleophilic attack of cyclic ethers on the propagating chain end is assumed to be one of the driving force in such copolymerizations. Reactivity of the monomers in cationic copolymerization is commonly affected by the reaction conditions, solvent, counter ion and temperature. Marked changes in the rate of copolymerization are observed when different solvents and counterions are used, because the structures of the propagating species in ionic polymerizations are sensitive to the nature of the solvent used. Displacement of the equilibrium, scheme 1.1, is caused by changing the solvent and / or temperature of polymerization.

## 1.7. Living polymerization

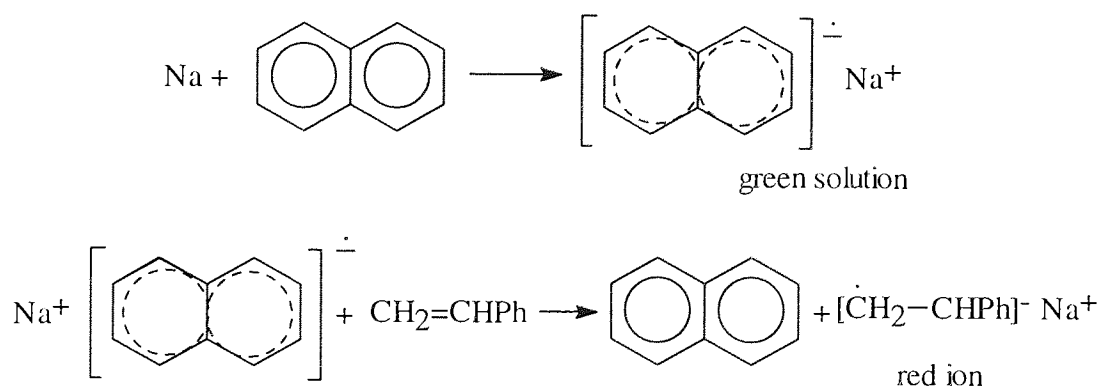
### 1.7.1. "Living" polymers concept

First described by Swarc<sup>69</sup> living polymerizations are polymerizations in which propagating centres do not undergo either termination or transfer. In the case of cationic polymerization, one could imagine the positively charged site still "active" and ready to react with more monomer molecules if they were reintroduced into the medium. Such properties of the system are full of interest for polymer chemists in order to increase chain length, have access to a better control of the molecular weight distribution and design new ranges of block copolymers.

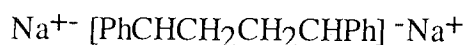
One of the first living polymerization was achieved in the anionic polymerization of styrene initiated by sodium naphthalene (figure 1.7.1.). The initiator for this type of polymerization is formed by adding sodium to a solution of naphthalene in an inert polar solvent, such as tetrahydrofuran.

The sodium dissolves to form an addition compound and, by transferring an electron, produces the green naphthalene anion radical. Addition of styrene to the system leads to electron transfer from the naphthyl radical-anion to the monomer to form a red styryl radical-anion.

Figure 1.7.1. Living polymerization of styrene



It is thought that a dianion capable of propagating from both ends, is formed.



The living character of the polymerization was demonstrated successfully by adding more styrene and by another monomer (isoprene) to increase the chain length and form a block copolymer, respectively.

### 1.7.2. Characterization of "living polymers"

The living nature of such systems is apparent in several ways. The added monomer is polymerized quantitatively, a plot of  $\overline{M}_n$  versus % conversion is linear. If the initiation is fast the molecular weight distribution is narrow. The concentration of the propagating chains remains constant and only propagation reactions take place. No termination or transfer reactions occur.

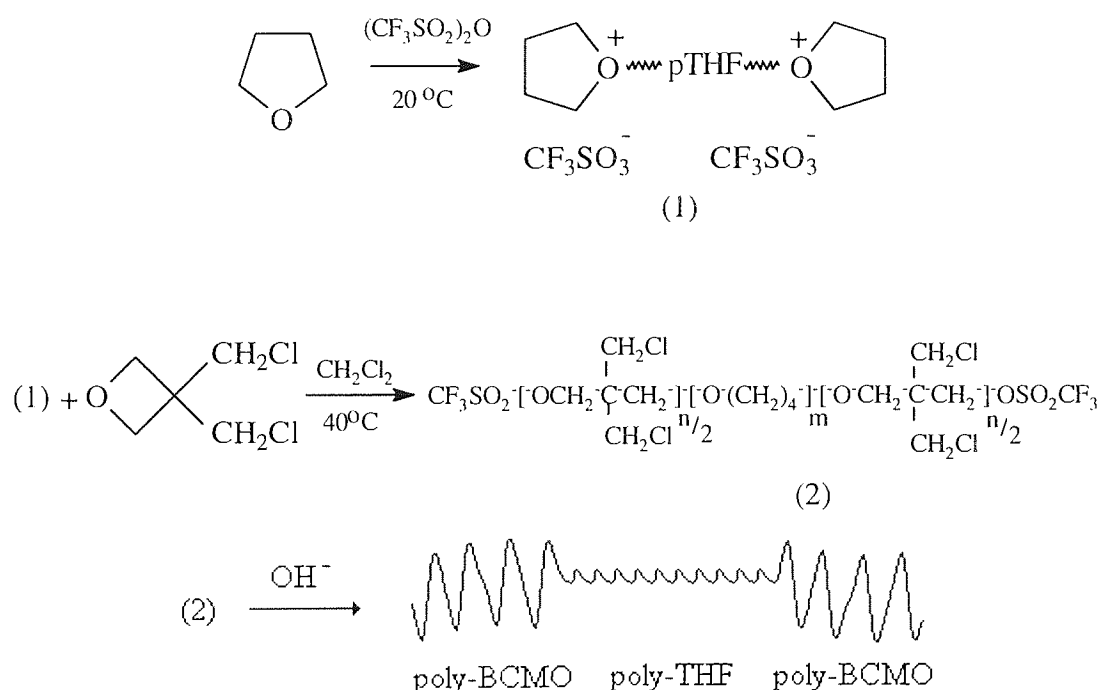
If the rate of initiation is slow, the molecular weight distribution is broader than that obtained with a rapid initiation system. Living polymerization may be terminated by the addition of a reagent such as a protic acid, water or an alcohol depending on the nature of the active end.

### 1.7.3. Living cationic polymerization

Carbocationic polymerizations are an area of growing interest in polymer synthesis. many types of monomers such as isobutylene, vinyl ethers, cyclic ethers, N-vinylcarbazole, p-alkostyrenes, oxiranes, and formaldehyde can be polymerized through cationic routes. Because of the inherent instability of the propagating ion, carbocationic polymerizations were believed for many years to be uncontrollable processes dominated by chain transfer and termination. However, since 1984, when Higashimura first reported the living cationic polymerization of isobutyl vinyl ether<sup>70</sup>, much work has been done in selecting the proper counteranion, temperature, and solvent conditions to allow for the living polymerization of many different monomer systems<sup>71-73</sup>. Much of the work focussed on the selection of a counteranion which was nucleophilic enough to stabilise the cation but still active enough to permit propagation. Such balances between stabilities and reactivities will be seen to be extremely important in living cationic polymerization.

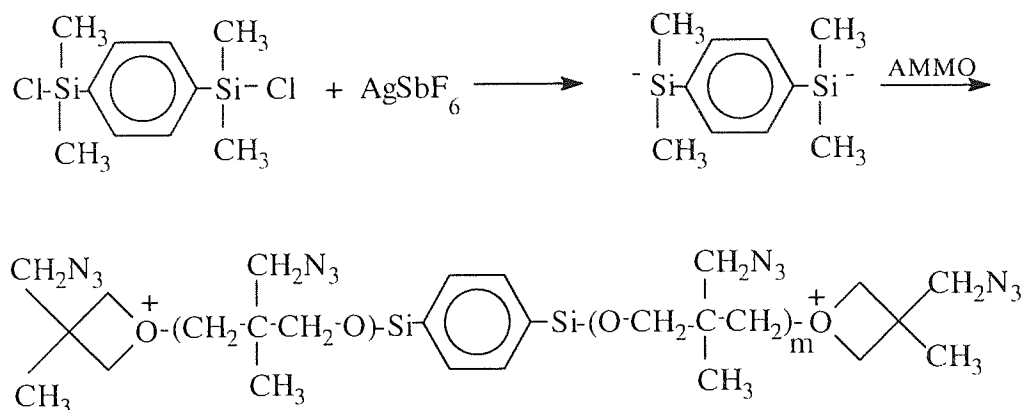
The living cationic polymerization of cyclic ethers was first observed for the polymerization of epichlorohydrin in the presence of ethylene glycol<sup>74</sup>. THF polymerization can proceed as a living system<sup>75,76</sup>. Smith and Hubin<sup>77</sup> reported that a bifunctional initiator, trifluoromethanesulfonic anhydride  $(\text{CF}_3\text{SO}_2)_2\text{O}$ , can be used for the living polymerization of THF. Recently Hsiue and co-workers<sup>78</sup> synthesised THF and 3,3-bis(chloromethyl) oxetane (BCMO) triblock copolymers having a narrow polydispersity via a living system, using this bifunctional initiator (figure 1.7.2).

**Figure 1.7.2. Synthesis scheme of triblock copolymers**



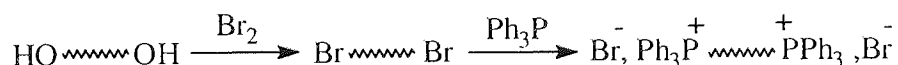
The use a bifunctional initiator system of bis-1,4-(chlorodimethylsilyl) benzene (BSB)/ $\text{AgSbF}_6$  in dichloromethane to prepare triblock copolymer via living cationic polymerization was described by Talukder<sup>79</sup>. The purity and dryness of the system is of importance in the success of the living polymerization of 3-azidomethyl-3-methyl-oxetane (AMMO) (figure 1.7.3).

**Figure 1.7.3. Polymerization of AMMO with BSB/AgSbF<sub>6</sub> initiator system**



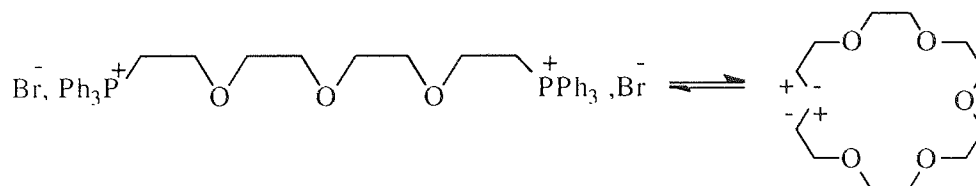
Recently polyethers of low and medium molecular weight containing stable ionic groups (phosphonium ions) at both ends, were obtained by living cationic polymerization of tetrahydrofuran initiated by trifluoromethane sulfonic anhydride, followed by termination with triphenyl phosphine<sup>80</sup>. The synthesis of diionically terminated polyethers was based on the conversion of hydroxyl end-groups of polyether diols, which can be obtained by the cationic Activated Monomer Polymerization (see section 1.5) of oxiranes and THF, into phosphonium ion end-groups. The transformation of the end groups was carried out by bromination in the presence of triphenylphosphine (figure 1.7.4.).

**Figure 1.7.4. Transformation of the end groups**



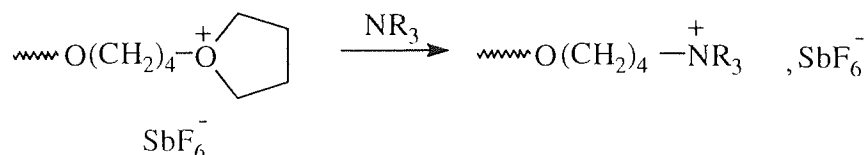
It was reported that intramolecular aggregation of the ionic terminal groups in such low molecular weight polyethylene oxides leads to cyclic structures resembling crown ethers and showing comparable efficiencies for complexing cations (figure 1.7.5.).

**Figure 1.7.5. Intramolecular aggregation of polyethers through the ionic end groups**



This approach differs from the direct use of terminating agents such as tertiary amines providing stable cationic end groups in the polymerization of THF or for ionenes of polyTHF<sup>81-83</sup> (figure 1.7.6.).

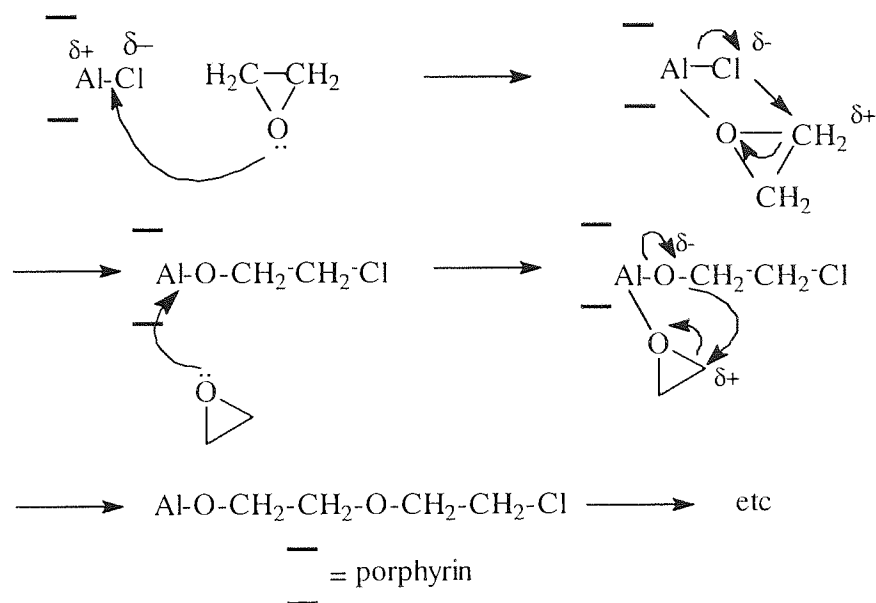
**Figure 1.7.6. Tertiary amine end group of living polyTHF**



#### 1.7.4. Immortal polymerization

The concept of immortal polymerization introduced by Inoue for the ring opening polymerization of epoxides and  $\beta$ -lactones<sup>84-86</sup> using catalysts such as metalloporphyrins of particularly zinc, aluminium and manganese. Living polymerization does not ensure immortality as termination can take place by addition of protonic reagents. A "coordinate anionic mechanism" was proposed<sup>87,88</sup>, in which the monomer was coordinated to the catalyst and activated towards nucleophilic attack, providing orientation of reacting molecules, and leading to stereospecific polymerization.

**Figure 1.7.7. Coordinate anionic mechanism of immortal polymerization of ethylene oxide**

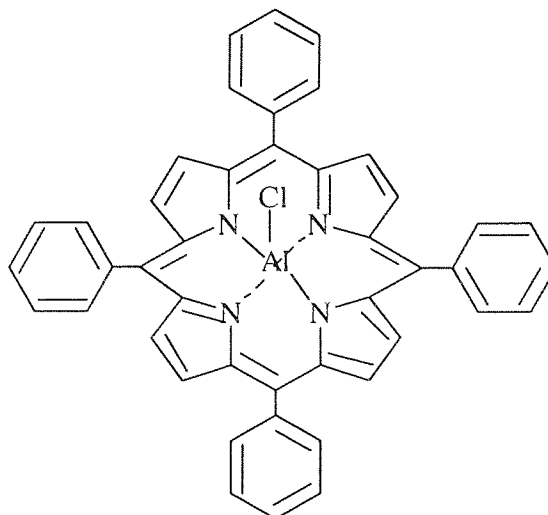


It is believed that the polymerization takes place by firstly coordinating the monomer at the electron-deficient aluminium atom, which then allows attack by the activated chlorine atom on the oxirane ring. Nucleophilic attack of the chloride ion on the  $\alpha$ -carbon of the monomer follows and the ring then opens to form the propagating structure. During propagation further coordination of the monomer occurs in a similar way. However nucleophilic attack at the  $\alpha$ -carbon is thought to occur by the ethereal oxygen atom which is directly linked to the Al atom.

Using the chloro-aluminium porphyrins (figure 1.7.8.) for the polymerization of propylene oxide, it was found that the reaction still continued even in the presence of a protic acid. This is remarkable considering that the growing polymer is of a nucleophilic nature and compounds such as water, chloric acid, alcohols were unable to terminate polymerization. The reaction gives a polymer with a narrow molecular weight distribution and, unlike living polymerization the number of polymer molecules is greater than that of the initiator. The immortal polymerization can be accounted for by the unusual reactivity of the aluminium atom-axial ligand bond (Al-Cl).



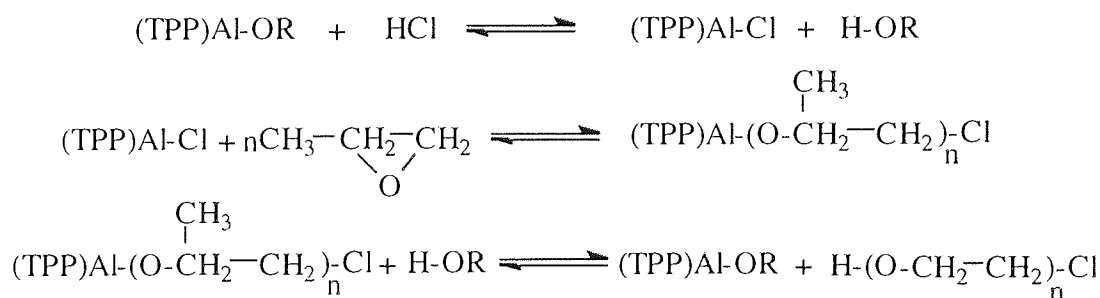
**Figure 1.7.8. (5,10,15,20-tetraphenylporphinato) aluminium chloride (TPP) AlCl**



When propylene oxide was polymerized using (TPP)Al-Cl, a living system was observed. Addition of HCl should have terminated the living polymerization, but instead it actually assisted the polymerization as further addition of propylene oxide was polymerized<sup>86</sup>.

The reaction scheme (figure 1.7.9.) indicates how the protic reagent might participate in the polymerization:

**Figure 1.7.9. Immortal polymerization of propylene oxide**

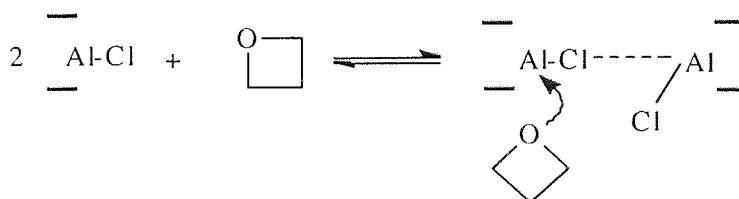


The addition of HCl generates the original catalyst which can be utilised to polymerize a further batch of monomer re-introduced into the system. The chain transfer reactions

shown above are reversible and occur much more rapidly than chain growth. The consequence of this is that narrow molecular weight distribution polymers are obtained. With immortal polymerization the number of polymer molecules is not limited by the amount of initiator but can be increased if required by the addition of a protic acid.

The polymerizations of oxetane and substituted oxetanes have been carried out with catalyst derived from the reaction of 5,10,15,20-tetraphenyl 21H, 23H-porphine and aluminium diethyl chloride<sup>89,90</sup>. This immortal polymerization leads to a polymerization that is slower than the corresponding polymerization of oxiranes but high conversions of monomer to polymer occur and the polymerization shows the properties of a living polymer; the molecular weight average of the polymer increases with conversion of the monomer to polymer closely correlating with conversion of the monomer polymerized to initiator used. The polydispersity indicates a narrow molecular weight distribution. The possible mechanism of the polymerization of oxetane (figure 1.7.10) was shown to involve two molecules of (TPP)AlCl taking part simultaneously during chain growth, and a single monomer molecule reacting with one active centre.

**Figure 1.7.10. Mechanism of the polymerization of oxetane using (TPP)AlCl**



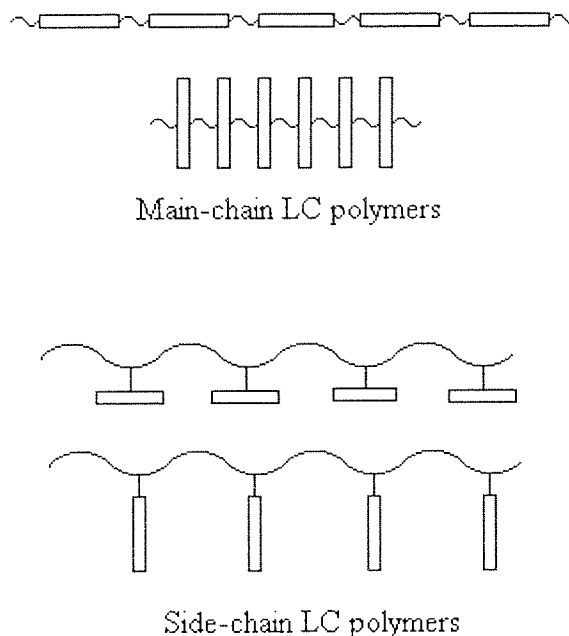
## 1.8. Applications of polyethers

### 1.8.1. Liquid crystals polymers

Liquid crystal (LC) behaviour is due to molecular rigidity rather than intermolecular attractive forces. A typical liquid crystal polymer is a rigid-rod macromolecule, the rigidity of which results from having rigid groups either within the polymer chain or as side groups on the polymer chain<sup>10</sup>. These two types of LC polymer, referred to as main chain and side chain LC polymers are depicted in figure 1.8.1. The rigid groups are referred as mesogens or mesogenic groups.

A large number of side-chain liquid crystal polymers have been synthesized in the last ten years. The influence of parameters such as the molecular weight of the polymer, the nature and the length of the spacer group, the nature of the mesogenic group and the polymer backbone had been studied<sup>91-94</sup>. Linear polyethers are selected for backbones because of their low T<sub>g</sub> and hence flexibility<sup>95,96</sup>. Recently, molecular design of novel side chain liquid crystalline polymers was reported using cationic ring opening polymerization of oxetane derivatives<sup>97</sup>. It was the first time that polyoxetane was used as the main chain. Cyclic oligomers of epichlorohydrin can be used as a backbone to create liquid crystal crown ethers, combining the capability to complex metal cations and LC properties<sup>98</sup>.

**Figure 1.8.1 Main chain and side chain liquid crystal polymers**



### 1.8.2. Energetic materials

Solid propellant rockets have a long history, which is interwoven with the development of gunpowder, artillery, and pyrotechnics. The propellants need to have high energy components, which, on combustion, give rise to low molecular weight gaseous products in order to produce a high specific impulse. It is essential that the propellant has a low vulnerability and the need for a propellant which is safe to make and to handle, has a long safe life without loss of performance and safety, and is cheap to make are fundamental requirements.

Recently, energetics and non-chlorine containing compounds, for clean storage, binders were developed using polyethers<sup>99,100</sup>. The synthesised polymers should incorporate the following properties:

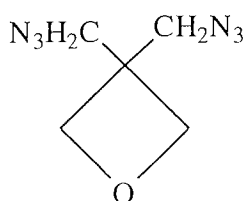
- 1- Molecular weight control
- 2- Low molecular weight polydispersity
- 3- Low glass transition temperature
- 4- Energetic characteristics

Therefore polyethers made from cyclic ethers, tetrahydrofuran, oxetane and their derivatives have attracted interest for these above desired properties<sup>78,101-103</sup>.

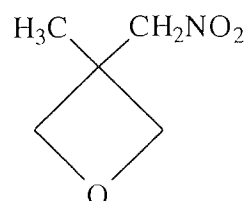
### 1.8.3. Scope of this project

Monomers, like 3,3 bis (azidomethyl) oxetane (BAMO) or 3-methyl-3-nitratomethyl-oxetane (NIMMO) depicted in figure 1.8.2., can be polymerized or copolymerized cationically using Lewis acid such as  $\text{BF}_3$  in dichloromethane<sup>104,105</sup>.

**Figure 1.8.2. Oxetane derivatives monomers**



3,3-bis (azidomethyl) oxetane  
BAMO



3-methyl-3-nitratomethyl oxetane  
NIMMO

Their respective polymers could be of interest in the synthesis of energetic and stable materials. It is known that intramolecular reaction, which produces cyclic oligomers notably tetramers and trimers, often occurs during the polymerization process.

The scope of this project is to collect informations concerning this phenomenon, studying and modelling the reaction of ring opening polymerization of oxetane using cationic species.

## CHAPTER 2

### EXPERIMENTAL TECHNIQUES

#### 2.1 High vacuum techniques

The high vacuum technique is one of several types of experiment techniques that can be employed to obtain a controlled experimental environment. The most usual reason for wanting this is the necessity to exclude oxygen and water and, less commonly, carbon dioxide from the reaction being studied. The intermediates involved in ring opening polymerizations, such as oxonium ions (cationic) or alkoxide ions (anionic), are known to be very sensitive to moisture and impurities. For this reason the distillation and purification of solvents or monomers were carried out using either high vacuum techniques or an inert atmosphere of argon in order to exclude these impurities from reactions.

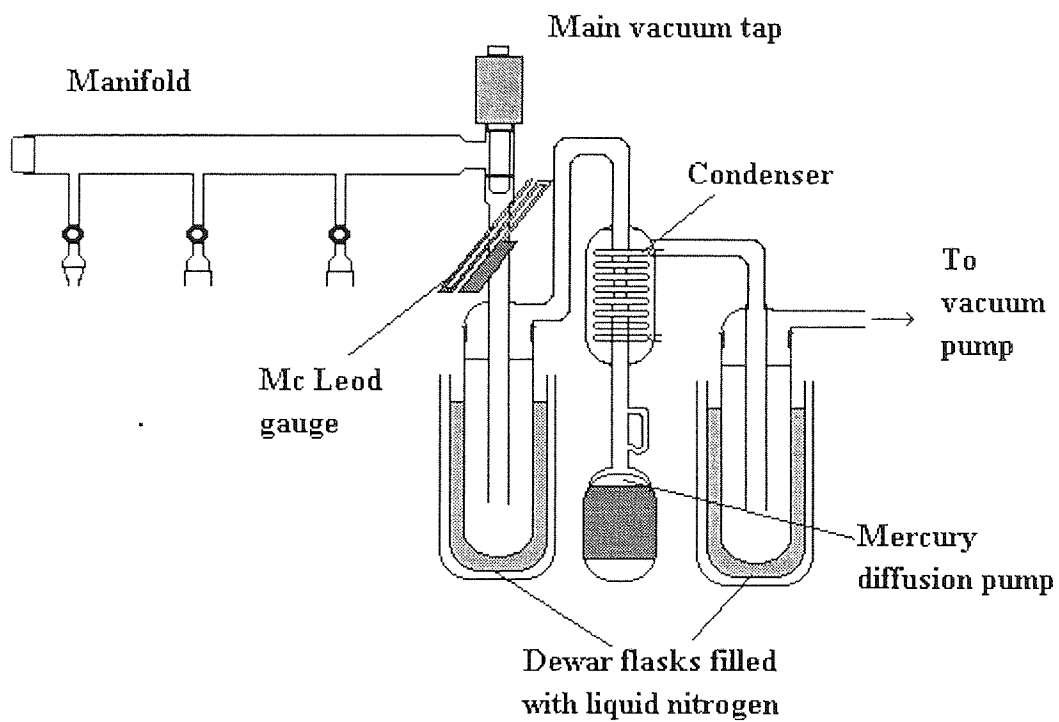
##### **2.1.1. The Vacuum line**

A typical vacuum line is shown in figure 2.1. For laboratory scale operations, a vacuum line is almost always suitable and efficient. It is constructed from glass and consists of a manifold fitted with PTFE taps connected to a system of two vacuum pumps placed in series. The latter is the most important part of the system, a mercury diffusion pump, in which mercury is heated so that it boils vigorously to produce a stream of mercury vapour, accelerated by the Venturi effect in a narrower tube section, then condensed on the walls of the water condenser. The second pump is an Edwards rotary pump which generates a pressure of approximately  $10^{-2}$  mm Hg. The whole system could provide a good working vacuum up to  $10^{-5}$  mm Hg in the best cases.

The purpose of the two cold traps is to trap volatile materials from the line on their way to the pumps, thus to protect the pumping system, and to trap as well the vapour and any pumping fluid before it can enter the line by back diffusion. The coolant used for the traps, liquid nitrogen (b.p.  $-195.8$  °C) which condenses the oxygen, has the advantage of being inert to combustion and of many uses in a laboratory.

In order to measure the absolute pressure in the vacuum line, and to check whether the system is free of leaks or ready to use, different gauges can be adapted. Electric gauges,

**Figure 2.1 The vacuum line**



such as Pirani type, or simple mercury MacLeod gauges are the most common and easy to use.

### **2.1.2 Freeze - thaw degassing of solvents**

Most liquids contain dissolved gaseous components such as oxygen, carbon dioxide or hydrogen, which need to be removed before vacuum distillation. The traditional method of removing such components is the "Freeze - Thaw degassing" and proceeds as follows:

A solvent flask (figure 2.3.) is attached to the vacuum line with the main tap closed. A Dewar vessel, filled with liquid nitrogen, is placed around the flask. When the liquid is frozen, the space above it is pumped by opening the main tap. After a while the main tap is closed and the solvent allowed to thaw. The same cycle is repeated until the bubbling ceases and a high vacuum is reached in the system. The duration of this process depends on the quantity of solvent to be distilled and, of course, on the amounts of gas dissolved. This procedure prevents "bumping" and "flashing over" during distillation.

### **2.1.3 Flasks**

The use of high vacuum techniques requires specially designed flasks for drying and storage of monomers and solvents. These flasks must be fitted with PTFE taps and joints which allow connection to the vacuum line. Two types of flasks were designed, a drying flask in which monomer was left over drying agent before distillation (figure 2.3.a), and a monomer solution storage flask, with both male and female greased joints, which could be connected to a polymerization vessel or distillation still (figure 2.3.b).

### **2.1.4 Trap to trap distillation**

Once degassed the solvent or monomer could be transferred to another storage flask by a trap to trap technique using the vacuum line, as shown in figure 2.2. This receiver flask is attached to the vacuum line, evacuated and then immersed into a Dewar filled with liquid nitrogen. By closing the main tap and opening the appropriate taps, the contents of the monomer flask are distilled into the receiver flask.



**Figure 2.2 Vacuum line distillation**

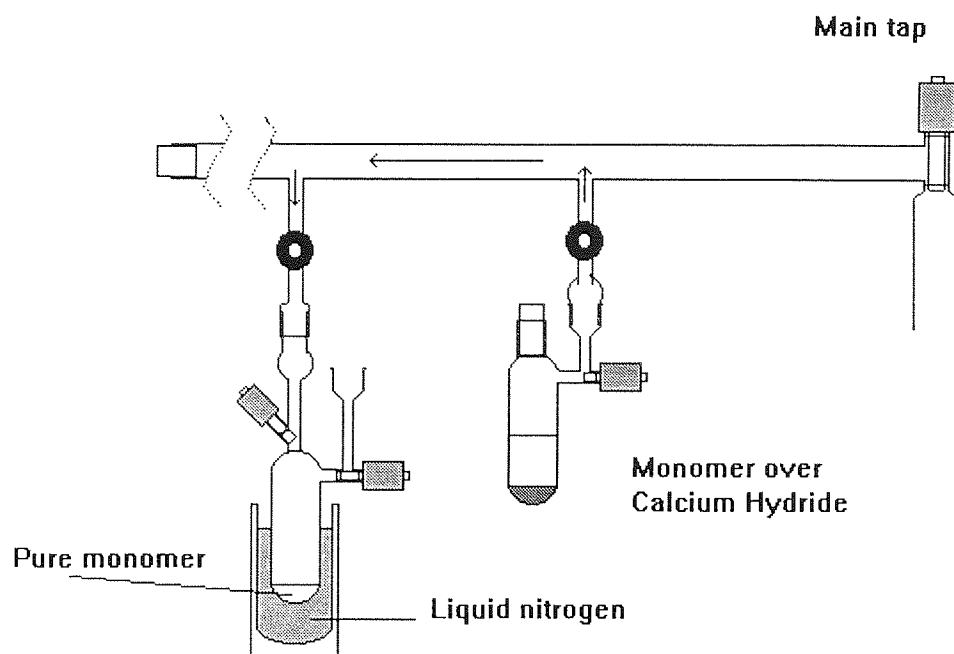


**Figure 2.3.a Monomer drying flask**

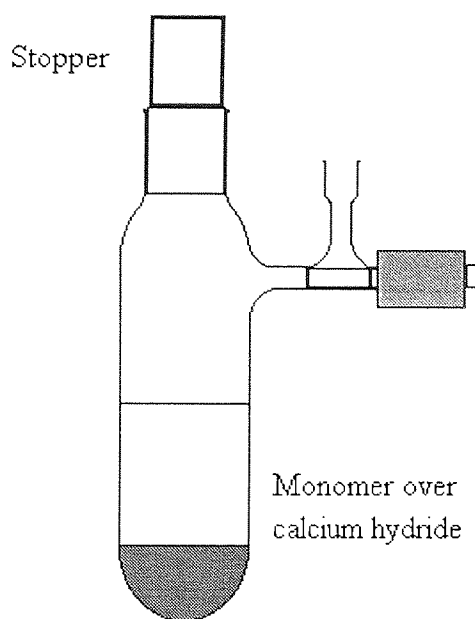
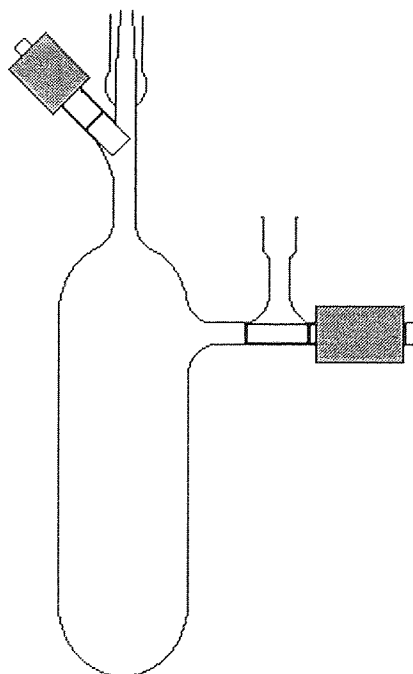


**Figure 2.3.b Monomer solution storage flask**



## **2.2. Treatment of glassware**

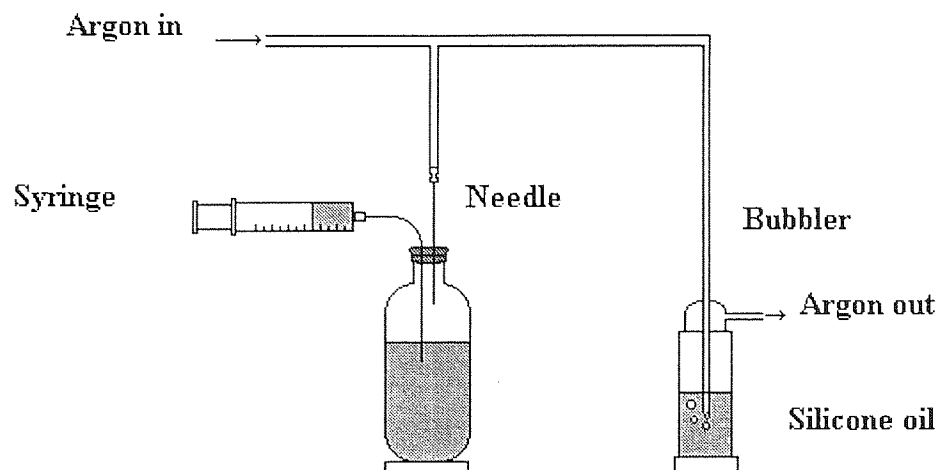
All the glass apparatus was cleaned thoroughly with a Decon solution and acetone. If necessary, for a deeper cleaning process, glassware was left soaking in a chromic acid solution for a period of 24 hours in order to get rid of particularly residual high vacuum silicon based grease and traces of polymers. Finally syringes, flasks, and all the reaction vessels were kept in an oven at 240 °C for few hours prior to use.

## **2.3. Manipulation techniques**

### **2.3.1. Inert gas techniques**

Many of the reactants used in ionic polymerization are sensitive to the presence of oxygen and moisture. Lewis acid-type catalysts are inefficient if "wet". A number of inert gas techniques were used to prevent decomposition, though in each case the inert gas was argon. Since argon is denser than air it provides a protective layer of inert gas above the liquid solution. In most cases argon was introduced into the flask via a needle through a rubber septum (see figure 2.4. The argon line). Dry argon was supplied by BOC with a purity guaranteed less than 3 vpm moisture and less than 3 vpm oxygen and no further purification carried out.

**Figure 2.4. The argon line**



### 2.3.2. Glove box techniques

Glove box techniques were used for manipulation, (and in some cases storage), of air and moisture sensitive reagents, such as initiators and polymerization solvents. A Miller-Howe box complete with a recirculation system was used with argon as the inert gas. The box was operated under positive pressure with a constant argon flow of 45 litres per minute through a series of columns containing 3 Å molecular sieves, BASF R311 catalyst and BDH activated charcoal. These columns were reformed periodically in order to attain moisture levels below 5 ppm and oxygen below 1 ppm (as confirmed by the manufacturer). An indication of dryness was given by measuring the length of time required for freshly exposed sodium metal to become tarnished. Flasks, syringes and equipment were introduced to the box by means of a port which was evacuated and purged with argon three times before opening the main door. The port was evacuated using an Edwards rotary vacuum pump which was vented to a fume cupboard in order to remove potentially harmful vapours.

## 2.4. Preparation and purification of materials

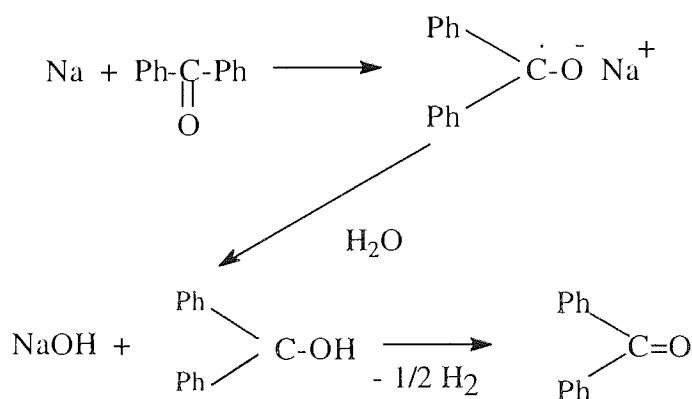
### 2.4.1. Monomers

#### 2.4.1.1. Oxetane

Oxetane, trimethylene oxide was obtained from Lancaster Chemicals Co. Before each distillation a fraction of 20-25 g was placed over calcium hydride for 48 hours in a stoppered flask (figure 2.3.a) with the tap slightly opened to allow hydrogen from the reaction with moisture to escape. The liquid was then degassed using the freeze-thaw technique described in section 2.1.2.

For a deeper and final drying, the monomer was transferred by trap to trap distillation (see section 2.1.3.) into another flask containing a mixture of benzophenone and slices of sodium metal previously degassed. It was apparent that oxetane was dry when a deep blue solution was produced by the mixture. (Scheme 2.1)

**Scheme 2.1. Sodium and benzophenone drying procedure**



The blue colour resulted from the production of a sodium benzophenone complex which is only observed in a completely dry environment. Immediately after this "colour test" the oxetane was distilled by the trap to trap method into a final dry storage flask (figure 2.3b). This was carried out because a reaction between sodium and oxetane took place if the mixture was allowed to stand for sometime at room temperature. This reaction was accompanied by the evolution of a gas, presumably hydrogen and the consumption of the monomer.

#### **2.4.1.2. 3,3-Dimethyloxetane**

3,3-dimethyloxetane was generously supplied by the Defence Research Agency, the same drying and distillation procedure was carried out as for oxetane.

#### **2.4.1.3. Tetrahydrofuran (THF)**

THF (hplc grade) was obtained from Fisons Chemicals Ltd. The purification procedure described for oxetane was adopted. In addition to the blue colour observed with sodium and benzophenone being an indication of dryness, it is also indicative of the absence of peroxides.

#### **2.4.1.4. Oxepane**

Oxepane (hexamethylene oxide) was supplied by Phase Separation Co. This cyclic ether was dried and purified following the procedure described in 2.4.1.1.

#### **2.4.1.5. Propylene oxide**

Propylene oxide (epoxy-propane) was supplied by Aldrich Co, dried and distilled using the procedure described in 2.4.1.1.

#### **2.4.1.6. Cyclohexene oxide**

Cyclohexene oxide was obtained from Aldrich Co and placed over fresh calcium hydride. The monomer was then degassed by freeze thaw technique and transferred to another dry flask by the trap-to-trap distillation method.

## **2.4.2. Catalysts**

### **2.4.2.1. Boron trifluoride etherate**

Boron trifluoride etherate,  $\text{BF}_3\text{OEt}_2$  is a self drying agent. It gives toxic fumes on hydrolysis and has to be handled at all times in the glove box. The required solution of  $\text{BF}_3\text{OEt}_2$  was prepared in dried and distilled dichloromethane and kept in the glove box.

### **2.4.2.2. Ethanediol**

Ethanediol was dried over fresh calcium hydride, degassed and distilled on the vacuum line. It was kept in the glove box as a solution in dichloromethane.

### **2.4.2.3. Tetrafluoroboric acid - diethyl ether complex 85 %**

$\text{HBF}_4 \cdot \text{O}(\text{C}_2\text{H}_5)_2$  was obtained from Aldrich Co, and used neat for terpolymerization between cyclic ethers.

### **2.4.2.4. Triflic acid**

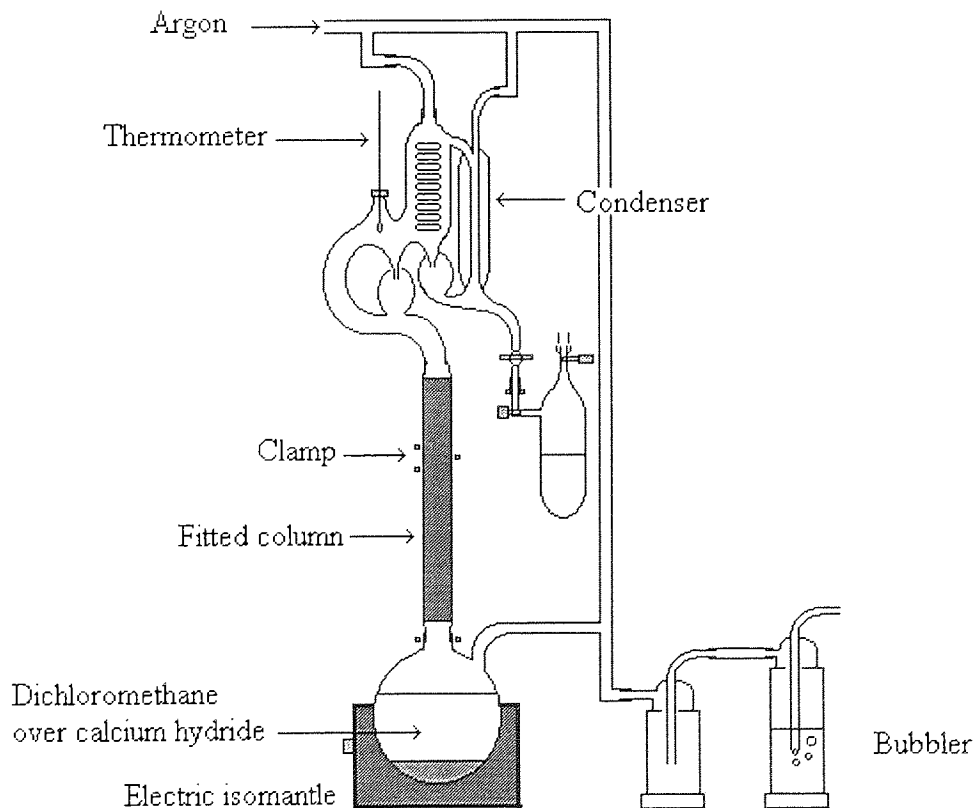
Triflic acid (trifluoromethane sulphonic acid), was obtained from Aldrich Co. in a 10g ampoule. Very hygroscopic, it gives toxic fumes with moisture. A solution in dry dichloromethane was kept in a storage flask in the glove box.

### 2.4.3. Solvents

#### 2.4.3.1. Dichloromethane

The polymerization solvent, dichloromethane (high purity grade) was obtained from Fisons Chemicals Co and placed over calcium hydride for a few days. It was then fractionally distilled under an inert atmosphere of argon. The distillation apparatus is shown in figure 2.5. The distillation was carried out in a closed system to prevent moisture contaminating the solvent. Before starting the distillation the system was purged with argon and a reflux was carried out for a few hours. A monomer storage flask was connected to the still before the distillation was started.

**Figure 2.5. Distillation apparatus used for the purification of dichloromethane**





#### **2.4.3.2. THF (gpc solvent)**

The Gel Permeation Chromatography solvent (hplc grade) was obtained from Fisons, no particular treatment was made. Solutions of polymers samples were prepared in this solvent and injected for analysis.

#### **2.4.4. Drying agents**

##### **2.4.4.1. Sodium metal**

Sodium metal was supplied in paraffin oil by BDH. The oil was removed by washing with hexane and tarnished surfaces cut away before use.

##### **2.4.4.2. Benzophenone**

Benzophenone was supplied by Janssen Chemica, no particular treatment was made prior to use.

##### **2.4.4.3. Calcium hydride**

Calcium hydride was obtained from Aldrich Co. A 40 mesh powder was found to be the more efficient to dry monomers and dichloromethane.

##### **2.4.4.4. Sodium sulphate**

Sodium sulphate was supplied by Aldrich Co., it was left in a furnace at 350 °C for few days prior to use.

## **2.4.5. Other chemicals**

### **2.4.5.1. Veratrole**

Veratrole (1,2-dimethoxybenzene) was obtained from Aldrich Co. A solution was made in dichloromethane and kept in the glove box.

### **2.4.5.2. Dibenzo-18-crown-6**

Dibenzo-18-crown-6 (2,3,11,12- dibenzo- 1,4,7,10,13,16- hexaoxacyclooctadeca-2,11- diene) was obtained from Aldrich Co.. A solution in dry dichloromethane was prepared and kept in the glove box.

### **2.4.5.3. 12-crown-4, 15-crown-5, 18-crown-6**

These three crown ethers were obtained from Aldrich. A solution of each was made in dry dichloromethane and kept in the glove box prior to use.

## **2.5. Polymerization techniques**

### **2.5.1. Calorimetric Techniques**

The ring opening polymerization of cyclic ethers is an exothermic process. Therefore a system capable of measuring the increase in temperature while the reaction is taking place under adiabatic condition could be used to measure rates of reaction for the system under study. For this reason the use of a calorimeter was employed.

The system used was a modified form of that used successfully for monitoring the cationic polymerization of cyclic ethers<sup>1</sup>, developed by Biddulph and Plesch<sup>106</sup>. The increase in temperature associated with the ring opening was measured using a GL23 2 k $\Omega$  thermocouple (supplied by RS Components Ltd.). The change in resistance as a function of temperature was measured by a Knauer auto potentiometer bridge itself linked to a Serviscribe IS Chart recorder. After calibration the apparatus was found to have a linear sensitivity to increases in temperature.

In a typical experiment the calorimeter (figure 2.6.), containing a magnetic flea both previously in the oven, was attached to the vacuum line through (A) with the monomer flask (figure 2.3.b) connected to (B). Tap (C) was closed and the whole system evacuated. After evacuation, tap (C) was closed and the required amount of monomer solution was poured into the bulb by opening (D). The calorimeter was placed on a magnetic stirrer and the thermistor was connected to the Knauer auto-potentiometer bridge. To ensure that ambient temperature did not have an effect on the experiments, water from a thermostated bath at 35 °C was continually passed through the double jacket. The balancing bridge was connected to chart recorder and the whole system was left to equilibrate at 35 °C for 15 minutes.

When the bridge was adjusted to zero and a stable line was obtained on the chart recorder, the required amounts of the co-catalyst first and then catalyst were injected through the rubber septum using syringes.

### **2.5.2 Discussion**

The trace of deflection against time was converted to °C.s<sup>-1</sup> by means of the calibration curve described above. The rate of increase in temperature during the reaction, measured

in  $^{\circ}\text{C}\cdot\text{s}^{-1}$  could then be used to estimate the rates of polymerization from the slopes of the lines obtained. A linear relationship between the maximum temperature increase and the concentration of monomer used in that experiment was observed. Figure 2.7. shows a typical thermogram of the homopolymerization of oxetane.

**Figure 2.6. The calorimeter**

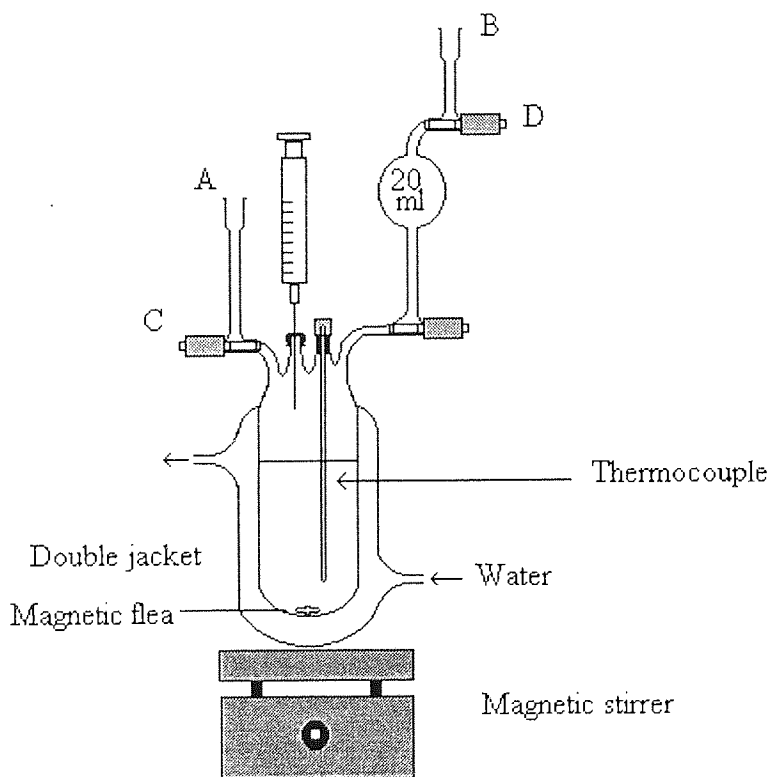
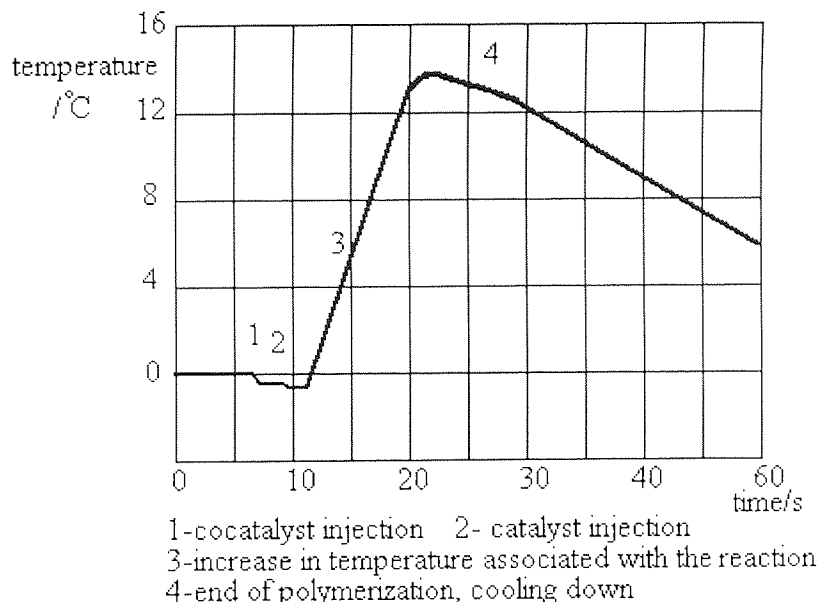


**Figure 2.7. A typical thermogram**

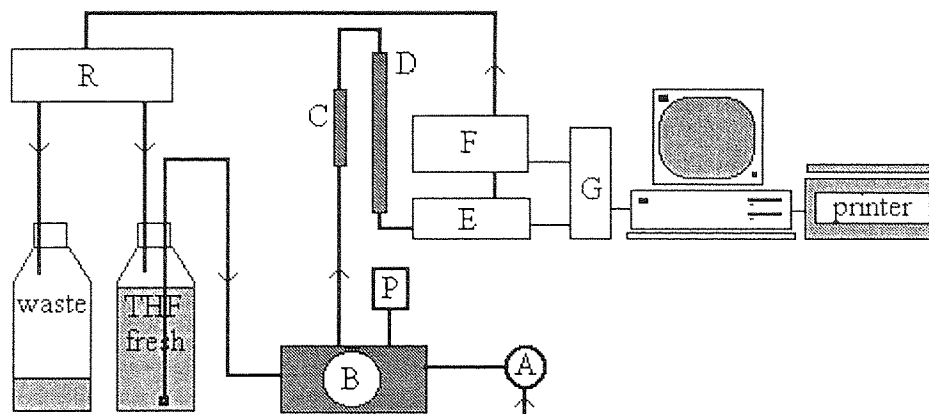


## **2.6. Analytical techniques**

### **2.6.1. Gel Permeation Chromatography**

Gel Permeation Chromatography (GPC), also known as Size Exclusion Chromatography, was used to determine the molecular weight distribution of polymers. The determination depends upon fractionation of polymer molecules in the sample according to their sizes. This is achieved by passing the sample in a mobile phase through a series of columns containing swollen cross-linked polystyrene beads. This stationary phase is constructed so that when swollen occurs, pores are produced in the beads, which are of different sizes and each pore allows only polymer chains of sufficiently small volume to enter it. This effectively slows down the passage of small molecules since they may occupy a larger pore volume, permeating the gel structures and taking a longer path through the column than larger polymer chains which are excluded from a greater fraction of the gel and elute more rapidly. Thus the large molecules leave the column first followed by progressively smaller molecules.

**Figure 2.8. The Gel Permeation Chromatography**



- |                    |                     |                   |
|--------------------|---------------------|-------------------|
| A- Injector system | B- HPLC pump        | C- Guard column   |
| D- Gel column      | E- RI detector      | F- UV detector    |
| G- DCU             | R- Solvent Recycler | P- Pressure gauge |

### 2.6.1.1. Experimental

The eluent used for GPC in this project was THF (hplc grade). It was delivered at 1 ml per minute by a Knauer high performance liquid chromatography pump (A). Samples of polymer made up in THF (1-2% w/v) were introduced into the column using a 100  $\mu$ l valve and loop injector system (B). The solution passes first through a short guard column (C) designed to filter the solution and then prevent blockages in the rest of the system, before entering then the main column set (D), supplied by Polymer Laboratories. Four columns were used with size exclusion limits between  $10^2$  to  $10^5$  Å. The eluted fractions from the column were analysed by a Knauer differential refractometer (E) and an ultra-violet spectrometer (F), connected in series. The differential refractometer monitors continuously the refractive index (RI) of the eluted solution and compares it with the refractive index of the eluent. Any difference owing to the presence of polymer in the eluent generates a deflection which is proportional to the concentration of the eluting polymer at that time. The UV detector only responds to polymers containing chromophoric groups, (which absorbs at a given wavelength) either attached to, or part, of the polymer back-bone (e.g. polystyrene). The output of each detector is recorded by a data collecting unit, (DCU), (G). The DCU is monitored by a PC computer running the software PL Caliber (from Polymer Laboratories). This

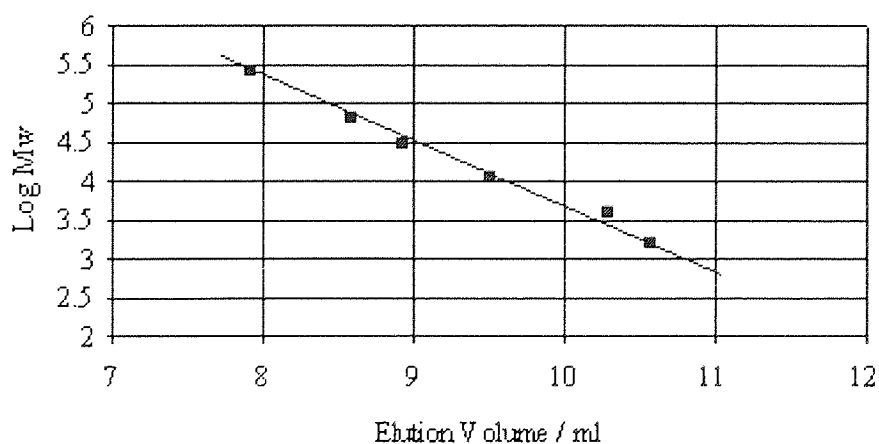
software allows the user to follow the analysis or to reanalyse previous chromatograms. At the end of the analysis calculations of molecular weight parameters are made according to the calibration equation of the column.

### 2.6.1.2. Calibration of the GPC column

To estimate the number and weight average molecular weights of a polymer it is necessary to determine how the molecular weight of the eluted polymer varies over the range of elution volumes. For this purpose polystyrene or polyTHF samples of narrow molecular weight distribution and of known molecular weights were injected in turn into the column. The volume of the solvent pumped through the column required to elute the polymer of specific molecular weight was measured and a calibration curve plotted, as shown in figure 2.9.

The system was calibrated with Polymer Laboratories polyTHF standard samples of known peak molecular weights ranging from 1600 to 258000. The calibration curve for the column used in these measurements is shown in figure 2.9.

**Figure 2.9. GPC calibration curve (PolyTHF)**



### 2.6.1.3. Calculations of average molecular weights

The data obtained from the chromatogram may be used to calculate number and weight average molecular weights, thus polydispersities and to gain information about the molecular weight distribution. Average molecular weights are calculated by the following equations:

$$\overline{Mn} = \frac{\sum wi}{\sum \left(\frac{wi}{Mi}\right)} \quad (1)$$

$$\overline{Mw} = \frac{\sum wiMi}{\sum wi} \quad (2)$$

where:

- $\overline{Mn}$  = number average molecular weight
- $\overline{Mw}$  = weight average molecular weight
- $wi$  = weight fraction of polymer of molecular weight  $Mi$  in a given sample
- $Mi$  = molecular weight of a given sample

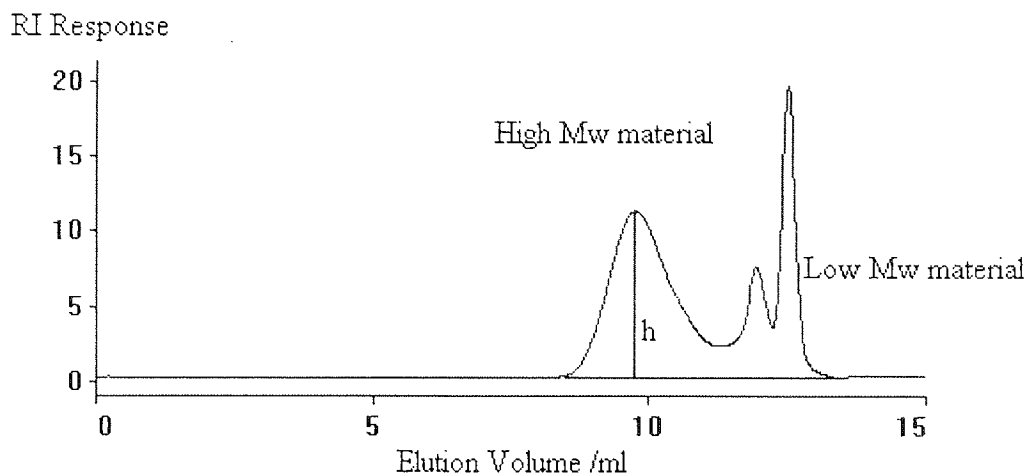
Since the detector response is proportional to the concentration of polymer in solution,  $wi$  may be replaced by  $hi$ , the height of the trace at a given elution volume. A typical size exclusion chromatogram is shown in figure 2.10.

$$\overline{Mn} = \frac{\sum hi}{\sum \left(\frac{hi}{Mi}\right)} \quad (3)$$

$$\overline{Mw} = \frac{\sum hiMi}{\sum hi} \quad (4)$$



**Figure 2.10. A typical GPC trace**



If the deflections obtained for a polymer sample across a range of elution volumes are measured and these elution volumes converted to molecular weight data by reference to a calibration curve, number and weight average molecular weights and polydispersities may be calculated. In practice these calculations were processed using the software PL Caliber run on a PC computer.

Some samples were also processed using a Gel Permeation Chromatograph located at the DRA site in Fort Halstead. This system consisted of a Waters 510 pump passing THF through an ERC 3522 degasser and into four PL gel columns having exclusion limits of  $10^5$ ,  $10^4$ ,  $10^3$ ,  $10^2$  Å. Samples were introduced to the column by a Waters 717 auto sampler and the output from the columns was detected by a differential refractometer and a Viscotek viscometer. The columns were calibrated with polyTHF standards and molecular weights were calculated, using a software (TriSEC) run on a PC computer.

### 2.6.2. Nuclear magnetic resonance spectroscopy (NMR)

Fourier transform high resolution NMR was used to characterise and determine the structure and the composition of monomers and polymers.  $^{13}\text{C}$  and  $^1\text{H}$  spectra were carried out using a Bruker AC 300 spectrometer. Solutions of the samples were made by dissolving the solids in deuterated chloroform ( $\text{CDCl}_3$ ) with a small quantity of tetramethyl silane (TMS) as reference to each solution. For the  $^{13}\text{C}$  analysis, a pulse technique, P.E.N.D.A.N.T.  $^{13}\text{C}$ , spectroscopy was used. This involves some noticeable differences on the conventional  $^{13}\text{C}$  spectrum. The signals corresponding to the carbon

are edited positively or negatively according to their types of substitution. Methyl and methine carbons peaks appear as positive peaks, whilst methylene and quaternary carbons appear as negative peaks. The P.E.N.D.A.N.T. spectrum slightly differs from one made using a D.E.P.T. sequence where signals belonging to quaternary carbons do not appear.

Both  $^1\text{H}$  and  $^{13}\text{C}$  spectrums were integrated and edited on a PC computer using software called WinNMR from Bruker.

## CATIONIC HOMOPOLYMERIZATIONS OF CYCLIC ETHERS

### 3.1 The cationic ring opening polymerization of oxetane

#### 3.1.1. Introduction

So far the collective work by Rose<sup>28,50</sup> and Farthing<sup>27</sup> has indicated that the polymerization of oxetane using  $\text{BF}_3\text{OEt}_2\cdot\text{H}_2\text{O}$  system includes three main stages: initiation, propagation and termination. The mechanisms have been discussed in chapter 1; the propagation step was considered as an  $\text{S}_{\text{N}}2$  step which is of second order type kinetics. Termination was considered to take place either by a transfer or a process of back-biting.

The initial objective of this project was to establish the kinetics of polymerization of oxetane using  $\text{BF}_3\text{OEt}_2$  as initiator in conjunction with a cocatalyst. Amongst the different cocatalysts tried in a previous research<sup>1</sup>, a difunctional cocatalyst such as ethanediol gave good results concerning the molecular weight of the polymer.

#### 3.1.2. Effect of the molar ratio $\text{BF}_3\text{OEt}_2$ :ethanediol on the rate of polymerization and on average molecular weights

The aim of this work was to establish the dependence of the rate of polymerization on the catalyst:cocatalyst molar ratio and hence to determine the optimal ratio of catalyst:cocatalyst for the polymerization of oxetane. A series of experiments was carried out in which the concentrations of  $\text{BF}_3\text{OEt}_2$  and monomer were kept constant and the concentration of ethanediol was varied. In this series constant volumes of monomer and catalyst solutions were added to the calorimeter and because the volume of cocatalyst used was varied, amounts of  $\text{CH}_2\text{Cl}_2$  were added to the solution to maintain the volume at  $25\text{ cm}^3$ . The rate of polymerization was recorded according to the procedure described in 2.5.1. After polymerization, the samples were recovered by allowing the solvent to evaporate from the solution. Polymer samples were then

parameters on molar ratio of  $\text{BF}_3\text{OEt}_2:\text{OH}$  is shown in table 3.1 and figures 3.1 and 3.2.

**Table 3.1. Effect of the molar ratio  $\text{BF}_3\text{OEt}_2:\text{OH}$  on the rate of polymerization,  $\overline{M}_n$ ,  $\overline{M}_w$  and Pd**

Molar ratio $\text{BF}_3\text{OEt}_2:\text{OH}$	Rate $^{\circ}\text{C}\cdot\text{s}^{-1}$	$\overline{M}_n$ $\text{g}\cdot\text{mol}^{-1}$	$\overline{M}_w$ $\text{g}\cdot\text{mol}^{-1}$	Pd
1:0.5	1.4	2220	3680	1.66
1:1	3.7	2930	4810	1.64
1:2	3.2	2460	4180	1.70
1:3	2.8	2280	3830	1.68
1:4	2.5	1960	3630	1.85

$[\text{OX}] = 2 \text{ M}$ ,  $[\text{BF}_3\text{OEt}_2] = 0.02 \text{ M}$ ,  $T = 35 \text{ }^{\circ}\text{C}$

**Figure 3.1. Effect of the initiator system ratio on the rate of polymerization**  
 $T_{\text{initial}} = 35 \text{ }^{\circ}\text{C}$ ,  $[\text{OX}]_{\text{initial}} = 2 \text{ M}$

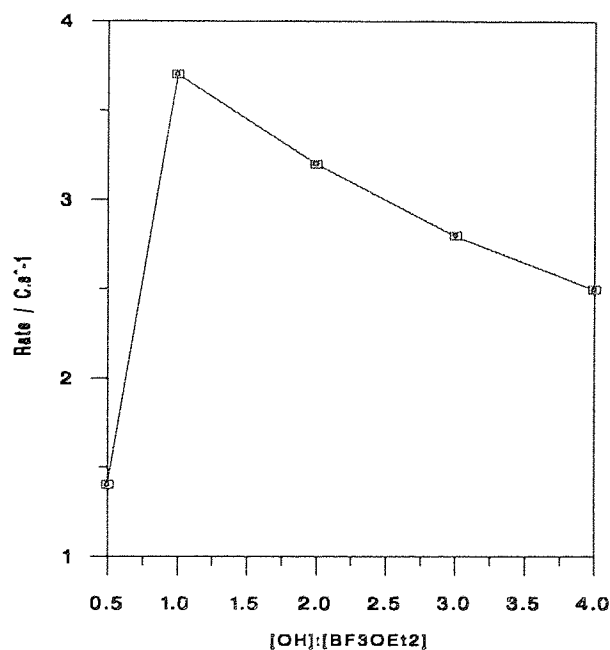
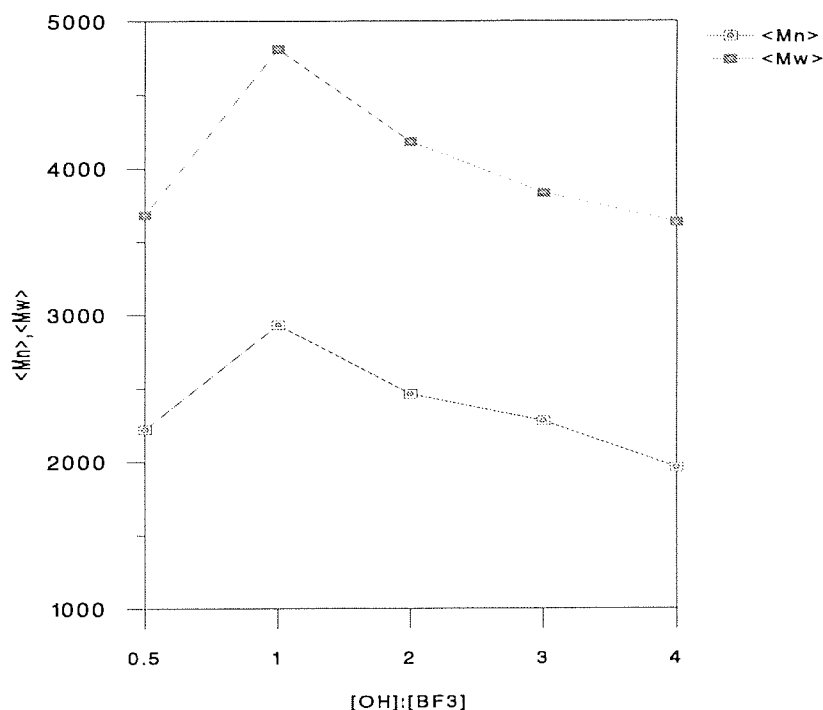


**Figure 3.2.** Effect of the initiator system ratio on  $\overline{Mn}$



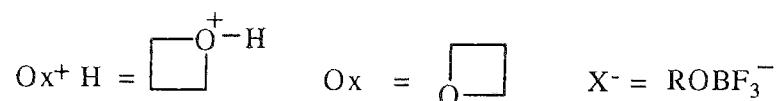
The results shown in table 3.1. and figure 3.1. would indicate that the rate of polymerization is a maximum when the molar ratio  $[\text{BF}_3\text{OEt}_2]:[\text{OH}]$  is 1:1. That the rate of polymerization reaches a maximum at this ratio suggests that the species responsible for initiation of the polymerization is a 1:1 complex of  $\text{BF}_3\text{OEt}_2$  and an hydroxyl group. Before this maximum the concentration of active catalyst is strictly dependent on the concentration of ethanediol, the excess of  $\text{BF}_3\text{OEt}_2$  is probably not involved in the protonation of the monomer.

When the concentration of OH groups exceeds that of the catalyst a steady decline in  $R_p$  is observed. This decline can attributed to protonation of excess ethanediol in competition with the monomer.

Thus:



with:



However, if the total concentration of protons is given by  $[\text{BF}_3\text{OEt}_2]$  (their source), then:

$$[\text{BF}_3\text{OEt}_2] = [\text{Ox}^+ \text{H}] + [\text{RO}^+ \text{H}_2]$$

and

$$\begin{aligned} \frac{[\text{Ox}^+ \text{H}]}{[\text{RO}^+ \text{H}_2]} &= \frac{[\text{Ox}^+ \text{H}]}{[\text{BF}_3\text{OEt}_2] - [\text{Ox}^+ \text{H}]} \\ &= \frac{K_1 [\text{Ox}]}{K_2 [\text{ROH}]_{\text{ex}}} \end{aligned}$$

$$\text{where } [\text{ROH}]_{\text{ex}} = [\text{ROH}] - [\text{BF}_3\text{OEt}_2]$$

It can then be shown that

$$\frac{1}{[\text{Ox}^+ \text{H}]} = \frac{1}{[\text{BF}_3\text{OEt}_2]} + \frac{K_2 [\text{OH}]_{\text{ex}}}{[\text{BF}_3\text{OEt}_2] K_1 [\text{Ox}]}$$

Since  $R_{p\text{max}} \propto [\text{BF}_3\text{OEt}_2]$  and  $R_p \propto [\text{Ox}^+ \text{H}]$

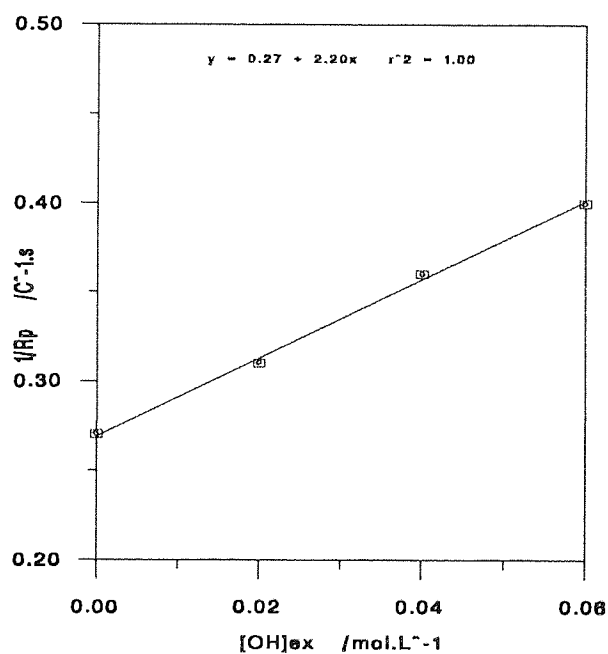
Then

$$\frac{1}{R_p} = \frac{1}{R_{p\text{max}}} + \frac{K_2 [\text{OH}]_{\text{ex}}}{R_{p\text{max}} K_1 [\text{Ox}]}$$

Figure 3.3. shows a plot of  $1/R_p$  against  $[\text{OH}]_{\text{ex}}$  which is linear and shows that the value of  $K_1/K_2$ , which can be estimated from the slope, is 0.06. This value shows that the protonation of the excess of ethanediol is predominant when the ratio  $[\text{OH}]:[\text{BF}_3\text{OEt}_2]$  is greater than 1, therefore the polymerization of oxetane is less favoured, the rate of polymerization decreases.

Figure 3.2. shows the variation of the average molecular weights as a function of the initiation system ratio. Like the rate of polymerization, it appears that  $\overline{M}_n$  and  $\overline{M}_w$  reach a maximum for the ratio 1:1. Increasing the concentration of ethanediol seems to decrease steadily both  $\overline{M}_n$  and  $\overline{M}_w$ . It can therefore be argued that the excess diol not only removes active catalyst from the system, but at the same time causes a reduction of molecular weight probably by increasing the rate of transfer.

**Figure 3.3. Dependence of  $1/R_p$  on the  $[\text{OH}]_{\text{ex}}$**



### 3.1.3. Effect of the concentration of oxetane

Several polymerizations were carried out using the system (1:1)  $\text{BF}_3\text{OEt}_2:\text{OH}$  as catalyst and in which the initial concentration of oxetane in the feed was changed. The concentrations of the catalyst, cocatalyst, and the total volume were kept constant. Table 3.2. summarises this study.

**Table 3.2. Homopolymerization of oxetane, effect of [OX] on the rate,  $\overline{M}_n$ ,  $\overline{M}_w$  and Pd**

[OX] mol.L <sup>-1</sup>	Rate °C.s <sup>-1</sup>	$\overline{M}_n$ g.mol <sup>-1</sup>	$\overline{M}_w$ g.mol <sup>-1</sup>	Pd
1	1.6	2010	3220	1.61
1.5	2.1	2340	3931	1.68
2	3.7	2930	4810	1.64
3	5.2	3660	6770	1.85
4	6.7	3940	7090	1.80

[BF<sub>3</sub>OEt<sub>2</sub>] = 0.01 M, T<sub>initial</sub> = 35 °C

Figure 3.4. shows the effect of monomer concentration on the rate of polymerization. A linear relationship is observed which is characteristic of a first order dependence. The effect of the monomer concentration on  $\overline{M}_n$  and  $\overline{M}_w$  is shown in figure 3.5., it appears that the effect follows a linear relationship. This can be explained by the fact that the degree of polymerization is probably kinetically controlled, thus:

$$\begin{aligned} \overline{DP}_n &= \frac{R_p}{R_t} \\ &= \frac{k_p [P^+_n][M]}{k_t [P^+_n][OH]} \end{aligned}$$

The degree of polymerization is proportional to the monomer concentration. In addition the increase of monomer concentration has no significant effect on the polydispersity index.



**Figure 3.4.** Dependence of rate of polymerization on [OX]

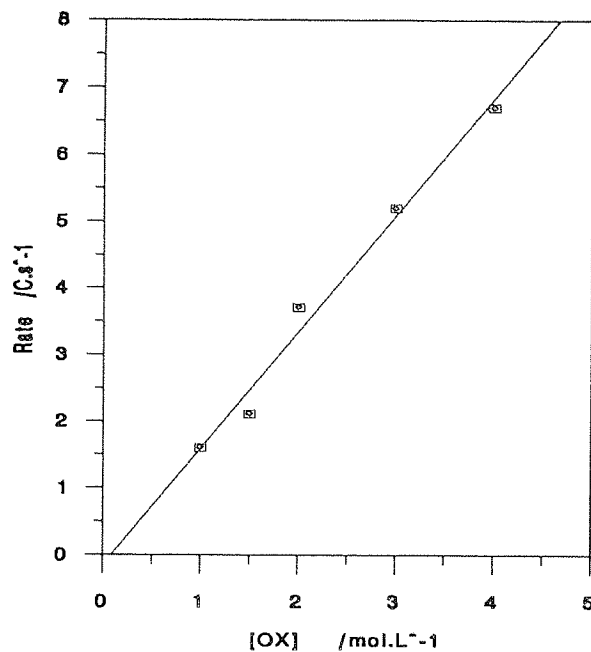
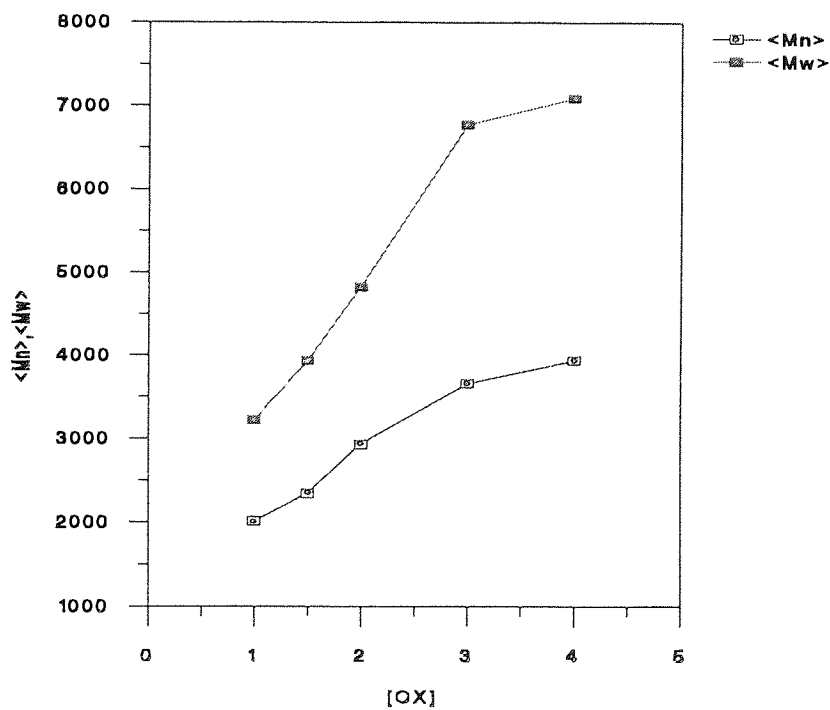


**Figure 3.5.** Dependence of  $\overline{M}_n$  and  $\overline{M}_w$  on [OX]



### 3.1.4 Effect of the concentration of catalyst on the rate of polymerization and on the average molecular weights

Using a ratio catalyst:cocatalyst ratio of 1:1, a series of experiments was carried out to study the effects of  $[\text{BF}_3\text{OEt}_2]$  on the rate of polymerization of oxetane. After the reactions, the polymers were analysed by GPC in order to measure the average molecular weights. The results are shown in table 3.3.

**Table 3.3.** Effect of  $[\text{BF}_3\text{OEt}_2]$  on  $\overline{M}_n$  and  $\overline{M}_w$  and on the rate of polymerization

$10^3 \cdot [\text{BF}_3\text{OEt}_2]$ mol.L <sup>-1</sup>	$1/[\text{BF}_3\text{OEt}_2]$ mol <sup>-1</sup> .L	Rate °C.s <sup>-1</sup>	$\overline{M}_n$ g.mol <sup>-1</sup>	$\overline{M}_w$ g.mol <sup>-1</sup>	Pd
6.4	156	0.42	4210	7310	1.74
7.6	131	0.60	3910	6920	1.77
9.4	106	0.86	3580	6350	1.77
12.1	83	0.95	3120	5680	1.82
17.6	57	1.20	2500	4050	1.62

[OX]= 1.8 M

The dependence rate of polymerization on  $[\text{BF}_3\text{OEt}_2]$  is linear as shown in figure 3.6. This would indicate that the kinetic is of first order in catalyst. The plot in figure 3.7. shows that  $\overline{M}_n$  is proportional to  $1/[\text{BF}_3\text{OEt}_2]$ .

**Figure 3.6.** Dependence of the rate on  $[\text{BF}_3\text{OEt}_2]$

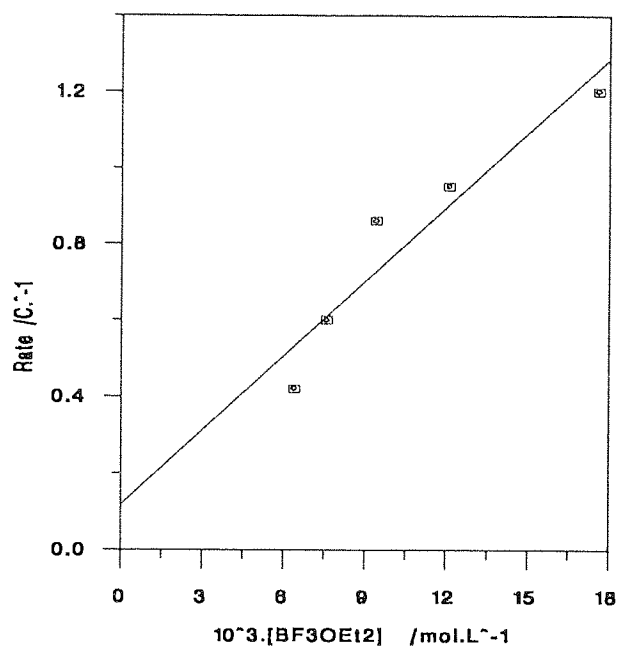
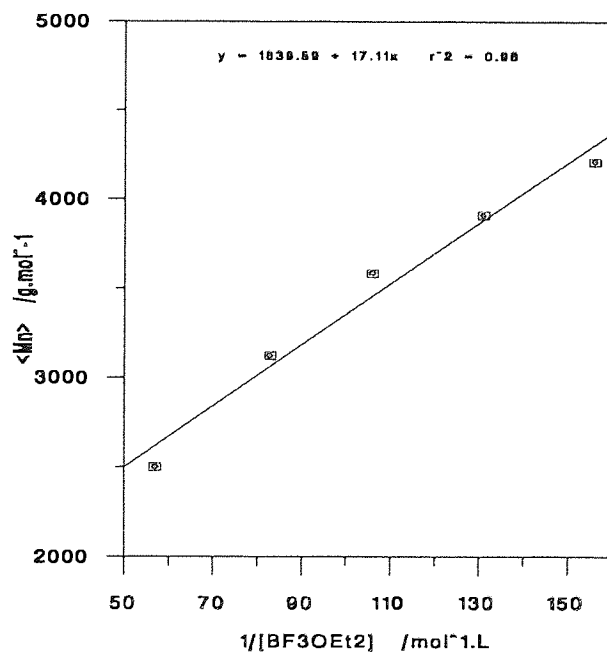


**Figure 3.7.** Dependence of  $\overline{Mn}$  on  $1/[\text{BF}_3\text{OEt}_2]$



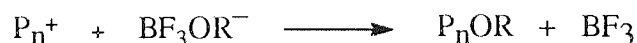
It has been shown that the rate of polymerization is dependent upon the concentrations of  $\text{BF}_3$ , OH and the monomer. Furthermore the dependence is first order with each reagent. However it should be noted that the polymerization is only possible when both  $\text{BF}_3$  and OH are present. In addition the rate of polymerization is dependent on the ratio of the concentrations of these two components, being a maximum when the ratio of their molar concentration is 1. If we consider that the initiation specie is a complex 1:1 between  $\text{BF}_3\text{OEt}_2$  and OH, we can simplify the equation:

$$R_p = k[\text{BF}_3:\text{OH}][\text{M}]$$

This give overall second order kinetics for the propagation reaction.

The dependence of the degree of polymerization on  $1/[\text{BF}_3\text{OEt}_2]$  can be explained by a kinetically controlled termination step involving the gegenion  $\text{BF}_3\text{OR}^-$ . The reaction is shown in scheme 3.1.

**Scheme 3.1. Termination involving the gegenion**



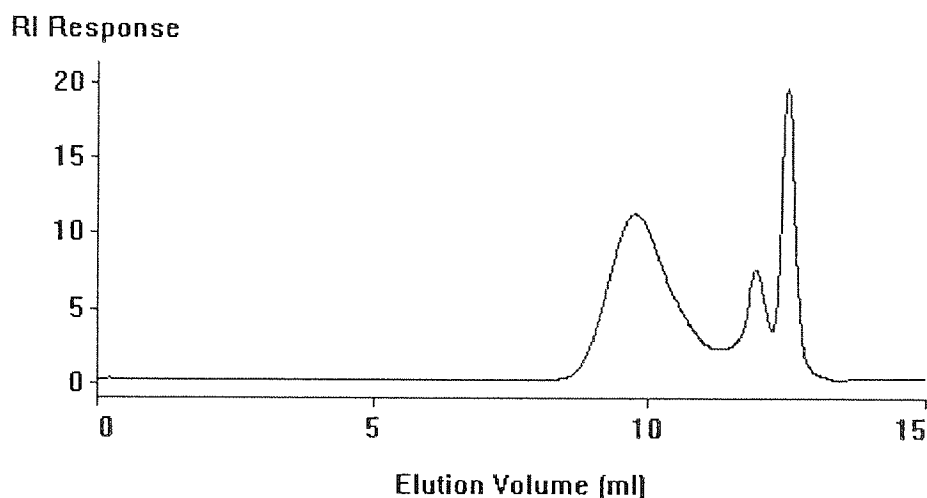
$$\begin{aligned} \overline{\text{DP}}_n &= \frac{R_p}{R_t} \\ &= \frac{k_p [\text{P}_n^+][\text{M}]}{k_t [\text{P}_n^+][\text{BF}_3\text{OR}^-]} \end{aligned}$$

**3.1.3. Molecular weight distribution (MWD) in homopolymerization of oxetane.**

It is known that the homopolymerization of oxetane leads to the formation of cyclic oligomers but particularly the cyclic tetramer (see section 1.5.1). A typical GPC chromatogram of polyoxetane with a cyclic tetramer peak is shown in figure 3.8. This oligomer is found in much higher proportions than any of the other cyclic oligomers, but studies carried out by Riat<sup>1</sup> suggested that such unusual effects are reduced when a monomer such as oxetane is copolymerized with tetrahydrofuran. The statistical copolymer formed appeared to reduce significantly the proportion of the cyclic tetramer

and it was suggested that the chain-end was in some way complexed as a crown-ether. This will be discussed in details in chapter 4.

**Figure 3.8. A typical GPC chromatogram of polyoxetane - Bimodal distribution**

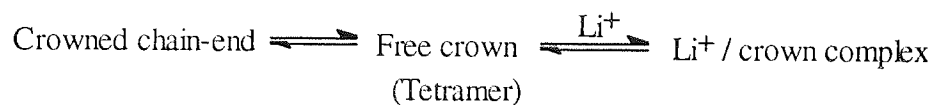


### 3.1.3.1. Effect of added salts on the MWD

Knowing the affinity of crown ether to complex small cations by template effect, the polymerization of oxetane was carried out in the presence of lithium chloride. This salt is slightly soluble in dichloromethane and it was added to the monomer solution so that the molar ratio monomer:LiCl was 100:1. Using the initiation system  $\text{BF}_3\text{OEt}_2$ :ethanediol described in section 3.1.2., the experiments were made following the usual procedure.

Figure 3.9. shows a GPC chromatogram of the polymer sample resulting from this experiment. When compared with the chromatogram from a normal polymer sample (figure 3.8), the oligomer peak corresponding to the tetramer ring has increased in intensity. It seems that the addition of lithium chloride has boosted the tetramer formation. It can be argued that in the polymerization of oxetane, the chain-end exists as a crown-ether complex in equilibrium with free crown-ether (tetramer). Addition of  $\text{Li}^+$  to the polymer displaces the equilibrium to the direction of crown formation because the free crown also complexes with the  $\text{Li}^+$  ion. Scheme 3.2 describes the equilibria between crowned chain-end, tetramer and the crown-ether/ $\text{Li}^+$  complex.

**Scheme 3.2. Equilibrium between the different forms of crown-ether**



The lithium ion is thought to complex to the polymer via the etheral oxygens. It is thought that with the homopolymer of oxetane the chains bend around to adopt a configuration in which four oxygen atoms are able to complex with the lithium ion, in a pseudo crown ether structure, then a tetramer ring can be formed as shown in figure 3.10.

**Figure 3.9. GPC chromatogram of polyoxetane with LiCl**

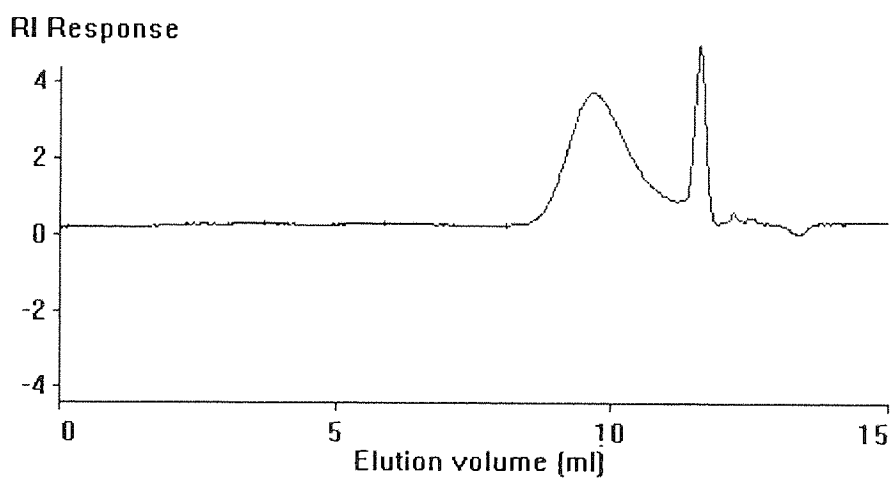
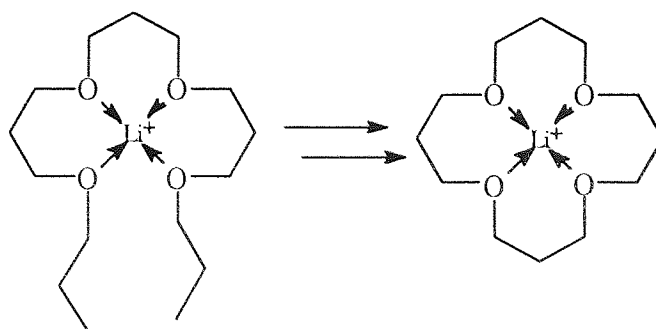


**Figure 3.10. Lithium ion complexation of the polymer chain and the tetramer**



## 3.2. Homopolymerization of 3,3-dimethyloxetane DMOX

### 3.2.1. Introduction

This section will discuss the homopolymerization of a substituted oxetane, 3,3-dimethyloxetane (DMOX). The objectives of these studies were to investigate the effects of the substitution on the kinetics of polymerization and the molecular weight distribution. The polymerization could be compared with that of oxetane and the effects of dimethyl substitution on the cyclooligomerisation process determined.

### 3.2.2. Kinetic studies

The homopolymerization of DMOX was carried out using the same reaction conditions as the oxetane study. Following the procedure described in 2.5, polymerizations were carried out using the catalyst system  $\text{BF}_3\text{OEt}_2$ /ethanediol. DMOX is a four membered ring, therefore its ring strain is equivalent to that of oxetane. The reaction associated with the ring opening is likely to be quite exothermic, so the rate of polymerization can be recorded calorimetrically. Using a catalyst:cocatalyst ratio of 1:1, several experiments were attempted changing the concentration of catalyst in the feed. The results are depicted in table 3.4.

**Table 3.4. Homopolymerization of DMOX, effect of  $[\text{BF}_3\text{OEt}_2]$  on the rate,  $\overline{M}_n$ ,  $\overline{M}_w$  and Pd**

$10^3 \cdot [\text{BF}_3\text{OEt}_2]$ mol.L <sup>-1</sup>	Rate °C.s <sup>-1</sup>	$\overline{M}_n$ g.mol <sup>-1</sup>	$\overline{M}_w$ g.mol <sup>-1</sup>	$1/[\text{BF}_3\text{OEt}_2]$ mol <sup>-1</sup> .L	Pd
7	0.30	1300	2145	143	1.65
10	0.62	2010	3660	100	1.82
13	0.85	2220	3860	77	1.74
20	1.20	3110	5220	50	1.68

[DMOX] = 2 M, T= 35 °C



**Figure 3.11. Effect of initiator concentration on the rate of polymerization**

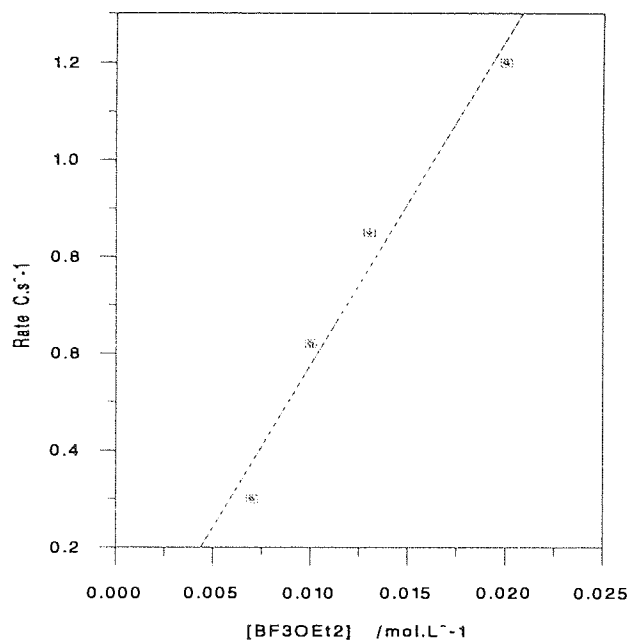


**Figure 3.12. Effect of initiator concentration on  $\overline{Mn}$ ,  $\overline{Mw}$**

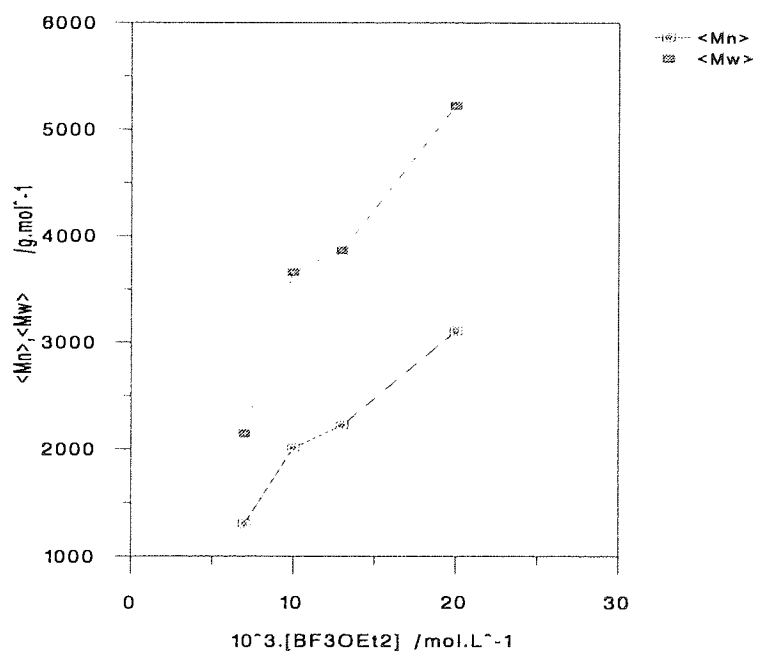


**Figure 3.13. Dependence of  $\overline{Mn}$  on  $1/[\text{BF}_3\text{OEt}_2]$**

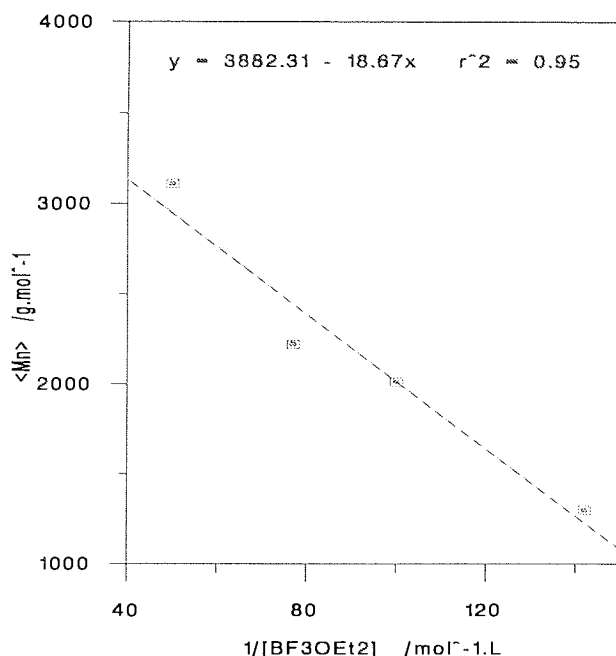


Figure 3.11. shows a linear dependence of the rate of polymerization on the catalyst concentration, this is characteristic of a first order kinetic in  $[\text{BF}_3\text{OEt}_2]$ . In comparison with oxetane it should be noticed that the calorimetrically determined rate of propagation of DMOX is slower than that of oxetane. This can be ascribed to a difference of reactivity between the two monomers. Although the ring strains are possibly close in value, it seems that the dimethyl substitution in position 3 on the oxetane ring slows the rate of propagation. Two factors can explain this. Firstly the methyl groups can create a steric hindrance for a monomer to attack the propagating end. Secondly if the growing specie has the structure of an oxonium ion, the inductive effect caused by the methyl group could attenuate the positive charge of the end group, therefore the propagation step is slowed. The difference in reactivity is discussed further in chapter 4 when copolymerization of OX and DMOX is studied.

The increase of catalyst concentration leads to an increase in number and weight average molecular weights, as shown in figure 3.12. This unusual phenomenon has to be correlated with the plot in figure 3.13 showing a linear decrease as a function of  $1/[\text{BF}_3\text{OEt}_2]$ . This result is in opposition to that obtained for the polymerization of oxetane. The increase of  $\overline{Mn}$  could be explained by the removal of active catalyst needed for the polymerization of DMOX, considering the presence of a side reaction between  $\text{BF}_3\text{OEt}_2$  and the cocatalyst. Therefore the DMOX monomer which differs from oxetane by the dimethyl substitution, does not behave in the same way during the

initiation step. It may be proposed that the dimethyl substitution creates a steric hindrance

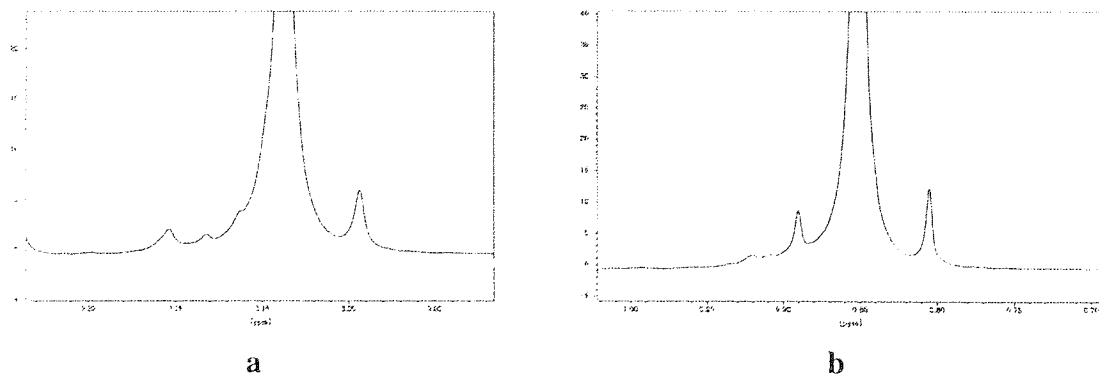
### 3.2.3. Homopolymerization of 3,3-dimethyloxetane and the formation of cyclic oligomers

Some samples of polyDMOX were analysed by  $^1\text{H}$  NMR spectroscopy. The spectrum is shown in appendix 1. Two singlets are normally expected and their assignments are as follow:

Protons	Multiplicity	$\delta$ ppm
$\begin{array}{c} \text{CH}_3 \\   \\ \text{-(O-CH}_2\text{-C-CH}_2\text{-O)-}_n \\   \\ \text{CH}_3 \end{array}$	Singlet	3.08
$\begin{array}{c} \text{CH}_3 \\   \\ \text{-(O-CH}_2\text{-C-CH}_2\text{-O)-}_n \\   \\ \text{CH}_3 \end{array}$	Singlet	0.85

Inspection of the spectrum indicates side peaks appear on both sides of each major peak, as shown in figure 3.14. This phenomenon was reproducible, appeared in all the NMR spectra of poly DMOX and even in the spectra of the copolymers made from DMOX and oxetane. We have attempted to explain in terms of structure the origin of such peaks in terms of structure.

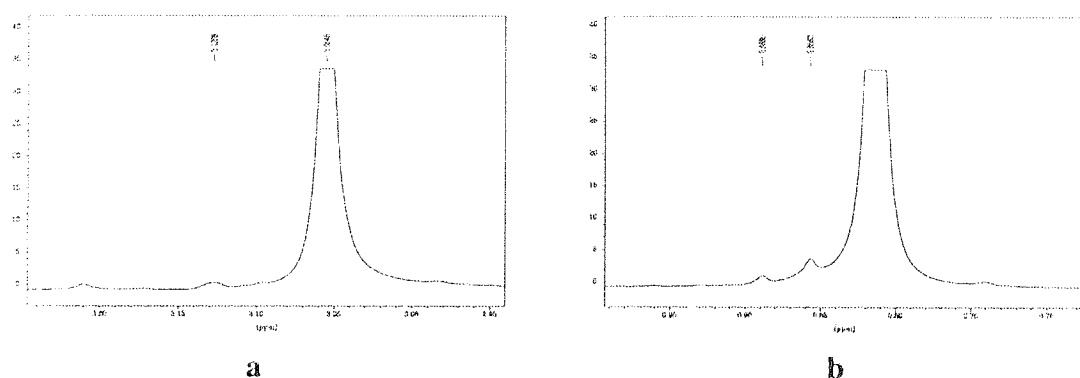
**Figure 3.14. Areas of the  $^1\text{H}$  NMR spectrum of polyDMOX showing side peaks a) O-CH<sub>2</sub>- (3.05-3.20 ppm) b) CH<sub>3</sub>- (0.8-1.1 ppm)**



COSY 2D spectrum of polyDMOX (shown in appendix 2) shows that there are no proton-proton couplings through the bonds. The major proton peaks can be surely identified as singlets assigned as shown. It seems that the unexpected smaller peaks belong to methyl or oxymethylene groups which are surrounded by different chemical environments.

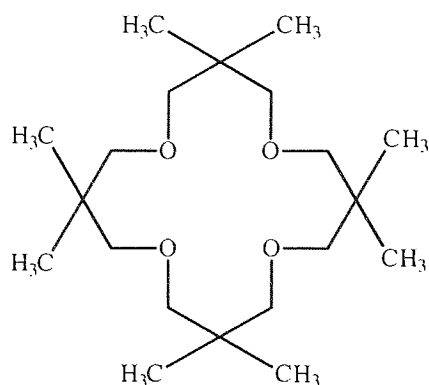
The gel permeation chromatogram shown in appendix 2 is characteristic of the polymer of 3,3-dimethyloxetane. It appears that the polymerization of 3,3-dimethyloxetane leads to the formation of cyclic oligomers. Previous work<sup>64,107</sup> has shown that the cyclic oligomers are mainly composed of tetramers. In an attempt to characterise the material giving rise to these peaks, the linear polymer was separated from the oligomers. Sufficient material of high molecular weight was separated and analysed by <sup>1</sup>H NMR. Figure 3.15. shows the modifications to the spectrum within the particular areas.

**Figure 3.15. Areas of the <sup>1</sup>H NMR spectrum of polyDMOX after separation from the oligomers a) O-CH<sub>2</sub>- (3.10-3.20 ppm) b) CH<sub>3</sub>- (0.80-1.10 ppm)**



The spectrum of the higher molecular weight linear polymer separated from the oligomer is slightly different from the one shown in figure 3.14. The small peaks at higher fields than the major signals have vanished. At the first sight, it can be concluded that the peaks in the higher field belong to the methyl and oxymethylene groups of the oligomer, possibly the tetramer ring. It is known that the chemical shifts of the protons of a cyclic structure slightly differ from those of a linear structure. Therefore the following assignments can be made for the cyclic tetramer, on the basis of their omission from the spectrum of the high molecular weight material. Concerning the low molecular weight fraction, it must be added that insufficient material was obtained to give meaningful spectrum.

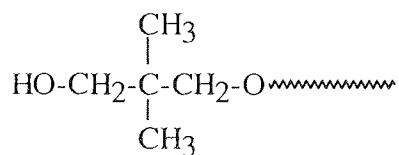
**Figure 3.16. Cyclic tetramer of DMOX**



	Multiplicity	$\delta$ ppm
- <u>C</u> H <sub>3</sub> (ring)	singlet	0.80
-O- <u>C</u> H <sub>2</sub> - (ring)	singlet	3.05

The small peaks down field remain, they seem to belong to the groups of the linear polymer. We know that one of the end groups is an hydroxyl group as shown in figure 3.17., therefore the oxymethylene and methyl groups of the DMOX unit adjacent to this OH end have different chemical shifts. The small peaks at 0.89 and 3.16 ppm, can be respectively assigned to the methyls and oxymethylene of the DMOX units adjacent to the OH end group.

**Figure 3.17. Hydroxyl end group of PolyDMOX**



### 3.3. Homopolymerization of tetrahydrofuran

#### 3.3.1. Introduction

Cationic polymerizations of THF were attempted using the initiator system ( $\text{BF}_3\text{OEt}_2/\text{ethanediol}$ ) that was used for the homopolymerization of four membered rings OX and DMOX. The experiments were unsuccessful, and no exotherm of polymerization was recorded. The inability of this initiator can be explained by the fact that THF is less basic than oxetane, therefore the initiation step involving the formation of an active site does not occur. Consequently a stronger acid is required for the polymerization of THF. Best results were provided by trifluoromethane sulfonic acid (or Triflic acid  $\text{CF}_3\text{SO}_3\text{H}$ ) diluted in dichloromethane. It is supposed that this super acid reacts by direct protonation of the ring, as described in section 1.3.2.1, and the propagation step is identical to the scheme of the homopolymerization of oxetane.

#### 3.3.2. Kinetic and GPC studies

Different amounts of a solution of triflic acid kept and syringed out into the drybox, were used to initiate tetrahydrofuran polymerization following the procedure described in section 2.5. A series of experiments were made varying the molar ratio between the catalyst and the monomer. Table 3.5. summarises the results of this study where the concentration of THF and the total volume were kept constant for all the series of experiment.

Table 3.5. Homopolymerization of THF with  $\text{CF}_3\text{SO}_3\text{H}$

Molar ratio [THF]:[ $\text{CF}_3\text{SO}_3\text{H}$ ]	[ $\text{CF}_3\text{SO}_3\text{H}$ ] $\text{mol.L}^{-1}$	Rate $^{\circ}\text{C.s}^{-1}$	$\overline{M}_n$ $\text{g.mol}^{-1}$	$\overline{M}_w$ $\text{g.mol}^{-1}$	Pd
100:1	0.020	0.40	1330	2130	1.60
200:1	0.010	0.35	1240	2140	1.73
300:1	0.007	0.20	1260	2050	1.63
400:1	0.005	0.15	980	1900	2.00

The rate of polymerization is less than  $0.5\text{ }^{\circ}\text{C}\cdot\text{s}^{-1}$ , which is indicative of a slower rate of propagation than oxetane. This can be explained by the lower ring strain of THF in comparison with that of the four membered ring. However, it seems that the amount of triflic acid used for the homopolymerization of tetrahydrofuran has little effect on the average molecular weights. The values of  $\overline{M}_n$  and  $\overline{M}_w$  stay relatively constant, and it can be argued that there is may be a termination step which occurs via transfer to the counter-anion  $\text{CF}_3\text{SO}_3^-$ .

### **3.4. Homopolymerization of oxepane**

The seven membered ring cyclic ether, oxepane, was found to be inactive towards the catalyst system  $\text{BF}_3\text{OEt}_2$ /ethanediol. Although it is known that the ring strain of oxepane is slightly greater than THF (respectively  $33\text{ kJ}\cdot\text{mol}^{-1}$  and  $23\text{ kJ}\cdot\text{mol}^{-1}$ ), this monomer does not homopolymerize. Like THF, oxepane undergoes copolymerization with oxetane, but this matter will be discussed in chapter 4.

## CHAPTER 4

# **COPOLYMERIZATIONS OF OXETANE AND OTHER CYCLIC ETHERS**

### **4.1. Copolymerization of oxetane and tetrahydrofuran (OX:THF)**

#### **4.1.1 Introduction**

A cationic initiator,  $\text{BF}_3\text{OEt}_2$  in conjunction with ethanediol as co-catalyst, has been used to copolymerize oxetane and THF. This initiation system was found to be inactive towards the homopolymerization of THF, but active towards a much more strained and basic monomer than THF. However it was of interest to understand the behaviour of four and five membered rings cyclic ethers in copolymerization.

#### **4.1.2. Procedure**

The copolymerizations were carried out at 35 °C in a sealed vessel (figure 2.6). The monomers were introduced into the vessel under a dry atmosphere together with the required volume of solvent necessary to ensure that the final volume of the system was constant. The required quantities of first cocatalyst and then catalyst solutions were injected by syringe out through a suba seal stopper. The increase of temperature associated with the ring opening polymerization was recorded using a thermocouple, connected to a Wheatstone bridge which was itself linked to a chart recorder. Rates of polymerization could be estimated from the initial slopes of the thermograms obtained and then compared with one another to gain an order of magnitude difference.

#### **4.1.3. Kinetic studies**

A series of experiments was carried out in which the ratio of the comonomers was kept constant and equal to 1 and the concentration of catalyst and cocatalyst were varied.



Table 4.1. depicts the effect of the initial concentrations of catalyst on the rate of polymerization.

**Table 4.1. Copolymerization OX:THF, initial conditions and rate observed.**

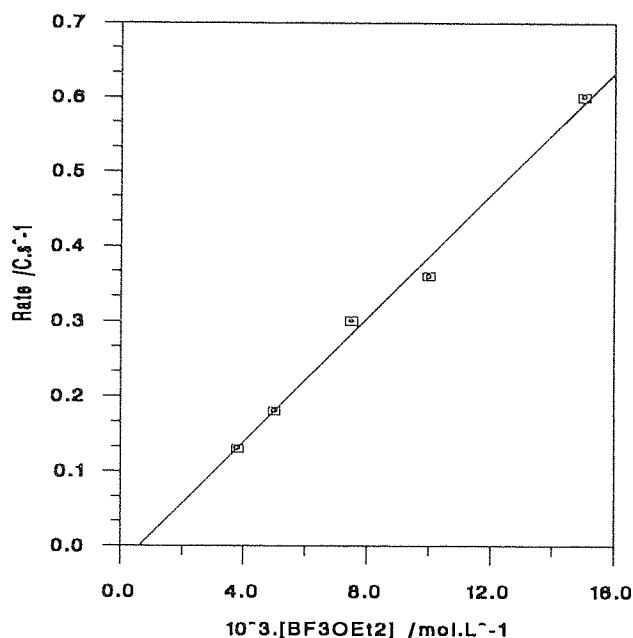
Ratio Monomer: Initiator	$10^3 \cdot [\text{BF}_3\text{OEt}_2]$ mol.L <sup>-1</sup>	Rate °C.s <sup>-1</sup>
400:1	3.8	0.13
300:1	5.0	0.18
200:1	7.5	0.30
150:1	10.0	0.36
100:1	15.0	0.60

[OX]= 1.5 M , [THF] = 1.5 M

The first observation derived from this series of experiments is that the rate observed for the copolymerization of oxetane and THF is much smaller than that recorded under similar conditions for the homopolymerization of oxetane (see section 3.1)

The effect of the catalyst concentration on the rate of polymerization at the constant concentration of monomer, observed calorimetrically, is shown in figure 4.1.

**Figure 4.1. Copolymerization Oxetane and THF**  
**Dependence of the catalyst concentration on the rate/[ox]**



The dependence of the catalyst concentration on the rate of polymerization shows a linear relationship kinetically characteristic of a simple mechanism of polymerization. This linear dependence is characteristic of a first order reaction to the catalyst.

#### 4.1.4. Molecular weight studies

After evaporation of the polymerization solvent, principally dichloromethane, polymer samples were analysed by gel permeation chromatography according to the procedure described in section 2.6.1. The molecular weight averages of the copolymers from the series are quoted against polyTHF standards and are depicted in table 4.2.

**Table 4.2. Copolymerization OX : THF, Molecular weight studies**

$10^3 \cdot [\text{BF}_3\text{OEt}_2]$ mol.L <sup>-1</sup>	$\overline{M}_n$ g.mol <sup>-1</sup>	$\overline{M}_w$ g.mol <sup>-1</sup>	$10^4/\overline{M}_n$ g <sup>-1</sup> .mol	Pd
3.8	2380	4080	4.2	1.72
5.0	2170	3560	4.6	1.64
7.5	1910	3040	5.2	1.59
10.0	1130	1970	8.8	1.74
15.0	1330	2230	7.5	1.67

[OX] = 1.5 M , [THF] = 1.5 M

In order to get more information concerning a mechanism of copolymerization, different graphs can be plotted. Figure 4.2. shows the dependence of the number average molecular weight on the catalyst concentration, and Figure 4.3. depicts the dependence of  $1/\overline{M}_n$  on the catalyst concentration.

**Figure 4.2. Copolymerization OX:THF, Dependence of  $\overline{M}_n$  on  $[\text{BF}_3\text{OEt}_2]$**

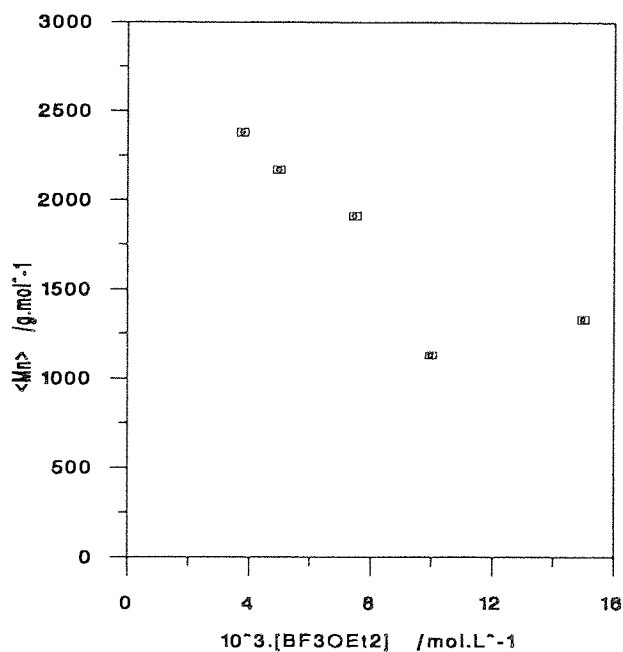
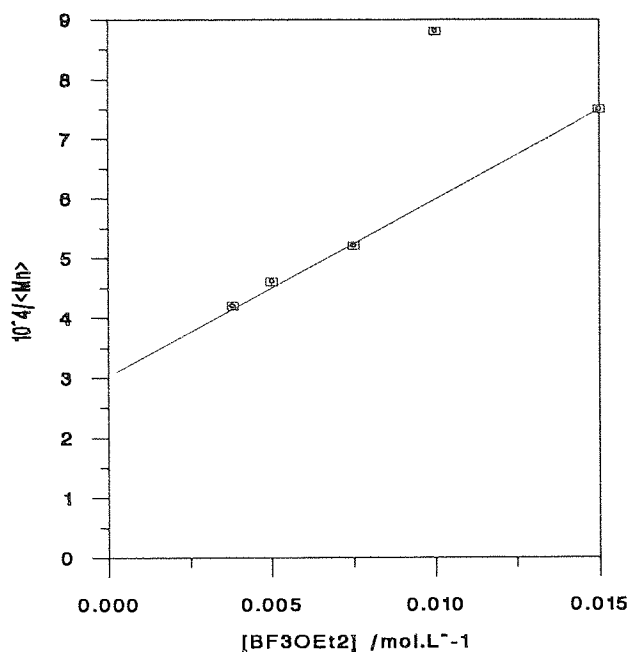


**Figure 4.3** Dependence of  $10^4/\overline{M}_n$  on  $[\text{BF}_3\text{OEt}_2]$



The above figures show that, the averages molecular weights  $\overline{M}_n$  and  $\overline{M}_w$  seem to be dependent from the catalyst concentration needed to initiate the copolymerization reaction. A slight decrease is observed. The explanation of the decrease of the average molecular weights is probably due to the termination step involving the catalyst. This can be related to the results obtained in section 3.1.4. for the homopolymerization of oxetane, wherein the degree of polymerization was controlled by termination with the gegenion. Figure 4.3 shows a linear relationship between  $1/\overline{M}_n$  and  $[\text{BF}_3\text{OEt}_2]$ , if one point is not taken in consideration.

Therefore :

$$\frac{1}{\overline{DP}_n} = a.[BF_3OEt_2] + b$$

$$\overline{DP}_n = \frac{R_p}{R_{t_1} + R_{t_2}}$$

$$= \frac{k_p[P^+_n][M]}{k_{t_1}[P^+_n][BF_3OEt_2] + b'}$$

The presence of the term b shows that another type of termination has to be considered. The chain growth does not only terminate by a transfer to the gegenion but also to other species existing in the medium, possibly monomer.

The evolution of the polydispersity index as a function of the catalyst concentration is stable. The values are stable and around 1.6-1.7 and we can conclude that the polydispersity index is independent from the ratio Monomer : Initiator.

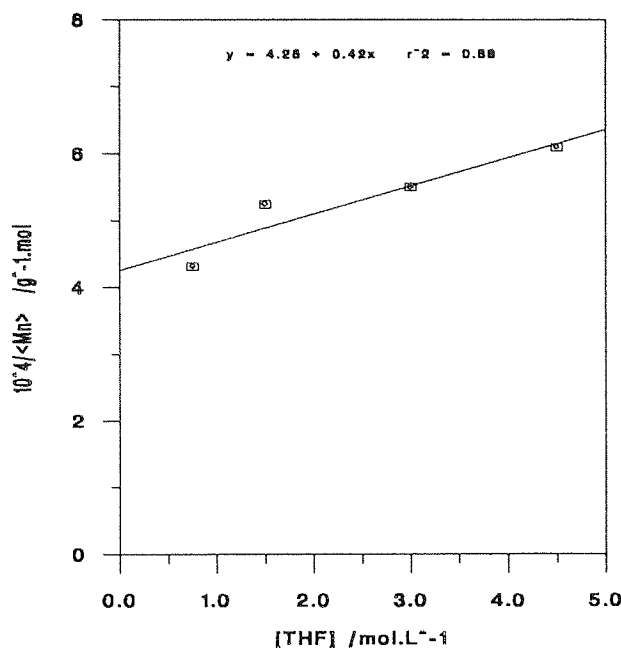
In another series of experiments, the molar ratio oxetane:catalyst was kept constant and the molar ratio OX:THF was changed. The effect of this change on the average molecular weights is shown in table 4.3.

**Table 4.3** Copolymerization OX:THF, Dependence of  $\overline{M}_n$  and  $\overline{M}_w$ , Pd on the OX:THF ratio

[THF] mol.L <sup>-1</sup>	$\overline{M}_n$ g.mol <sup>-1</sup>	$10^4/\overline{M}_n$ mol.g <sup>-1</sup>	Pd	Rate °C.s <sup>-1</sup>
0.75	2320	4.31	1.72	1.10
1.50	1910	5.23	1.59	0.30
3.00	1820	5.49	1.62	0.20
5.40	1640	6.09	1.65	0.04

[OX]= 1.5 M , [BF<sub>3</sub>OEt<sub>2</sub>]= 0.0075 M , T= 35 °C

**Figure 4.4. Dependence of  $10^4/\overline{Mn}$  on [THF]**



The table shows that increasing the concentration of THF in the feed decreased the number average molecular weight, the polydispersity index staying relatively constant. In addition the rate of polymerization recorded calorimetrically decreased with increasing THF concentration, but it must be noted that the rate recorded is an overall rate of polymerization and in this type of copolymerization the heat associated with the ring opening is probably coming in a great part from the polymerization of oxetane. Such data cannot be treated quantitatively.

Figure 4.4 shows a linear dependence between  $1/\overline{Mn}$  and the concentration of THF.

Thus

$$\frac{1}{\overline{DP}_n} = a.[\text{THF}] + b$$

In this case the degree of polymerization is

$$\begin{aligned} \overline{DP}_n &= \frac{R_p}{\sum R_t} \\ &= \frac{k_p[P^+_n][M]}{k_{t1}[P^+_n][\text{BF}_3\text{OEt}_2] + k_{t2}[P^+_n][\text{THF}]} \end{aligned}$$

Therefore it can be proposed that the other termination is likely to involve the monomer THF and possibly also oxetane.

#### 4.1.5. Copolymer composition study

The composition of the copolymer made from the reaction of oxetane and THF, was determined by  $^{13}\text{C}$  and  $^1\text{H}$  NMR spectroscopy in  $\text{CDCl}_3$ . The NMR spectra are shown in appendix 1. The signals used for this determination are detailed as follows:

##### $^{13}\text{C}$ NMR ( $\text{CDCl}_3$ ) assignments

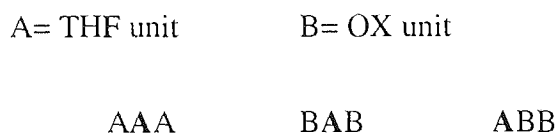
Polyoxetane:	$\delta$ ppm
$-(\text{-O-}\underline{\text{C}}\text{H}_2\text{-CH}_2\text{-}\underline{\text{C}}\text{H}_2\text{-O-})_n$	67.9
$-(\text{-O-CH}_2\text{-}\underline{\text{C}}\text{H}_2\text{-CH}_2\text{-O-})_n$	29.8
PolyTHF:	
$-(\text{-O-}\underline{\text{C}}\text{H}_2\text{-CH}_2\text{-CH}_2\text{-}\underline{\text{C}}\text{H}_2\text{-O-})_n$	70.9
$-(\text{-O-CH}_2\text{-}\underline{\text{C}}\text{H}_2\text{-}\underline{\text{C}}\text{H}_2\text{-CH}_2\text{-O-})_n$	26.4

##### $^1\text{H}$ NMR ( $\text{CDCl}_3$ ) assignments

Polyoxetane:	Multiplicity	$\delta$ ppm
$-(\text{-O-}\underline{\text{C}}\text{H}_2\text{-CH}_2\text{-}\underline{\text{C}}\text{H}_2\text{-O-})_n$	Triplet	3.42
$-(\text{-O-CH}_2\text{-}\underline{\text{C}}\text{H}_2\text{-CH}_2\text{-O-})_n$	Quintuplet	1.77
PolyTHF:		
$-(\text{-O-}\underline{\text{C}}\text{H}_2\text{-CH}_2\text{-CH}_2\text{-}\underline{\text{C}}\text{H}_2\text{-O-})_n$	Triplet	3.34
$-(\text{-O-CH}_2\text{-}\underline{\text{C}}\text{H}_2\text{-}\underline{\text{C}}\text{H}_2\text{-CH}_2\text{-O-})_n$	Quintuplet	1.57

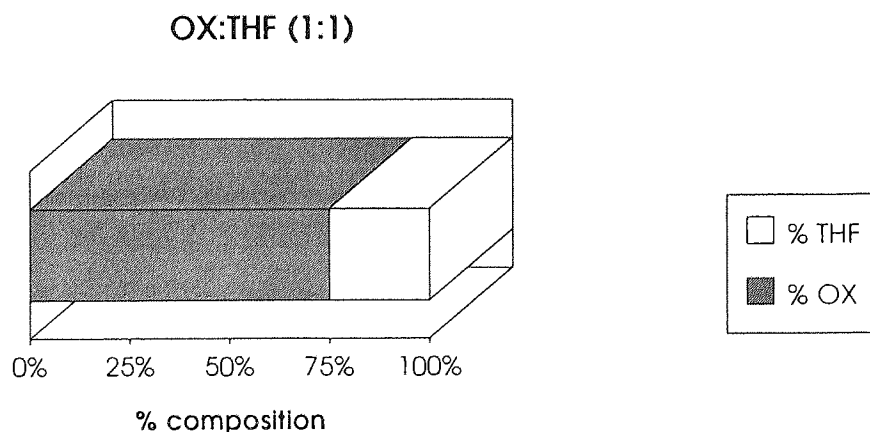
The  $^{13}\text{C}$  study shows that the signals belonging to the carbon of the oxymethylene group ( $-\text{OCH}_2$ ) of both oxetane and THF units are in fact divided into three singlets. This observation leads to the idea of a statistical distribution of THF units in the copolymer chain.

Therefore at the first sight, considering only the first neighbouring groups, three different positions in the copolymer chain are possible for a THF unit:



The areas of the  $^1\text{H}$  NMR signals can be used to determine the percentage of THF and oxetane units in the copolymer. Although the feed molar ratio of the monomers was 1:1, it was found that the proportion of THF units did not exceed 25 %. (Figure 4.5.)

**Figure 4.5. Copolymerization OX:THF (feed ratio 1:1), Percentage of the monomers units in the copolymer.**





## 4.2. Copolymerization of oxetane and oxepane (OX:OXP)

### 4.2.1. Introduction

Oxepane is a seven membered ring cyclic ether, its ring strain is greater than THF, but much smaller than oxetane. Using the catalyst system  $\text{BF}_3\text{OEt}_2$ /ethanediol, it was found that this monomer does not homopolymerize (see section 3.3). Its behaviour in a copolymerization with oxetane was studied and compared with that for THF.

### 4.2.2. Kinetic study

The procedure described in section 4.1.2. was carried out for the copolymerization of oxetane and oxepane. Different experiments were made varying the molar ratio monomers to catalyst. The increase of temperature associated with the reaction was recorded. Table 4.4. summarises this study.

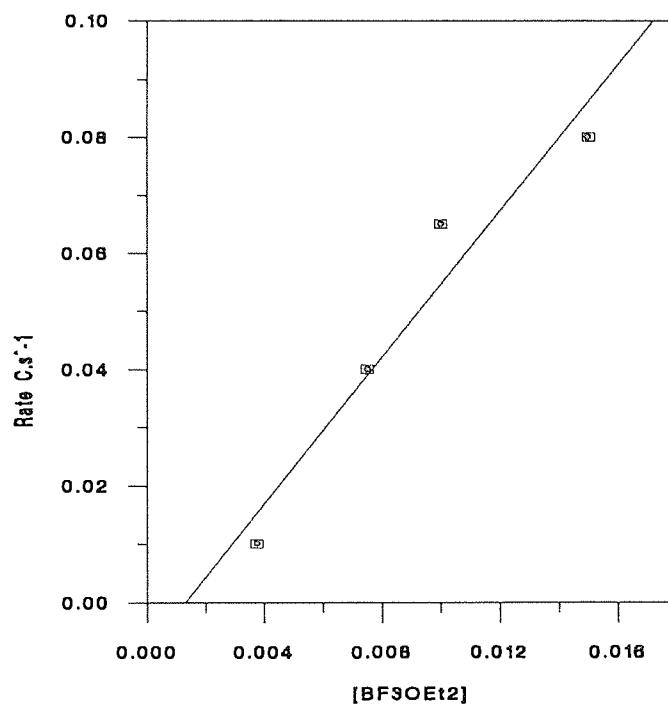
**Table 4.4. Copolymerization OX:OXP, Initial conditions and rate observed**

<b>Ratio Monomer:Initiator</b>	<b><math>10^3 \cdot [\text{BF}_3\text{OEt}_2]</math> mol.L<sup>-1</sup></b>	<b>Rate °C.s<sup>-1</sup></b>
400:1	3.8	0.01
200:1	7.5	0.04
150:1	10.0	0.06
100:1	15.0	0.08

$$[\text{OX}] = 1.5 \text{ M}, [\text{OXP}] = 1.5 \text{ M}$$

The effect of the catalyst concentration on the rate of polymerization is plotted in Figure 4.6. It shows a linear dependence characteristic of a first order on the catalyst concentration. The same observation was observed previously for the copolymerization of oxetane and THF.

**Figure 4.6. Copolymerization OX:OXp, Dependence of the Rate on [BF<sub>3</sub>OEt<sub>2</sub>]**



#### 4.2.3. Molecular weight studies

The results of the GPC analysis ran for each copolymer samples are presented in table 4.5 and graphically in figure 4.7

**Table 4.5 Copolymerization OX:OXp, Molecular weight studies**

Ratio [M]:[I]	10 <sup>3</sup> . [BF <sub>3</sub> OEt <sub>2</sub> ] mol.L <sup>-1</sup>	$\overline{M}_n$ g.mol <sup>-1</sup>	$\overline{M}_w$ g.mol <sup>-1</sup>	Pd
400:1	3.8	520	1160	2.23
200:1	7.5	700	1150	1.64
150:1	10.0	640	1080	1.68
100:1	15.0	750	1250	1.66

[OX]= 1.5 M , [OXp]= 1.5 M , T= 35 °C

**Figure 4.7. Copolymerization OX:OXE, Dependence of  $\overline{Mn}$  and  $\overline{Mw}$  on  $[\text{BF}_3\text{OEt}_2]$**

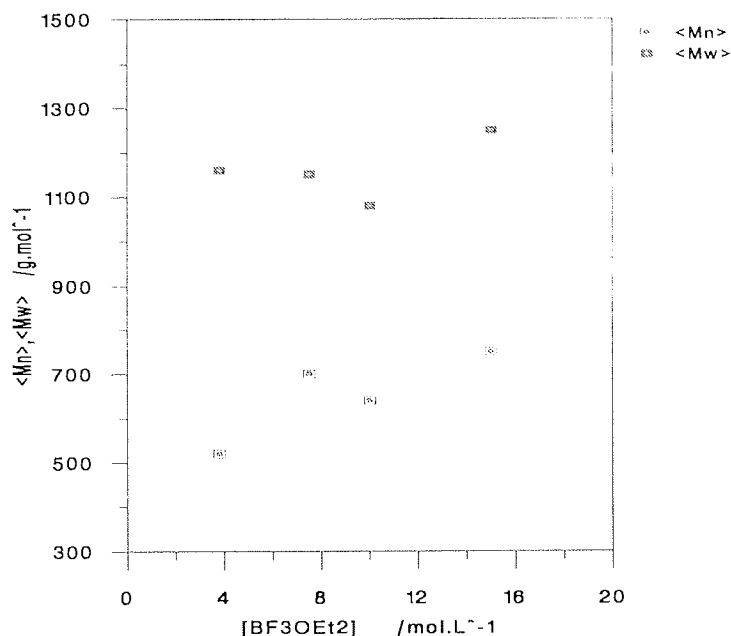


Figure 4.7 shows that the relationship between  $\overline{Mn}$ ,  $\overline{Mw}$  and the ratio monomer:initiator is fairly independent. The same conclusion can be drawn for the polydispersity index which stays constant except for one sample showing a broad molecular weight distribution.

In this case, it can be drawn that termination involving the gegenion is not likely to occur in the same way as it does for the copolymerization between oxetane and THF. Therefore the degree of polymerization is probably not subject to a control involving this type of termination.

The effect of the variation of the feed molar ratio oxetane : oxepane was studied carrying out the same procedure as the study made for the copolymerization oxetane and THF. It is depicted in table 4.6. The ratio [OX]:[Initiator] was kept constant and equal to 200:1.

**Table 4.6. Copolymerization OX:OXP, Dependence of  $\overline{M}_n$  and  $\overline{M}_w$ , Pd on the concentration of OXP**

[OXp] mol.L <sup>-1</sup>	$\overline{M}_n$ g.mol <sup>-1</sup>	$1/\overline{M}_n$ g <sup>-1</sup> .mol	Pd	Rate °C.s <sup>-1</sup>
0.75	1310	7.63	1.65	0.70
1.50	700	14.28	1.63	0.04
3.00	530	18.87	1.72	0.03

[OX]= 1.5 M , [BF<sub>3</sub>OEt<sub>2</sub>]= 0.075 M , T= 35 °C

The average molecular weights decrease when increasing the concentration of oxepane in the feed. This can be correlated quantitatively to the decrease of the rate of polymerization recorded calorimetrically. An explanation is the difference of reactivity of the two monomers in the different steps of polymerization. Subsequent analysis of the copolymers (section 4.2.4.) showed that the copolymerization was heavily weighted in favour of oxetane, therefore the heat associated with the ring opening is possibly caused by the polymerization of oxetane. The dependence of  $1/\overline{M}_n$  on the concentration of oxepane is shown in figure 4.8, a linear relationship can be exhibited. Therefore like in the case OX:THF, the degree of polymerization is likely to be kinetically controlled by a termination by transfer to oxepane.

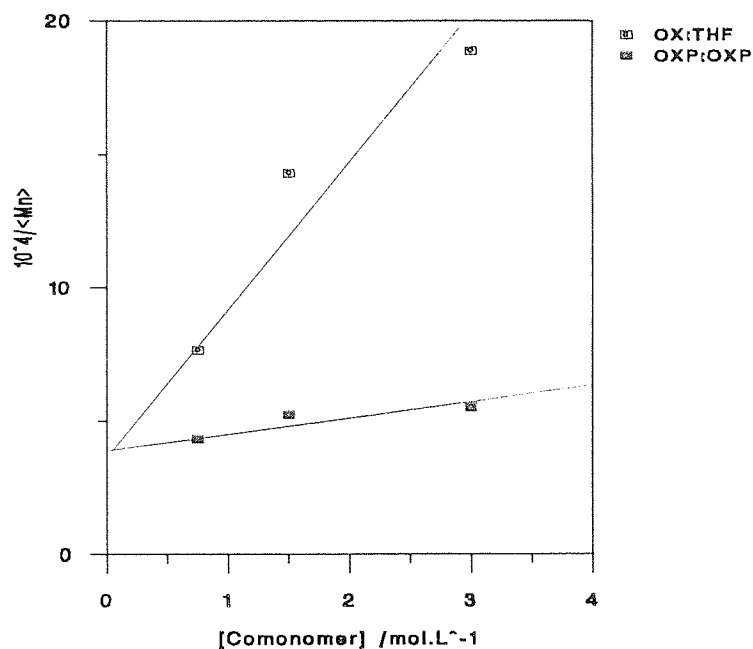
$$\frac{1}{\overline{DP}_n} = a.[\text{OXp}]$$

$$\overline{DP}_n = \frac{R_p}{R_t}$$

$$= \frac{k_p [P^+_n][M]}{k_t [P^+_n][\text{OXp}]}$$

The plot of  $1/\overline{M}_n$  against concentration of THF is also shown in figure 4.8 for comparative purposes. The contributions of each type of reaction to the overall termination differ markedly.

**Figure 4.8** Dependence of  $10^4/\overline{M}_n$  on [OXP] and [THF]



#### 4.2.4. Copolymer composition

The samples were analysed by  $^{13}\text{C}$  and  $^1\text{H}$  NMR spectroscopy, the spectra are shown in appendix 1. The signals used for the determination are listed below.

##### $^{13}\text{C}$ NMR assignments

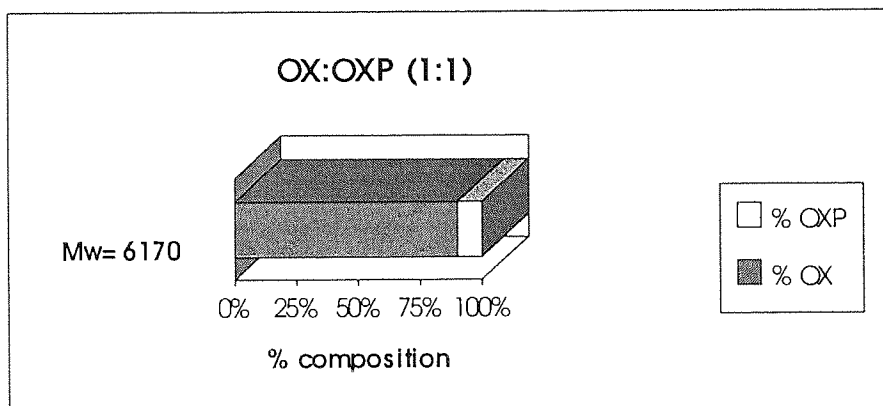
Polyoxepane:	$\delta$ ppm
$-(\text{-O-}\underline{\text{C}}\text{H}_2\text{-CH}_2\text{-CH}_2\text{-CH}_2\text{-CH}_2\text{-}\underline{\text{C}}\text{H}_2\text{-O-})_n$	71.4
$-(\text{-O-CH}_2\text{-}\underline{\text{C}}\text{H}_2\text{-CH}_2\text{-CH}_2\text{-CH}_2\text{-}\underline{\text{C}}\text{H}_2\text{-CH}_2\text{-O-})_n$	29.6
$-(\text{-O-CH}_2\text{-CH}_2\text{-}\underline{\text{C}}\text{H}_2\text{-}\underline{\text{C}}\text{H}_2\text{-CH}_2\text{-CH}_2\text{-O-})_n$	26.1

##### $^1\text{H}$ NMR assignments

Polyoxepane:	Multiplicity	$\delta$ ppm
$-(\text{-O-}\underline{\text{C}}\text{H}_2\text{-CH}_2\text{-CH}_2\text{-CH}_2\text{-CH}_2\text{-}\underline{\text{C}}\text{H}_2\text{-O-})_n$	Triplet	3.67
$-(\text{-O-CH}_2\text{-}\underline{\text{C}}\text{H}_2\text{-CH}_2\text{-CH}_2\text{-CH}_2\text{-}\underline{\text{C}}\text{H}_2\text{-CH}_2\text{-O-})_n$	Multiplet	1.82
$-(\text{-O-CH}_2\text{-CH}_2\text{-}\underline{\text{C}}\text{H}_2\text{-}\underline{\text{C}}\text{H}_2\text{-CH}_2\text{-CH}_2\text{-O-})_n$	Multiplet	1.35

The areas of the  $^1\text{H}$  NMR signals were used to determine the ratio oxetane : oxepane within the copolymer. The highest percentage of oxepane units in the copolymer chain did not exceed 10% (Figure 4.9).

**Figure 4.9. Copolymerization OX:OXP (feed ratio 1:1), Percentage of the monomers units in the copolymer.**



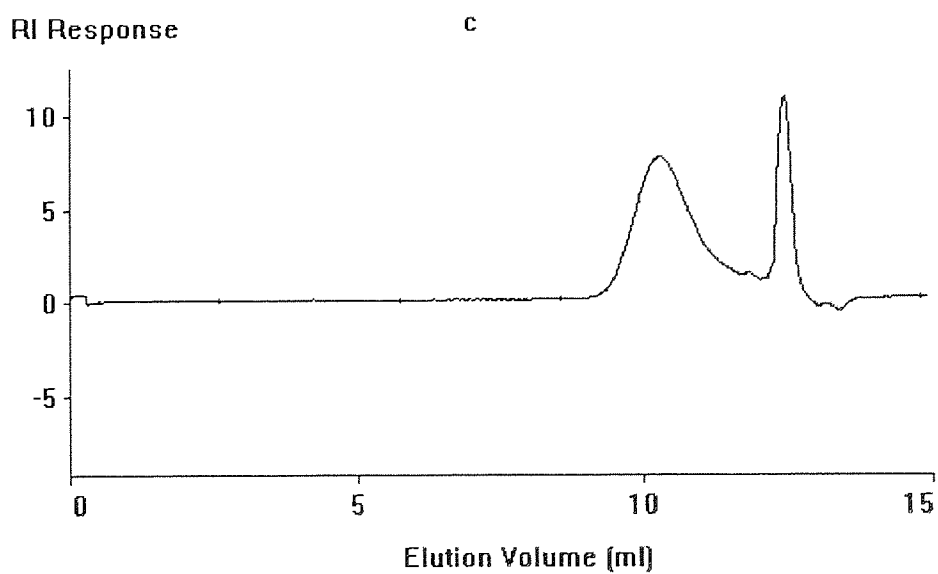
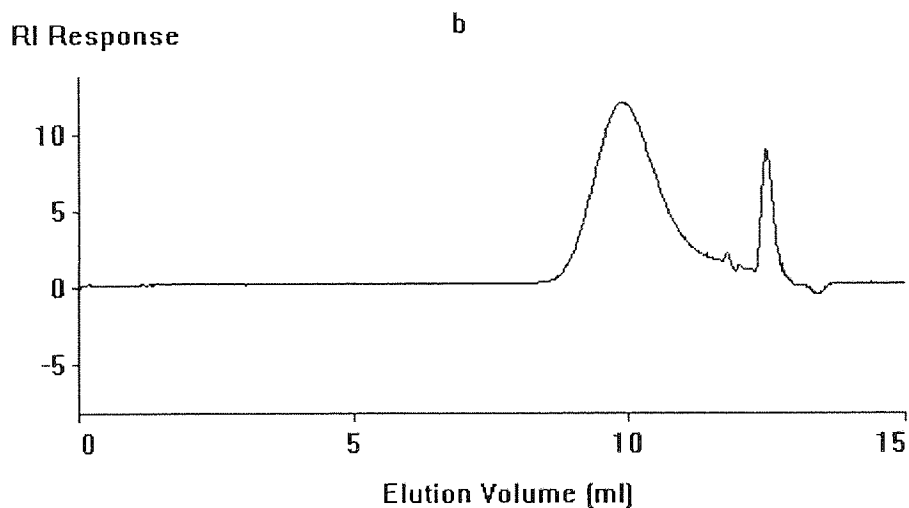
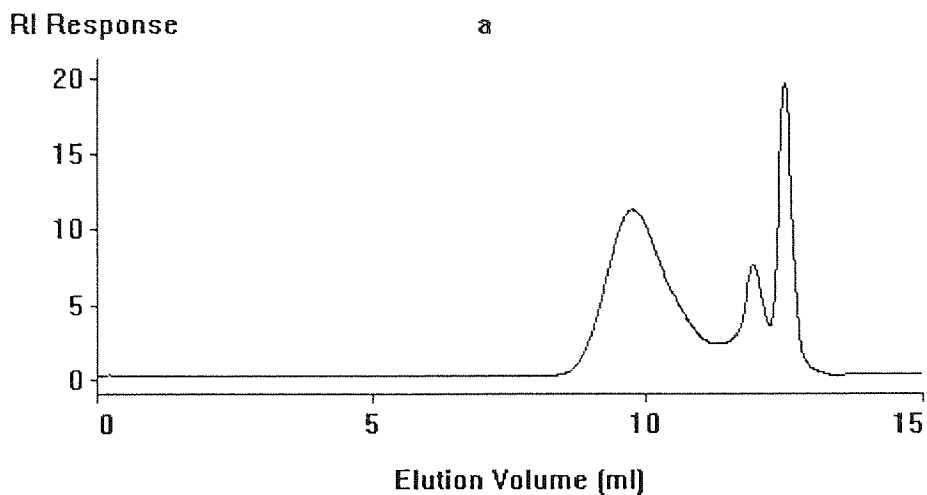
### 4.3. Copolymerizations and cyclooligomerization.

Figure 4.10. shows typical GPC Chromatograms of the products of

- the homopolymerization of oxetane
- the copolymerization of oxetane  $M_1$  and tetrahydrofuran  $M_2$  ( $M_1:M_2 = 1:1$ )
- the copolymerization of oxetane  $M_1$  and oxepane  $M_2$  ( $M_1:M_2 = 1:1$ ).

In all polymerizations the concentration the concentration of oxetane was  $1.5 \text{ mol.dm}^{-3}$  and the molar ratio oxetane : catalyst : cocatalyst was 200:1:1. All polymerizations were carried out with an initial temperature of  $35 \text{ }^\circ\text{C}$ . The different data and characteristics collected are shown in table 4.7. for comparison.

**Figure 4.10. Typical GPC chromatograms of a) polyoxetane b) copolymer oxetane and thf c) copolymer oxetane and oxepane.**



**Table 4.7. Comparison of homopolymerization and copolymerization characteristics**

Monomer	GPC	$\overline{M_w}$ g.mol <sup>-1</sup>	Pd	Rate C.s <sup>-1</sup>	MWD	% Composition
OX	a	5220	1.5	2.11	bimodal	100/0
OX : THF	b	3040	1.6	0.30	unimodal	74/26
OX : OXP	c	1150	1.6	0.04	unimodal	90/10

The polydispersities of the polymers are virtually constant around 1.6-1.7, which is indicative of a simple mechanism being applicable to each polymerization. These data were determined using only the high molecular weight region of the chromatogram.

Incorporation of tetrahydrofuran and oxepane into the polymerization system has led to a significant decrease in the molecular weight of the polymer produced. This decrease in molecular weight is accompanied by a decrease in the rate of polymerization, as observed calorimetrically. A problem associated with the use of calorimetry for the measurement of the rate of polymerization is that the heat of polymerization of one mol. of oxetane is greater than that of one mol. of THF or oxepane. As a result such measurements may only effectively record the rate of incorporation of oxetane into the copolymer and not the overall rate of monomer consumption. The initial rates of polymerization determined from the calorimeter traces are shown in table 4.7.

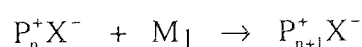
If a kinetic chain mechanism applies to this type of polymerization then it would be reasonable to suppose that :

$$\overline{DP}_n = \frac{R_p}{\sum R_t}$$

Where  $\overline{DP}_n$  is the degree of polymerization,  $R_p$  is the rate of propagation and  $R_t$  the rate of termination steps.

Consequently it can be argued that the decrease in molecular weight observed in such systems is in part associated with the overall decrease in propagation rate.

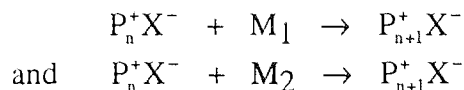
The propagation reaction may be proposed simply as:



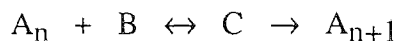
for the homopolymerization of oxetane.



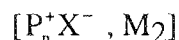
In the case of copolymerization of oxetane  $M_1$  with other monomers  $M_2$  one should postulate at least two types of propagation reaction.



The propagation step can be simplified as followed:



where  $A_n$  is the growing polymer chain, B is the comonomer molecule and C is an intermediate species which could have the following structure:



The stability of the intermediate C is of importance because it determines not only the rate of the propagation step but also the rate of termination

In the copolymerization of oxetane and oxepane it can be argued that the intermediate is more stable than its oxetane equivalent involved in the copolymerization between oxetane and tetrahydrofuran. This possible interpretation could explain the difference between the rates recorded calorimetrically.

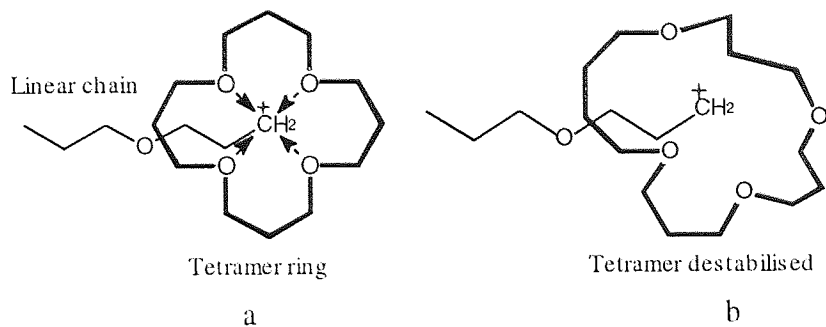
The shapes of the chromatograms a, b, and c indicates differences in the molecular weight distributions. In the homopolymerization of oxetane, cyclic oligomers were found in a quite large quantity. Their presence was not found in such amounts in the copolymer samples, and the MWD can be considered as unimodal.

Considering the homopolymerization of oxetane, a possible explanation of this phenomenon can be due to the incorporation of a tetramer ring at the end of the growing chain. (see figure 4.11a.)

Hence the positive charge of the cation is stabilised by the presence of the oxygen atoms arranged as in a crown ether. Therefore the "back-biting" reaction which produces the cyclic oligomers is aided.

During the copolymerization of oxetane and THF or oxepane, the relative absence of the oligomer peak can be explained by the incorporation of the comonomer into the polymer back-bone which disrupts the regularity of the polymer chain and also the structure of the propagating end (see figure 4.11b.). The positive charge is destabilised and the cyclooligomerization occurs with difficulty.

**Figure 4.11. Possible structure of the propagating end in a) homopolymerization of OX and b) copolymerization OX:THF**



#### 4.4. Copolymerization of oxetane and 3,3-dimethyloxetane. (OX:DMOX)

It was interesting to study the copolymerization between the two four membered rings, oxetane and its disubstituted equivalent, 3,3-dimethyloxetane. It is well known that their homopolymerizations lead to the formation of cyclic oligomers notably a significant amount of cyclic tetramers. Comparisons of the reactivities of the monomers can be made on basis of the absolute rate constants of polymerization. It was found that oxetane polymerises more rapidly than 3,3-dimethyloxetane using the initiator system  $\text{BF}_3\text{OEt}_2$ /ethanediol. However, for a better understanding of the factors influencing these "reactivities", rate constants of homopolymerization are not very useful because two factors are changed simultaneously: the growing species and the monomers (See section 3.2.2).

Following the copolymerization procedure described in section 4.2 for the system OX:THF, different experiments were made varying the monomers molar ratio OX:DMOX, but keeping constant the ratio OX:Catalyst (200:1). The polymers were analysed by GPC, the composition was determined by  $^1\text{H}$  and  $^{13}\text{C}$  NMR spectroscopy. The spectra of the three corresponding experiments are shown in appendix 1.

##### $^1\text{H}$ NMR ( $\text{CDCl}_3$ ) assignments:

	Multiplicity	$\delta$ ppm
Polyoxetane :		
$-(\text{-O-}\underline{\text{CH}}_2\text{-CH}_2\text{-}\underline{\text{CH}}_2\text{-O-})_n\text{-}$	Triplet	3.42
$-(\text{-O-CH}_2\text{-}\underline{\text{CH}}_2\text{-CH}_2\text{-O-})_n\text{-}$	Quintuplet	1.77
PolyDMOX :		
$\begin{array}{c} \text{CH}_3 \\   \\ -(\text{-O-CH}_2\text{-C-CH}_2\text{-O-})_n\text{-} \\   \\ \text{CH}_3 \end{array}$	Singlet	3.13
$\begin{array}{c} \text{CH}_3 \\   \\ -(\text{-O-CH}_2\text{-C-CH}_2\text{-O-})_n\text{-} \\   \\ \text{CH}_3 \end{array}$	Singlet	0.85

**$^{13}\text{C}$  NMR ( $\text{CDCl}_3$ ) assignments:**

	$\delta$ ppm
Polyoxetane :	
-(-O- <u>C</u> H <sub>2</sub> -CH <sub>2</sub> - <u>C</u> H <sub>2</sub> -O-) <sub>n</sub>	67.9
-(-O-CH <sub>2</sub> - <u>C</u> H <sub>2</sub> -CH <sub>2</sub> -O-) <sub>n</sub>	30.2
PolyDMOX :	
$\begin{array}{c} \text{CH}_3 \\   \\ \text{-(O-CH}_2\text{-C-CH}_2\text{-O-)}_n\text{-} \\   \\ \text{CH}_3 \end{array}$	77.5
$\begin{array}{c} \text{CH}_3 \\   \\ \text{-(O-CH}_2\text{-C-CH}_2\text{-O-)}_n\text{-} \\   \\ \text{CH}_3 \end{array}$	36.6
$\begin{array}{c} \text{CH}_3 \\   \\ \text{-(O-CH}_2\text{-C-CH}_2\text{-O-)}_n\text{-} \\   \\ \text{CH}_3 \end{array}$	22.3

**Table 4.8. Copolymerization OX:DMOX, Effect of the feed molar ratio on the average molecular weights and on the copolymer composition.**

Monomer Ratio OX:DMOX	[OX] mol.L <sup>-1</sup> (feed)	$\overline{M}_n$ g.mol <sup>-1</sup>	$\overline{M}_w$ g.mol <sup>-1</sup>	Pd	Composition %OX - %DMOX
1:1	1.5	3260	5740	1.76	33 - 67
2:1	3.0	4040	8080	2.00	57 - 43
3:1	4.5	6310	11810	1.87	76 - 24

[DMOX]= 1.5 M , T= 35 °C

Table 4.8 shows that the increase of the concentration of OX leads to an increase of molecular weight as expected. The  $^{13}\text{C}$  NMR spectra show a statistical distribution of the DMOX units in the chain. Three types of peaks are distinctly observed for the carbons corresponding to the DMOX units. The chemical shifts of the oxymethylene

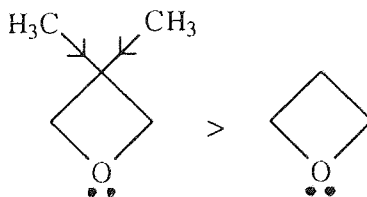
carbon and the quaternary carbon show the existence of different triads characterised by different chemical environments.

	A= DMOX unit	B= OX unit	
AAA	-O-CH <sub>2</sub> -C(CH <sub>3</sub> ) <sub>2</sub> -CH <sub>2</sub> -O		77.2 ppm
	-O-CH <sub>2</sub> -C(CH <sub>3</sub> ) <sub>2</sub> -CH <sub>2</sub> -O		36.7 ppm
AAB	-O-CH <sub>2</sub> -C(CH <sub>3</sub> ) <sub>2</sub> -CH <sub>2</sub> -O		77.1 ppm
	-O-CH <sub>2</sub> -C(CH <sub>3</sub> ) <sub>2</sub> -CH <sub>2</sub> -O		36.6 ppm
BAB	-O-CH <sub>2</sub> -C(CH <sub>3</sub> ) <sub>2</sub> -CH <sub>2</sub> -O		76.9 ppm
	-O-CH <sub>2</sub> -C(CH <sub>3</sub> ) <sub>2</sub> -CH <sub>2</sub> -O		36.4 ppm

Considering the first experiment (feed ratio 1:1) the composition of the polymer shows an unexpected result that the incorporation of DMOX in the copolymer is greater than that of oxetane although the rate of polymerization of DMOX in homopolymerization is lower than oxetane. This can be explained as follows.

Because of the inductive effect created by the substitution of the methyl group in position 3 on the ring, the nucleophilicity of DMOX is greater than OX.

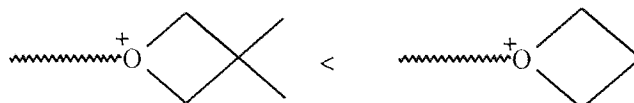
Nucleophilicity:



The ring strains of the two molecules are in theory similar (both four membered rings), but the steric hindrance created by the dimethyl substitution probably lowers slightly the ease of ring opening. This can explain the difference of propagation rates observed in homopolymerization.

We have to consider that in the copolymerization OX:DMOX, two types of end groups are involved. Because of the inductive effect created by the dimethyl substitution, the

positive charge of the oxygen atom is possibly attenuated, therefore we can establish the following scheme, that the oxonium end from DMOX is less reactive than the OX end assuming that the end groups have this type of structure:



The greater presence of DMOX units in the polymer chain (67% versus 33% of OX units whereas the feed ratio equals 1:1), can be ascribed to the better nucleophilicity of the DMOX monomer, which permits, via the  $S_N2$  propagation step, a better incorporation of DMOX.

The GPC chromatograms of the copolymers OX:DMOX (Appendix 2) show the presence of cyclic oligomers. In contrast with the copolymerization OX:THF and OX:OX, the cyclooligomerization by back-biting is not suppressed. Making copolymers with oxetane and 3,3 dimethyl oxetane does not modify the overall structure of the polymer chain which is still constituted of 4-membered units, therefore the back biting can occur for tetramer to be produced.

#### **4.5. Terpolymerizations between oxetane and other cyclic ethers**

Terpolymerizations using specific combinations of 3 membered ring cyclic ether (propylene oxide), 4 membered rings (oxetane, 3,3-dimethyloxetane), 5 (THF) and 7 (oxepane), were attempted. The catalyst used was a strong acid, tetrafluoroboric acid-diethyl ether complex 85% ( $\text{HBF}_4 \cdot \text{O}(\text{C}_2\text{H}_5)_2$ ). The molar ratio in the feed between monomers was equal to 1:1:1 and the molar ratio monomer:catalyst was 200:1.

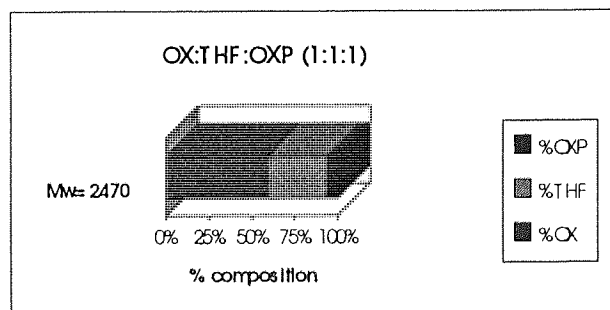
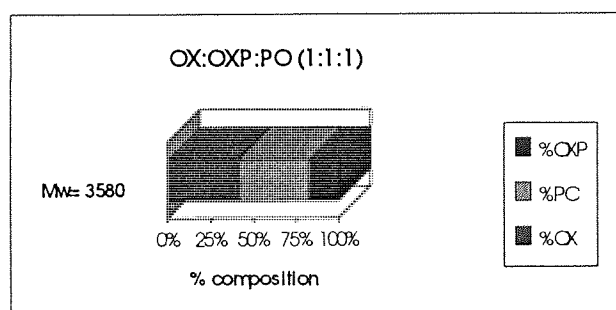
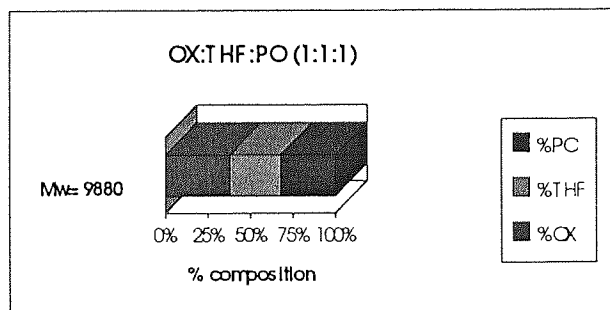
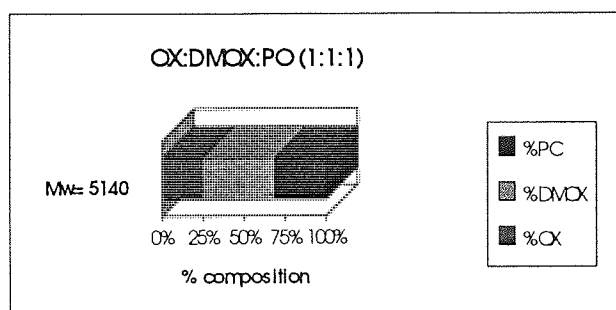
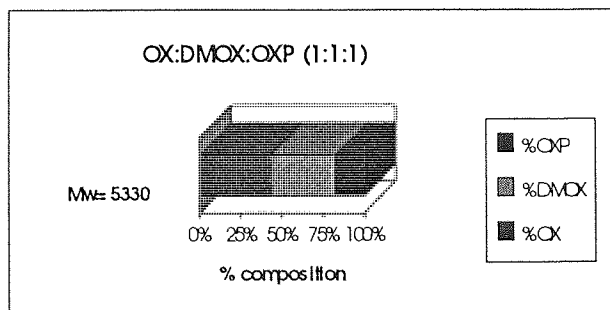
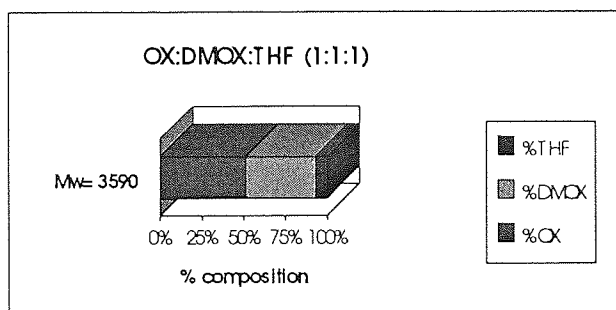
Table 4.9. summarises the GPC analyses and the composition of the polymers determined by NMR spectroscopy.

**Table 4.9. Terpolymerizations, GPC analysis and polymer composition**

Terpolymerization 1:1:1	$\overline{M}_n$ g.mol <sup>-1</sup>	$\overline{M}_w$ g.mol <sup>-1</sup>	Pd	% Composition
OX:THF:DMOX	2180	3590	1.65	OX=51 DMOX=42 THF=7
OX:OX:DMOX	3420	5330	1.56	OX=43 DMOX=39 PO=18
PO:OX:DMOX	3100	5140	1.66	OX=24 DMOX=44 PO=32
PO:OX:THF	6160	9880	1.60	OX=38 DMOX=30 THF=32
PO:OX:OX	2480	3580	1.44	OX=41.5 PO=41 OXP=17.5
OX:THF:OX	1450	2470	1.70	OX=59 THF=34 OXP=7

Table 4.9. shows that the monomers can be polymerized using this catalyst. The highest average molecular weight, quoted against polyTHF, is for the combination propylene oxide - oxetane - THF showing that these monomers are less sensitive to termination. Surprisingly the composition of this terpolymer is close to the initial ratio in the feed. Figure 4.12. is of interest to visualise the composition of the terpolymers. It appears that in terpolymerization the four membered rings are present in a high concentration, and propylene oxide units are found in a significant quantities (30-40%). This can be ascribed to the strong ring strain of oxiranes and oxetanes. The last experiment is of interest and shows the behaviour of unsubstituted cyclic ethers in terpolymerization. It appears that in the combination oxetane- THF- oxepane, oxetane is found in the largest quantity, but oxepane is only found in a small amount although it is a bit more strained than THF. This observation has to be correlated with the results found for the copolymerizations OX:THF and OX:OX. It seems that in copolymerization and terpolymerization oxepane is a bit less reactive than THF.

**Figure 4.12. Composition of the terpolymers**





## CHAPTER 5

# LIVING POLYMERIZATIONS

### 5.1. Introduction

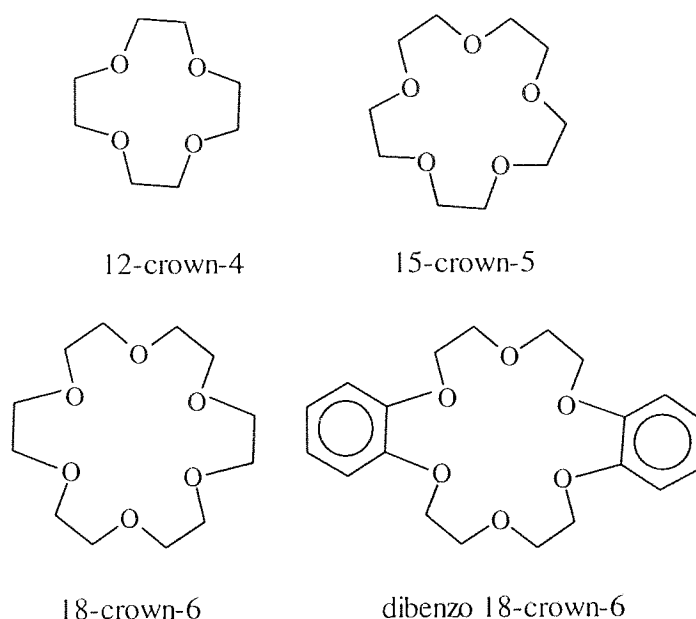
In this chapter, the possibility of polymerizing cyclic ethers in a living polymerization will be discussed. This type of polymerization is described in section 1.7 as a polymerization wherein the termination step does not occur and the propagating end remains "active". A living system is of interest for making of polymers of well controlled chain length. In the polymerization of oxetane, we have described the propagating end as a dynamic equilibrium between a tertiary oxonium ion and a carbocation surrounded by a cyclic ether tetramer molecule arranged like a crown ether, but the kinetics of polymerization suggest transfer and termination mechanisms still occur. In order to make a living polymer, the positive charge of the active end has to be stabilised and "protected" to hinder termination. In order to stabilised the carbocation, an array of compounds was tried.

### 5.2. Use of crown-ethers

It is known that in the homopolymerization of oxetane, the concentration of tetramer deviates markedly from the Jacobson-Stockmayer's prediction model. In chapter 4, this has been explained in terms of a back-biting process that promotes the formation of the tetramer structure that then complex as a crown-ether with the propagating centre, effectively stabilising the carbocationic propagating centre. The aim of these series of experiments is to see the effect of the addition of well known crown-ethers to the polymerization feed. The different crown-ethers used are based on an open ethylene oxide unit and shown in figure 5.1. The literature available on the use of such compounds in cationic polymerization is limited. No systematic investigation of the effect of crown-ethers on homopolymerization or copolymerization could be found. It has to be said that the crown-ethers are not likely act as a monomer and to undergo ring opening polymerization, therefore there is no interference with the linear polymer of oxetane.

Experimentally the polymerizations were carried out in the calorimeter vessel, following the same procedure as for the homopolymerizations. The required amount of crown ether in solution in dichloromethane was introduced by syringe into the vessel and mixed with the monomer solution prior to initiator injection. The catalyst and cocatalyst used in all these investigations were boron trifluoride etherate and ethanediol respectively. In each reaction the ratio of monomer to catalyst and crown ether was maintained at 100:1:1.

**Figure 5.1. Crown-ethers added to the feed as complexing agents**



### 5.2.1. Effect of the addition of crown-ethers on the homopolymerization of oxetane

The initial rates of reaction were estimated from the calorimetry traces and GPC studies were carried out on the samples as described previously. Table 5.1. shows the effect of the presence of crown-ethers on the polymerization of oxetane. For comparison the results obtained under the same experimental conditions, for the homopolymerization of oxetane without crown ether are also shown in the table.

**Table 5.1. Effect of crown ether addition on the homopolymerization of oxetane**

Experiment	$\overline{M}_n$ g.mol <sup>-1</sup>	$\overline{M}_w$ g.mol <sup>-1</sup>	Pd	Rate °C.s <sup>-1</sup>
OX	2930	4810	1.64	3.7
OX:12crown4	2650	4400	1.66	3.2
OX:15crown5	3260	5670	1.74	2.9
OX:18crown6	4210	7370	1.75	3.1
OX:db18crown6	10840	19870	1.83	2.6

$$[\text{OX}] = 2 \text{ M}, [\text{BF}_3\text{OEt}_2] = [\text{Crown-ether}] = 0.02 \text{ M}, T = 35 \text{ }^\circ\text{C}$$

From the information shown in table 5.1 and the relevant traces, the following conclusions can be drawn. The smaller crown-ether (12-crown-4) involved in the study has no significant effect on the polymerization of oxetane. Only bigger rings have an effect on the values of  $\overline{M}_n$  and  $\overline{M}_w$ . As expected the size of the cavity within the crown-ether is of importance. The 12-crown-4, compared with the tetramer of oxetane (16-crown-4), is too small to accommodate the propagating carbocation. The other crown-ethers are big enough to stabilise the end, therefore the increases in average molecular weight observed can be explained by the end capping of the carbocation by the crown-ether, temporarily preventing the termination step. The propagating end once partially stabilised, still allows the back-biting process to produce cyclic oligomers such as the tetramer (16-crown-4) again because there is no disruption of the structure of the chain-end.

The rates of polymerizations as measured calorimetrically, show that oxetane is a very reactive monomer and the addition of crown-ethers affects slightly the rate of propagation. The values must be treated with caution due to the accuracy with which the measurements may be made. However the slower rate of polymerization has to be correlated with an increase of molecular weight. This is most noticeable in the case in the last experiment wherein the value of  $\overline{M}_n$  was found to be four times greater than that found in the first homopolymerization at a rate of propagation of only 70 % of the original. This reduction in the observed rate, being considered to be a result of this induced greater stability of the propagating species, must also lead to a species that slows termination/transfer an even greater factor.

Table 5.1. also shows that the addition of dibenzo 18-crown-6 to oxetane has significantly increased the molecular weight of the product. From the chromatogram showed in appendix 3, it was observed that the addition of this crown ether has apparently reduced the quantity of cyclic tetramer. The implication of this result is that

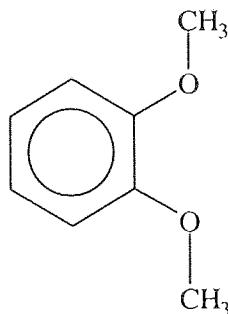
the back biting reaction is less favoured when such complexing agent is present during the course of polymerization.

For the two last experiments described, the sizes of the cavity of the crown ether are identical, however a dramatic increase of  $\overline{Mn}$  occurs when two benzene rings are present on the crown. It could therefore be proposed that the dibenzo-18-crown-6 offers a better stabilisation of the positive chain-end via its overall electron density than 18-crown-6 itself. Figure 5.1 shows that dibenzo-18-crown-6 is, as well as being a crown ether, also an aromatic ether which was considered to be an important factor in the determination of the stability of the propagating species.

### 5.3. Use of Veratrole

Given the results obtained using dibenzo-18-crown-6 as a complexing agent, 1,2 methoxy benzene, (veratrole - figure 5.2.) was used as a complexing agent for the polymerization of oxetane. It was dissolved in dichloromethane and different amounts of this solution were added to the monomer solution prior to the catalyst injection.

Figure 5.2. Molecule of Veratrole



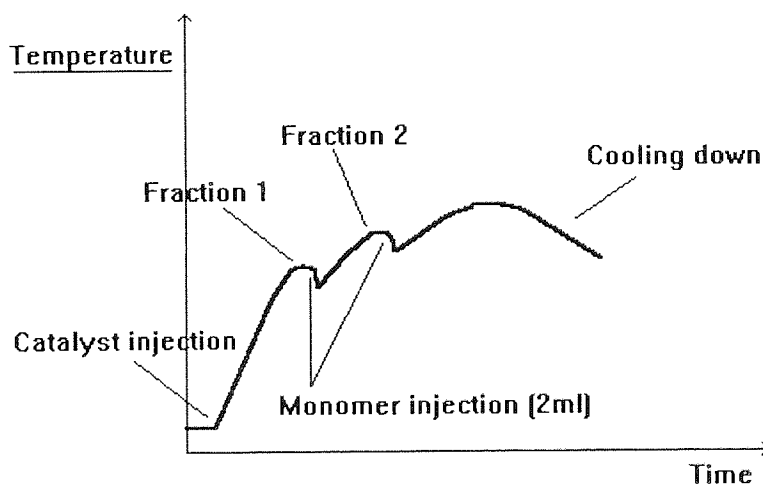
#### **5.3.1. Effect of Veratrole on the homopolymerization of oxetane**

A series of experiments was attempted under the same conditions as these described for the crown-ethers study, but replacing the crown ether by veratrol and using a monomer:veratrole molar ratio equal to 100:1. The rate of polymerization recorded

calorimetrically was used to indicate the progression of the reaction. After the injection of the catalyst-cocatalyst system, the observed rate increased normally and after a short time a small fraction of the mixture was syringed out for analysis. Then an amount of veratrole-free fresh monomer solution was injected into the vessel. The resulting increase of observed temperature indicated that the reaction continued until a second fraction was taken for analysis. The injection of another small amount of monomer solution was carried out and at the end of the reaction the final material and the previous fractions were analysed by GPC.

Figure 5.3. shows the thermogram recorded for this experiment.

**Figure 5.3. Thermogram and procedure of the homopolymerization of oxetane with veratrole**



This experiment displayed characteristics typical of living polymerization systems.

- i) The polymerization started again after addition of fresh amounts of monomer .
- ii) The GPC analysis of the fractions show that the chain length increased with adding of more monomer to a polymerization as shown in figure 5.4.

It could be proposed that propagating end was still "active" during the course of the experiment, therefore the freshly added monomer can polymerize at the end of the polymer increasing the chain length. This result can be ascribed to a change in the structure of the growing species compared with that of a conventional oxetane polymer. It may be proposed that veratrole is stabilising the positive charge on the propagating

species, as shown in figure 5.5 favouring propagation over termination reactions and resulting in the formation of higher molecular weight polymer. This stabilisation may occur by interactions between the lone pairs of electrons on the oxygen atoms of veratrole and the positively charged growing end.

**Figure 5.4.** Variation of  $\overline{M}_n$  after addition of fractions of fresh monomer

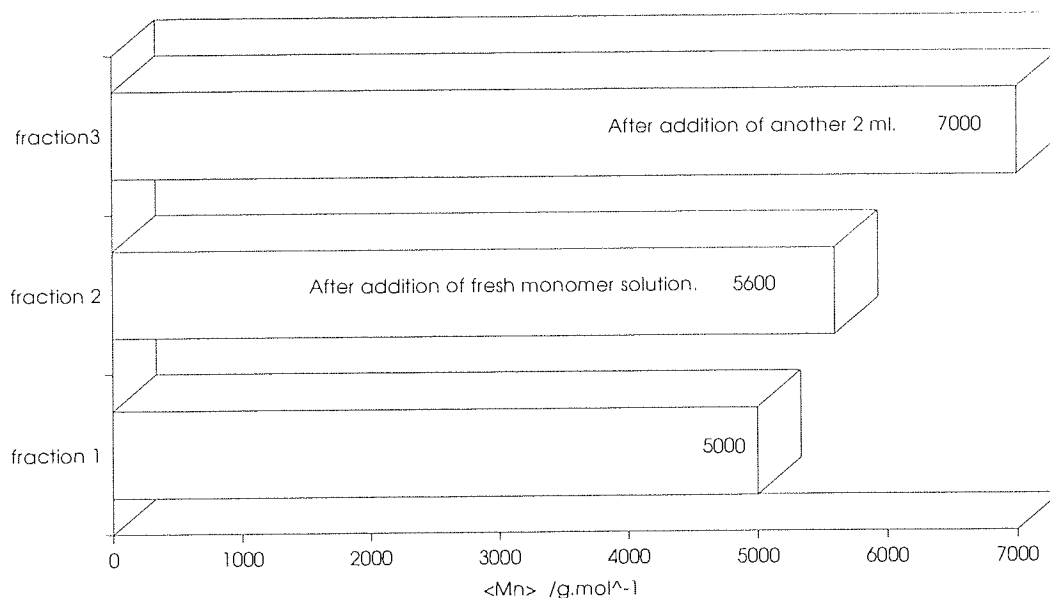
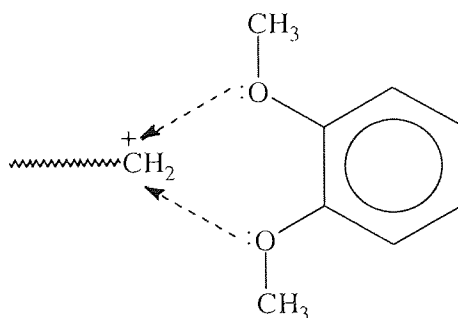


**Figure 5.5.** Stabilisation of the propagating end



### 5.3.2. Effect of the concentration of oxetane on the molecular weight

In order to check the validity of this living system, further experiments were carried out to see the effect of the concentration of oxetane on the average molecular weights keeping constant the molar ratio monomer:veratrole at 300:1 and the concentration of initiator. The results of this series are shown in table 5.2.

It can be seen that the number average molecular weight increased with increasing concentration of monomer. Molecular weights of 25000 are unusually high for such polymer systems. In a genuine living system the expected value can be calculated taking account of the fact that the initiator used was difunctional. Figure 5.6. shows the effect of the initial concentration of oxetane on the calculated value of  $\overline{Mn}$  and that observed by GPC. In theory this variation is likely to be linear, but figure 5.6 shows that the variation of the observed values increased with increase of monomer concentration. However they were markedly below the theoretical values of  $\overline{Mn}$ . The observed values of  $\overline{Mn}$  appear to be the half of those expected, but for the last experiment in which the ratio Monomer:Initiator was equal to 80:1 and the observed value matched the expected. This deviation could have different explanations, such as the quality of the initiation or some early terminations occurring by charge transfer if the stabilisation of the end by veratrole is not completely efficient. The values of the polydispersities indicate a fairly broad molecular weight distribution. This strengthens the idea that some chains could have terminated and that the polymerization is not truly living. If the initiation step is fast the expected polydispersity of a living system is close to 1, this is the case in living polymerization of monomers like styrene, but it seems that with the natures of an oxetane molecule and the growing species more or less stabilised by a veratrole molecule, this value is never reached. It can be argued that the polymer chains undergo transesterification with the active site as shown in scheme 5.1. This is the reason why the polydispersities are close to the value of 2, therefore the term pseudo-living polymerization will be more acceptable.

**Scheme 5.1. Transesterification between the propagating end and the polymer chain**

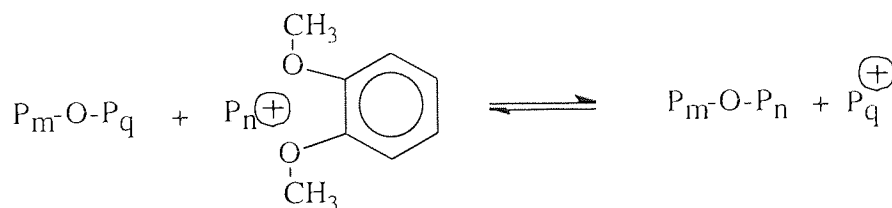
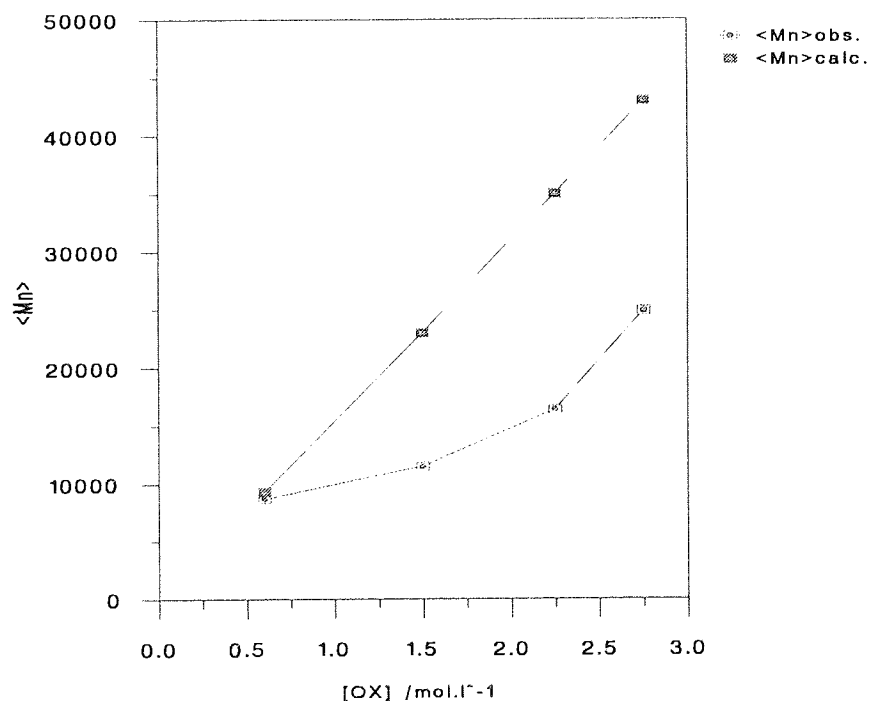


**Table 5.2. Homopolymerization of oxetane with Veratrole**  
**Effect of the variation of [OX] on  $\overline{Mn}$ ,  $\overline{Mw}$  and Pd.**

Experiment	[OX] mol.L <sup>-1</sup>	[M]/[I]	$\overline{Mn}_{calc.}$ g.mol <sup>-1</sup>	$\overline{Mn}_{obs.}$ g.mol <sup>-1</sup>	Pd
1	2.75	367	43000	24920	1.95
2	2.25	300	35000	16380	1.98
3	1.50	200	23000	11490	2.09
4	0.60	80	9300	8670	1.86

[catalyst] = 0.0075 M , T= 35 °C

**Figure 5.6. Homopolymerization of oxetane with veratrole, Effect of [OX] on  $\overline{Mn}$  calculated and  $\overline{Mn}$  observed**



In addition the overlay chromatograms of the samples related to this study are shown in appendix 3. The figure shows that the control of the molecular weight distribution is



possible using veratrole as a stabilising end agent. The chromatograms indicate that cyclic oligomers are still formed in the homopolymerization of oxetane with veratrole.

### 5.3.3. Effect of veratrole on the homopolymerization of 3,3-dimethyloxetane

The experiments described above were attempted using veratrole in the homopolymerization of 3,3-dimethyloxetane. No significant change in the average molecular weight was observed after the addition of small amount of fresh monomer solution. In addition the chart recorder following the reaction indicated no further reaction. This suggested that the polymer end underwent termination. For indication table 5.3. and figure 5.7. show the effect of the variation of monomer:initiator ratio on  $\overline{Mn}$ , the ratio monomer:veratrole remaining constant and equal to 300:1. If this system is "living" the plot shown in figure 5.7. is expected to be similar to figure 5.6. The values of  $\overline{Mn}$  do not increase when increasing the concentration of monomer, therefore it can be concluded that veratrole has probably no effect on the stabilisation of the growing species involved in the homopolymerization of 3,3-dimethyloxetane.

This monomer differs from oxetane by the presence of substituents in position 3. The substitution creates some steric effect which possibly prevents the veratrole to act in the same way as in the homopolymerization of oxetane.

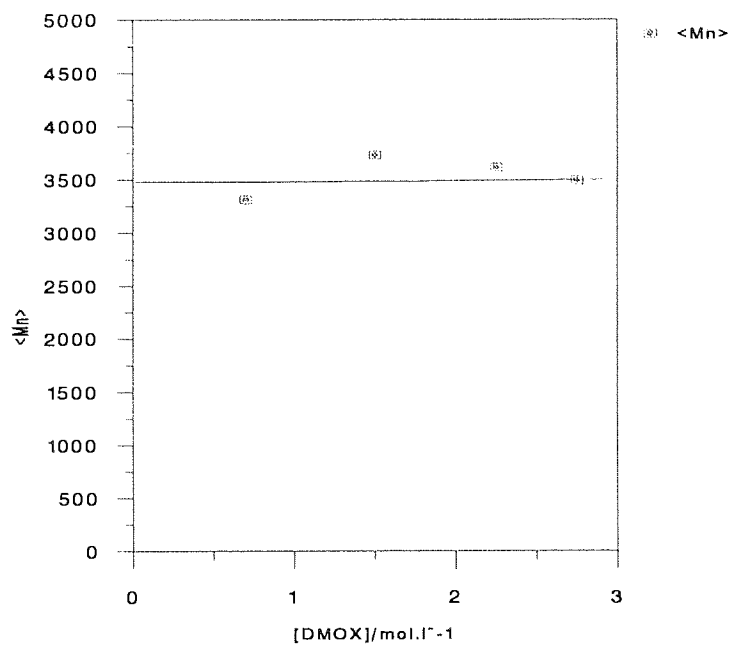
**Table 5.3. Homopolymerization of DMOX with Veratrole**  
**Effect of the variation of [DMOX] on  $\overline{Mn}$ , and Pd.**

[DMOX] mol.L <sup>-1</sup>	[M]/[I]	$\overline{Mn}$ g.mol <sup>-1</sup>	Pd
2.75	370	3490	1.63
2.25	300	3610	1.62
1.50	200	3730	1.65
0.70	80	3310	1.56

[catalyst] = 0.0075 M , T= 35 °C

Figure 5.7. Homopolymerization of DMOX with veratrole, Effect of [DMOX] on

$$\overline{Mn}$$



## 5.4. Pseudo-living copolymerizations of cyclic ethers

Crown-ethers, like dibenzo 18-crown-6, and compounds such as veratrole were believed to promote the formation of living polymers from oxetane. Specific combinations of oxetane and veratrole have shown a good control of the polymerization process. In some cases the virtually absence of termination enables the formation of polymers having a well defined chain length. It was interesting to investigate the effect of such additives in the copolymerizations of oxetane and other cyclic ethers like THF, oxepane and 3,3-dimethyloxetane.

### 5.4.1. Copolymerizations of oxetane : THF and oxetane : oxepane

These monomers have already been copolymerized using  $\text{BF}_3\text{OEt}_2$ /ethanediol as initiator system and it was found that the incorporation of tetrahydrofuran into the polymer did not exceed 25% (and 10% for oxepane). The NMR analysis has shown that the distribution of the THF (or oxepane) units in the chain was statistical. In this section we have attempted to make copolymers in the presence of dibenzo-18-crown-6 or veratrole. In each case the molar ratio between the monomers and veratrole or the crown ether was 100:1. The molecular weights were determined by GPC and the compositions of the copolymers were determined by  $^1\text{H}$  NMR according to areas underneath the specific peaks. The results of this studies are shown in table 5.4.

**Table 5.4. Copolymerizations OX:THF and OX:OXP with dibenzo 18-crown-6 (db18c6) and veratrole (VTL),**

Experiment	$\overline{M}_n$ g.mol <sup>-1</sup>	Pd	Composition
OX:THF	1330	1.56	%OX=75 %THF=25
OX:THF:db18c6	3570	1.70	%OX=72 %THF=28
OX:THF:VTL	10320	1.80	%OX=70 %THF=30
OX:OXP	3590	1.72	%OX=90 %OXP=10
OX:OXP:db18c6	4530	1.90	%OX=88 %OXP=12
OX:OXP:VTL	8850	1.70	%OX=91 %OXP=9

[monomers]= 2M , T= 35 °C

For the copolymerization between oxetane and THF, no significant changes in the composition of the copolymers are observed. The percentage of THF units in the polymer is around 25 to 30. Therefore the use of dibenzo 18 crown 6 or veratrole does not particularly affect the relative rates of incorporation of the monomers. The main change observed is for the value of  $\overline{Mn}$  which increases significantly by addition of dibenzo 18-crown-6 and dramatically increases with veratrole. The polydispersity index seems to be affected by the use of the additives varying from 1.56 to 1.80 with veratrole. The same tendencies are observed concerning the composition and the values of  $\overline{Mn}$  of the copolymers made from oxetane and oxepane.

The addition of small amounts of dibenzo-18-crown-6 and veratrole brings some new results in the copolymerizations of cyclic ethers. We have found that the average molecular weights of the copolymers can be increased significantly without significant changes in the composition. As in the homopolymerization of oxetane, this can be ascribed to the fact that dibenzo-18-crown-6 and especially veratrole are responsible of the stabilisation of the propagating end, preventing the termination and therefore increasing  $\overline{Mn}$ .

In these cases the molecular weight distributions of the copolymers are unchanged. The oligomer peak does not appear on the GPC chromatograms of the copolymers OX:THF and OX:OXP. The incorporation of THF or OXP units disrupts the regularity of the polymer chain. Therefore the formation of the tetramer, as described in section 4.3, is limited.

#### **5.4.2. Copolymerizations with DMOX and other cyclic ethers**

Different copolymerizations involving 3,3-dimethyloxetane and four, five, seven members cyclic ethers were carried out in the presence of dibenzo 18-crown-6 and veratrole following the same conditions as in section 5.4.1. The results of this study are shown in table 5.5.

**Table 5.5. Copolymerizations DMOX:THF, DMOX:OXP and DMOX:OX with dibenzo 18-crown-6 (db18c6) and veratrole (VTL)**

Experiment	$\overline{M}_n$ g.mol <sup>-1</sup>	Pd	Composition
DMOX:THF	2700	1.8	%DMOX=87 %THF=13
DMOX:THF:db18c6	4790	2.2	%DMOX=80 %THF=20
DMOX:THF:VTL	2800	3.2	%DMOX=93 %THF=7
DMOX:OXP	2450	1.7	%DMOX=97 %OX=3
DMOX:OXP:db18c6	2660	1.8	%DMOX=98 %OX=2
DMOX:OXP:VTL	2510	1.9	%DMOX=95 %OX=5
DMOX:OX	3260	1.8	%DMOX=67 %OX=33
DMOX:OX:db18c6	3680	2.0	%DMOX=60 %OX=40
DMOX:OX:VTL	2530	1.6	%DMOX=64 %OX=36

[Monomers]= 2M , T= 35 °C

Table 5.5. shows that the veratrole does not seem to have as significant effect on the copolymers of DMOX as it does on the copolymers made from oxetane. This result has to be correlated to the inefficiency of veratrole in the homopolymerization of DMOX.

It has to be stressed that steric effects created by the dimethyl substitution seem to be responsible for the inability of veratrole to take part in the stabilisation of the propagating end.

In all samples the compositions of the copolymers are not significantly affected.

However in some cases such as DMOX:THF or DMOX:OX, the addition of dibenzo 18-crown-6 provokes a slight increases of  $\overline{M}_n$ . Therefore it can be proposed that dibenzo 18-crown-6 is probably a better stabilising agent than veratrole for the propagating end of polyDMOX.

## CHAPTER 6

### CONCLUSIONS AND FURTHER WORK

#### 6.1. Kinetic studies

The work presented in this thesis investigated the kinetics and mechanisms of ring opening polymerization of different cyclic ethers using mainly a cationic system of initiation,  $\text{BF}_3\text{OEt}_2$ /ethanediol. The cyclic ethers studied reacted differently. Four membered rings, such as oxetane and 3,3-dimethyloxetane, homopolymerized instantaneously whereas tetrahydrofuran and oxepane were not found to undergo homopolymerization using this type of initiator. This is in accordance with the fact that ring strain and basicity are likely to be the driving forces in cationic ring opening polymerization.

For the homopolymerization of oxetane, the rate of polymerization and the number average molecular weight were a maximum when the ratio  $[\text{OH}]:[\text{BF}_3\text{OEt}_2]$  was 1. Above this value, when the concentration of OH groups exceeded that of the catalyst, a steady decline in  $R_p$  was observed. This is attributed to the protonation of excess ethanediol in competition with protonation of the monomer. A linear dependence was found between  $1/R_p$  and the concentration of OH in excess. It was also found that the excess of cocatalyst not only removes active catalyst from the system, but at the same time causes a reduction in molecular weight by increasing the rate of transfer.

When the ratio  $[\text{OH}]:[\text{BF}_3\text{OEt}_2]$  was maintained at a value of 1, the plot of  $\text{DP}_n$  against  $1/[\text{BF}_3\text{OEt}_2]$  was linear. This dependence is explained by a kinetically controlled termination step involving the counterion.

For the homopolymerization of 3,3-dimethyloxetane,  $\overline{Mn}$  increased when the concentration of catalyst was increased. This unexpected result may be explained by the removal of the active catalyst through a side reaction between the  $\text{BF}_3\text{OEt}_2$  and the cocatalyst. However further investigations are required to support this tentative hypothesis.

Copolymerizations between cyclic ethers gave interesting outcomes. It was found that monomers such as THF or oxepane could copolymerize with oxetanes using  $\text{BF}_3\text{OEt}_2$ /ethanediol. The composition of the copolymers determined by  $^1\text{H}$  NMR showed that the distribution of the units was statistical and the presence of THF units

did not exceed 25% (10% for oxepane) in the copolymer. In the case of the copolymerization of oxetane and THF, a linear dependency was observed between  $1/\overline{Mn}$  and  $[\text{BF}_3\text{OEt}_2]$ , and, by increasing the ratio  $[\text{THF}]:[\text{OX}]$ , the degree of polymerization was found to be dependent on  $1/[\text{BF}_3\text{OEt}_2]$  and  $1/[\text{THF}]$ . The explanation of this is that  $\text{DP}_n$  is controlled kinetically via termination with the gegenion  $\text{BF}_3\text{OR}^-$  and transfer to monomers, principally THF

$$\overline{\text{DP}}_n = \frac{R_p}{\sum R_t}$$

The copolymerization of oxetane and oxepane led to the same conclusions, namely that the degree of polymerization is kinetically controlled by terminations. However it was found that the contribution of each type of reaction to the overall termination differs markedly. The major part was ascribed to the termination with oxepane monomer.

## 6.2. Molecular weight distribution

The Gel permeation chromatography studies showed that the molecular weight distributions of the samples of polyoxetane and poly3,3-dimethyloxetane were bimodal. This was in accordance with previous work of Rose<sup>28</sup> establishing that cyclic tetramer is found in much higher proportions than any of the other cyclic oligomers. Because of the affinity of crown ether to complex lithium ion by way of a template effect, the addition of LiCl to the medium resulted in a significant increase in the production of cyclic tetramer. On the other hand the molecular weight distribution of the copolymers made from oxetane and THF or from oxetane and oxepane were shown to be unimodal. The presence of cyclic tetramers was not found in the same amounts as for the homopolymerization of oxetane.

The model developed by Rose explained the formation of cyclic tetramer in terms of "back-biting" reaction, involving the propagating end described as an oxonium ion. Although being totally acceptable in the case of the homopolymerization of oxetane, this model of growing end was found to be restrictive for the explanation of the phenomena observed in the experiments with lithium salts and in the copolymerizations.

These observations could be explained by a change in the structure of the growing end involved in the cationic polymerization. For the homopolymerization of oxetane, it is proposed that the growing species could be represented as a tetramer ring at the end of the growing chain. The positive charge of the cation is stabilised by the presence of the

oxygen atoms arranged as in a crown ether. This allows the "back-biting" reaction to produce cyclic tetramers in large quantities. Therefore it is argued that the chain end exists as a crown ether complex in equilibrium with free crown ether (Tetramer). It is not unreasonable to argue that a cyclic tetramer would complex more readily with a propagating carbonium ion than a monomer molecule to form an oxonium ion.

During the copolymerization, the regularity of the polymer chain is disrupted by the incorporation of the comonomer into the polymer back-bone; the structure of the propagating end is modified, destabilising the positive charge. The production of cyclic tetramers by "back-biting" process occurs with difficulty. On the other hand, for the copolymerization of oxetane and 3,3-dimethyloxetane (both four membered rings), the presence of tetramer is explained by the non-disruption of the polymer chain during the incorporation of DMOX units. Thus, the cyclooligomerization occurs in the same way as described for the homopolymerization of oxetane.

### **6.3. Pseudo-living polymerizations**

The work presented in chapter 5, has introduced some new possibilities for the cationic ring opening polymerization of oxetane, and strengthens the evidence for the model of the structure of the propagating end. The addition of crown-ethers such as 18-crown-6 to the polymerization is found to increase the number average molecular weight. It is proposed that the cavity of these crown-ethers is large enough to end-cap the propagating carbocation, preventing terminations from occurring. This was particularly noticeable with dibenzo-18-crown-6, and it is proposed that the stabilisation of the positive chain-end is increased by the high density of delocalised electrons of the benzene rings supported by the crown-ether. With this stable end created by the strong interactions between the carbocation and the dibenzo crown-ether, the rate of propagation is slowed and the formation of cyclic tetramer apparently reduced but not suppressed.

By adding veratrole to the homopolymerization of oxetane, high molecular weight polymers were obtained, and evidence of a pseudo living system was found. This is ascribed to the stabilisation by interaction of the positive charge of the carbocation of the growing end and the lone pairs of electrons on the oxygen atoms of veratrole.

It was also found that the use of dibenzo-18-crown-6 and veratrole in the copolymerization did not affect the composition of the statistical copolymers and their molecular weight distribution.



Veratrole was found to be ineffective in the attempts to make living polymers of polyDMOX. Could this result be correlated to the unexpected dependence of the degree of polymerization on the catalyst concentration?

It can be argued that the different structures of the propagating ends involved in the homopolymerization of DMOX and oxetane are responsible for this behaviour. The dimethyl substitution seems to create a steric hindrance for the veratrole molecule to the stabilisation of the end, and to the prevention of termination reactions. Thus, this research throws up an entirely new question: Is the model of the propagating end for the homopolymerization of oxetane limited by the presence of the substituents on the ring? The priority in further experiments has to be given to the homopolymerization of DMOX using dibenzo-18-crown-6. In spite of the existence of steric effects created by the presence of methyl groups, we could expect this crown-ether to be a suitable agent for the stabilisation of the propagating end.

## REFERENCES

- 1 "The ring opening polymerization of ring strained cyclic ethers"  
D.P.S. Riat, PhD Thesis, The University of Aston in Birmingham, (1992)
- 2 "Recent Advances in Cationic Polymerization"  
J.P. Kennedy, A.W. Langer, *Advances in Polymer Science*, **3**, 508-512, (1964)
- 3 "Kinetics and mechanisms of the cationic polymerization of tetrahydrofuran in solution. THF-CH<sub>3</sub>NO<sub>2</sub> system"  
K. Matyjaszewski, S. Slomkowski, S.Penczek, *J. Polym. Sci., Polym. Ed.*, **17**, 69-74, (1979)
- 4 "Kinetics and mechanisms of the cationic polymerization of tetrahydrofuran in solution. THF-CH<sub>2</sub>Cl<sub>2</sub>/CH<sub>3</sub>NO<sub>2</sub> systems"  
K. Matyjaszewski, S. Slomkowski, S. Penczek, *J. Polym. Sci., Polym. Ed.*, **17**, 2413-2422, (1979)
- 5 "The mechanism of the initiation reaction of the cationic polymerization of tetrahydrofuran by stable cationic salts"  
Y. Yamashita, *Makromol. Chem.*, **142**, 171-181, (1971)
- 6 "Macroions pairs and macroions in the kinetics of polymerization of hexamethylene oxide"  
Brezinska K., Matyjaszewski K., Penczek S., *Makromol. Chem.*, **179**, 2387-2395, (1978)
- 7 "Carbanions Living Polymers and Electron Transfer Processes", M. Swarc, Interscience Ed, New York, (1968)
- 8 "The cationic polymerization of THF in CH<sub>3</sub>NO<sub>2</sub>"  
P. Dreyfuss., M.P. Dreyfuss, *Adv. Chem Ser.*, **91**, 335, (1969)
- 9 "The Synthetic Importance and Industrial Applications of Ring Opening Polymerization"  
J.E. Mc Grath, *Makromol Symp., Macromol. Symp.*, **42-3**, 69-91, (1991)
- 10 "Principles of Polymerization, Third Edition"  
G. Odian, Wiley Interscience Ed, New York, (1991)
- 11 "Polymers: Chemistry and Physics of Modern Materials"  
J.M.G. Cowie, Intertext Books, Glasgow, (1973)
- 12 "Ring Opening Polymerization"  
K.C. Frisch, S.L. Reegen, Marcel Dekker Ed, New York, (1969)

- 13 "Polymerization and halogen scrambling behavior of phenyl substituted cyclotriphosphazenes"  
H.R. Allock, M.S. Connoly, *Macromolecules*, **18**, 1330, (1985)
- 14 "Polymerization of 2-methoxy -2-oxo -1,3,2 -dioxaphospholane, kinetics and polymer structure"  
S. Penczek, Libiszowski, *Die Makromol. Chem.*, **189**, 1765-1786, (1988)
- 15 "The Polymerization of Lactic Acid Anhydrosulphite by Anionic initiators",  
L.R. Adams, PhD Thesis, The University of Aston in Birmingham, (1994)
- 16 "Cationic Ring Opening Polymerization of Heterocyclic Monomers", Penczek S., Kubisa P., Matyjaszewski K., *Advances in Polymer Sci.*, **37**, (1980)
- 17 "Some thermodynamic and kinetic aspects of addition polymerization"  
F.S. Dainton, K.J. Ivin, *Chem. Soc. Quart. Revs.*, **12**, 61-90, (1958)
- 18 "Copolymerization of substituted tetrahydrofuran with some cyclic ethers"  
A. Ishigaki, T. Shono, Y. Hachihama, *Die Makromol. Chem.*, **79**, 170-179, (1964)
- 19 W. Gordy, S.C. Stansford, *J. Chem. Phys.*, **7**, 93-99, (1939)
- 20 "Correlation of cationic copolymerization parameters of cyclic ethers, formals and esters"  
Y. Yamashita, T. Tsuda, M.Okada, S. Iwatsuki, *J. Polym. Sci., Part A*, **1**, 2121-2131, (1966)
- 21 "Basicity and Complexing Ability of Ethers"  
S. Searles Jr., M. Tamres, "The Chemistry of the Ether Linkage", S. Patai, London, New York, Sidney, Wiley(Ed), (1967)
- 22 "Correlation of base strengths of cyclic compounds"  
H. K. Hall Jr, *J. Am. Chem. Soc.*, **79**, 5441, (1957)
- 23 "Houben-Weyl Methoden der Organischen Chemie"  
H. Meerwein, E. Muller (Ed), 4th Edition, George Thieme Verlag, Stuttgart, (1965)
- 24 "Superacids and their derivatives. V Kinetics and mechanisms of the cationic polymerization of 3,3-(bischloromethyl) oxacyclobutane initiated by Ethyl trifluoromethanesulfonate. Evidence for ester type propagating species"  
S. Kobayashi, H. Danda, T. Saegusa, *Bull. Chem. Soc.*, Japan, **47**, 2699-2705, (1974)
- 25 "Cationic block copolymerization of THF with 3,3 bis(chloromethyl) oxacyclobutane"  
T. Saegusa, S. Matsumoto, Y. Hashimoto, *Macromolecules*, **3**, 377-381, (1970)

- 26 "Polymerizacion cationica del oxetano iniciada por hexafluoroantimoniato de trietiloxonio"  
E. Perez, A. Bello, J.G. Fatou, *Anales de Quimica*, **81**(1), 73-78, (1985)
- 27 "Preparation and polymerization of some 3,3 disubstituted oxacyclobutanes"  
A.C. Farthing, *J. Chem. Soc.*, 3648-3649, (1955)
- 28 "Cationic polymerization of oxacyclobutanes- Part I"  
J.B. Rose, *J. Chem. Soc.*, 542-543, (1956)
- 29 "Kinetics and mechanism of cationic epoxide copolymerization"  
S. Entelis, G.V. Korovina, *Die Makromol. Chem.*, **175**, 1253-1280, (1974)
- 30 "Study by <sup>19</sup>F Nuclar Magnetic Spectroscopy of the cationic polymerization of tetrahydrofuran initiated by PF<sub>5</sub>"  
F. Andruzzi, A. Prescia, G. Ceccarelli, *Die Makromol. Chem.*, **176**, 977-990, (1975)
- 31 "Some new cocatalysts for the polymerization of four and five membered cyclic ethers by Lewis acid catalysts"  
T. Saegusa, H. Imai, J. Furakawa, *Die Makromol. Chem.*, **54**, 218-221, (1962)
- 32 "Aluminium alkyl catalysts for the polymer of four and five membered cyclic ethers"  
T. Saegusa, H. Imai, J. Furakawa, *Die Makromol. Chem.*, **65**, 60-73, (1962)
- 33 "Polymerization of tetrahydrofuran by the AlEt<sub>3</sub>- H<sub>2</sub>O- Promoter system"  
T. Saegusa, S. Matasumoto, T. Vershima, *Die Makromol. Chem.*, **105**, 132-137, (1967)
- 34 "Trimethylsilyl triflate as an initiator for cationic polymerization, Improved initiation through the use of promoters"  
J.S. Hrkach, K. Matyjazewski, *J. Polym.Sci. -A: Polym. Chem.*, **33**, 285-298, (1995)
- 35 "Complex triarylsulfonium salt photoinitiators. I- The identification, characterization and syntheses of a new class of triarylsulfonium salt photoinitiators"  
J.V. Crivello, H.W. Lam, *J. Polym. Sci.-A: Polym. Chem.*, **18**, 2677-2695, (1980)
- 36 "Photoinitiated cationic polymerization by dialkyl-4-hydroxyphenyl sulfonium salts"  
J.V. Crivello, H.W. Lam, *J. Polym. Sci.-A: Polym. Chem.*, **18**, 1021-1034, (1980)

- 37 "Photosensitized cationic polymerization using dialkylphenacylsulfonium and dialkyl (4-hydroxyphenyl) sulfonium salt initiators"  
J.V. Crivello, H.W. Lam, *Macromolecules*, **14**, 1141-1147, (1981)
- 38 "Synthesis, characterization and photoinitiated cationic polymerization of difunctional oxetane"  
H. Sasaki, J.V. Crivello, *JMS, Pure Appl. Chem.*, A(29) **10**,915-930, (1992)
- 39 "Photochemical cationic polymerization of cyclohexene oxide in solution containing pyridinium salt and polysilane"  
Y. Yagci, *Eur. Polym. J.*, **28**, 387-390, (1992)
- 40 "N-Alkoxy-pyridinium and N- Alkoxy-quinolinium salts as initiators for cationic photopolymerizations"  
Y. Yagci, *J. polym. Sci. -A: Polym. Chem.*, **30**, 1987-1991, (1992)
- 41 "Block copolymers by combination of radical and promoted cationic polymerization routes"  
Y. Yagci, *Macromolecules*, **24**, 4620-4623, (1991)
- 42 "Photosensitized cationic polymerization using N-ethoxy-2-methylpyridinium hexafluorophosphate"  
Y. Yagci, *Polymer*, **34**, 1130-1134, (1993)
- 43 "Polymeric pyridinium salts as photoinitiators for cationic polymerization"  
O. Karal, A. Onen, Y. Yagci, *Polymer*, **35**, 4694-4696, (1994)
- 44 "Activated monomer propagation in cationic polymerizations"  
S. Penczek, *Die Makromol. Chem., Macromol. Symp.*, 203-220, (1986)
- 45 "Cationic polymerization of ethylene oxide. I-Stannic chloride"  
D. J. Worsfold, A.E Eastham, *J. Am Chem Soc*, **79**, 897-900, (1957)
- 46 "Cationic polymerization of ethylene oxide. II-Boron Trifluoride"  
D. J. Worsfold, A.E Eastham, *J. Am Chem Soc*, **79**, 900-903, (1957)
- 47 "Cationic polymerization of ethylene oxide. III-Depolymerization of polyglycols by oxoniums fluoroborates"  
G.A. Latremouille, G.T. Merral, A.M. Eastham, *J. Am Chem Soc*, **82**, 120-124, (1960)
- 48 "<sup>13</sup>C Nuclear Magnetic Resonance studies on the polymerization of cyclic ethers"  
S. Kobayashi, K. Morikana, T. Saegusa, *Macromolecules*, **8**, 954-957, (1975)
- 49 "Macrocyclic Tetrahydrofuran oligomers. 2- Formation of macrocycles in the polymerization of tetrahydrofuran macrocycles with triflic acid."  
G. Pruckmayr, T.K. Wu, *Macromolecules*, **11**, 265-270, (1978)

- 50 "Cationic polymerization of oxacyclobutanes"  
J.B. Rose, J.Chem Soc., 546-548, (1956)
- 51 "The formation of cyclic oligomers in the polymerization of cyclic ethers"  
P. Dreyfuss, M.P. Dreyfuss, Polymer Journal, **8**, 8181-8196, (1976)
- 52 "Equilibrium ring concentrations and statistical conformations of polymer chains: Part 7 Cyclics in poly (1,3- dioxolane)"  
J.M. Andrews, J.A. Semlyen, Polymer, **13**, 141-151, (1972)
- 53 "Determination of secondary and tertiary oxonium ions in the polymerization of cyclic acetals initiated by HOSO<sub>2</sub>CF<sub>3</sub>"  
P. Kubisa, S. Penczek, Die Makromol. Chem., **180**, 1821-1823, (1979)
- 54 "Macrocyclic polydimethylsiloxanes"  
J.F. Brown, G.M.J. Slusarczuk, J. Am. Chem Soc., **87**, 931-934,(1965)
- 55 "Mechanism of the formation of macrocycles during the cationic polymerization of cyclotrisiloxanes. End to end ring closure versus ring expansion"  
J. Chojnowski, M. Scibiorek, J. Kowalski, Die Makromol. Chem.,**178** ,1351-1366, (1977)
- 56 "Cyclic polyethers and their complexes with metal salts"  
C.J. Pedersen, J. Am. Chem. Soc, **89**, 7017-7036, (1967)
- 57 "Openings rings to polyethers"  
M. Mullins, E.P. Woo, Chemtech, **23**, 25-28, (1993)
- 58 "The conformational consequences of replacing methylene groups by ether oxygen"  
J. Dale, Tetrahedron, **30**, 1683-1694,(1974)
- 59 "Lithium salts complexes of 1,5,9,13 -tetraoxacycloheadecanes"  
J. Dale, J Krane, J.C.S. Chem. Comm., 1021-1013, (1972)
- 60 "The mechanism of cationic cyclooligomerization and polymerization of ethylene oxide"  
J. Dale, K. Daatsvatn, T. Gronnberg, Die Makromol. Chem., Short Comm., **178**, 873-879, (1977)
- 61 "Macrocyclic oligoethers related to ethylene oxide"  
J. Dale, P.O. Kristiansen, Acta. Chem. Scan., **26**, 1471-1478, (1972)
- 62 "Application of macrocyclic polyethers"  
J.S. Shih, J. Chinese. Chem. Soc., **39**, 551-559, (1992)

- 63 "Strontium extraction with a polymer bound 18 crown 6 polyether"  
G. Zirnheld, J. Leroy, G. Brunette, *Separation Sci. and Tech.*, **28**, 2419-2429 (1993)
- 64 "Cyclic oligomers in cationic polymerization of 3,3- dimethyloxetane"  
M. Bucquoye, E.J. Goethals, *Die Makromol. Chem.*, **179**, 1681-1688, (1978)
- 65 "Intramolecular reaction - The theory of linear systems"  
H. Jacobson, W.H. Stockmayer, *J. Chem. Phys.* 1600-1607, (1950)
- 66 "Carbon 13 NMR in Polymer Science"  
W.M. Pasika (Ed), ACS Symposium Series 103, Washington D.C., (1979)
- 67 "Copolymers obtained by means of anionic ring opening polymerization. Poly (2,2-dimethyltrimethylene carbonate), tapered  $\epsilon$  caprolactone"  
H. Keul, H. Hocker, E. Leitz, K.H. Ott, L. Morbitzer, *Die Makromol. Chem.*, **189**, 2303-2321, (1988)
- 68 "Polylactones 2a) Copolymerization of glycolide with  $\beta$ -propiolactone,  $\gamma$ -butyrolactone or  $\delta$ -valerolactone"  
H.R. Kricheldorf, Mang T., J.M. Jonte, *Die Makromol Chem.*, **186**, 955-976, (1985)
- 69 "Carbanions, living polymers, and electron transfer processes"  
M. Swarc, Interscience Publishers Inc (Ed), New York, (1968)
- 70 "Living polymerization of isobutyl vinyl ether with the hydrogen iodide / iodine initiating system"  
T. Higashimura, M. Sawamoto, M. Miyamoto, *Macromolecules*, **17**, 265-268, (1984)
- 71 "Living carbocationic polymerization. IV Living polymerization of isobutylene"  
R. Faust, J.P. Kennedy, *J. Polym. Sci - A: Polym Chem*, **25**, 1847-1869, (1987)
- 72 "Criteria for living systems with a special emphasis on living cationic polymerization of alkenes"  
K. Matyjaszewski, *J. Polym. Sci. - A: Polym. Chem.*, **31**, 995-999, (1993)
- 73 "Living cationic polymerization of isobutyl vinyl ether. 1- Initiation by hydrogen iodide (tetraalkyl ammonium salts)"  
O. Nuyken, H. Kroner, *Die Makromol. Chem.*, **191**, 1-23, (1990)
- 74 "Cationic ring opening polymerization of epichlorohydrin in the presence of ethylene glycol"  
Y. Okamoto, *Polymer Preprints*, **25**, 264-266, (1984)

- 75 "Synthesis of telechelic polytetrahydrofuran having a carboxyl group using ketene silyl acetal as a terminator"  
S. Kobayashi, H. Uyama, M. Ogaki, T. Yoshita, T. Saegusa, *Macromolecules*, **22**, 4412-4415, (1984)
- 76 "Synthesis and the preliminary analysis of block copolymers of 3,3' bis-(azidomethyl)-oxetane and 3-nitratomethyl-3'-methyloxetane"  
M.A.H. Talukder, G.A. Lindsay, *J. Polym. Sci. -A: Polym. Chem.*, **28**, 2393-2401, (1990)
- 77 "The preparation and chemistry dicationically active polymers of tetrahydrofuran"  
S. Smith, A.J. Hubin, *J. Macromol. Sci. Chem.*, **A7(7)**, 1399-1413, (1973)
- 78 "Tetrahydrofuran and 3,3 bis(Chloromethyl) oxetane triblock copolymers synthesised by two end living cationic polymerization"  
G.H. Hsie, Y.L. Liu, Y.S. Chiu, *J. Polym. Sci. -A: Polym. Chem.*, **31**, 3371-3375, (1993)
- 79 "Ring opening polymerization of oxetanes by cationic initiators: polymerization of 3- azidomethyl -3- methyloxetane with bis(chlorodimethylsilyl) benzene/silver hexafluoroantimonate initiating system.  
M.A.H. Taludker, *Macromol. Symp.*, **42/43**, 501-511, (1991)
- 80 "Polyethers containing stable ionic end groups"  
P. Kubisa, T. Biedron, *Macromol. Symp.*, **85**, 129-141, (1994)
- 81 "Recent advances in cationic ring opening polymerization"  
E.J. Goethals, *Makromol. Chem. Symp.*, **6**, 53, (1986)
- 82 "Structure-property behaviour of segmented poly(tetramethylene oxide)-based bipyridinium ionene elastomers"  
D. Feng, G.L. Wilkes, B. Lee, J.E. Mc Grath, *Polymer*, **33**, 526-536, (1992)
- 83 "Living cationic ring opening polymerization of tetrahydrofuran- Part I"  
E.J. Goethals, D. Van Meeirvenne, G Trossaert, R. Deveux, *Die Makromol. Chem.*, *Macromol. Symp.*, **32**, 11, (1990)
- 84 "Living and immortal polymerization with metalloporphyrins"  
S. Inoue, *Polymer Peprints*, **2**, 42-43, (1988)
- 85 "Immortal polymerization. Polymerization of epoxide and  $\beta$ -lactone with aluminium porphyrin in the presence of protic compound"  
T. Aida, Y. Maekawa, S. Asano, S. Inoue, *Macromolecules*, **21**, 1195-1199,(1988)



- 86 "Living polymerization of epoxides with metalloporphyrin and synthesis of block copolymers with controlled chain lengths"  
T. Aida, S. Inoue, *Macromolecules*, **14**, 1162-1166, (1981)
- 87 "The polymerization of 1-propylene oxide"  
C.C. Price, M. Osgen, *J. Am. Chem. Soc.*, **78**, 690-691, (1956)
- 88 "Synthesis of propylene oxide-ethylene oxide block copolymers with controlled molecular weights, using metalloporphyrin as a catalyst"  
T. Aida, S. Inoue, *Makromol. Rapid. Comm.*, **11**, 677-680, (1980)
- 89 "Studies in ring opening polymerization. 12. The ring opening polymerization of oxetane to living polymers using a porphinato-aluminium catalyst"  
A.J. Amass, M.C. Perry, D.P.S. Riat, B.J. Tighe, E. Colclough, M.J. Stewart  
*Eur. Polym. J.*, **30**, 641-646, (1994)
- 90 "The ring opening polymerization of ring strained cyclic ethers using metalloporphyrin initiator"  
D.P.S. Riat, Internal report, The University of Aston in Birmingham, (1992)
- 91 "Side chain liquid cristal polymers"  
V. Percec, C. Pugh, C.B. Mc Ardle Ed., Blackie, Glasgow, London, (1989)
- 92 "Thermotropic hydrocarbon side chain liquid crystalline polymers. 1- Synthesis and characterization of liquid crystalline phases"  
J.J. Mallon, S.W. Kantor, *Macromolecules*, **22**, 2070-2077, (1989)
- 93 "Thermotropic hydrocarbon side chain liquid crystalline polymers. 3- Characterization of liquid crystalline phases"  
J.J. Mallon, S.W. Kantor, *Macromolecules*, **23**, 1249-1256, (1989)
- 94 "A novel route to block copolymer by changing the mechanism from living ring opening metathesis polymerization of cyclic olefins to adol condensation polymerization of silyl vinyl ethers"  
V. Percec, B. Hahn, *Macromolecules*, **22**, 1588-1592, (1991)
- 95 "Synthesis of liquid crystalline polymers with a polyoxetane main chain"  
Y. Kawakami, K. Takahashi, H. Hibino, *Macromolecules*, **24**, 4531-4537, (1993)
- 96 "Side chain liquid crystalline polydiene"  
Y. Kawakami, K. Toida, Y. Ito, *Macromolecules*, **26**, 1177-1179, (1993)
- 97 "Molecular design and synthesis of novel side chain liquid crystalline polymers."  
Y. Kawakami, *Macromol. Symp.*, **84**, 167-181, (1994)

- 98 "Liquid crystal crown ether derived from tetramer of epichlorohydrin"  
A. Le Borgne, V. Trentin, N. Lacoudre, N. Spassky, *Polymer Bulletin*, **30**, 1-6, (1993)
- 99 " The degradation and stabilization of solid rocket propellants"  
P. Bunyan, A.V. Cunliffe, A. Davis, F.A. Kirby, *Polym. Degradation and Stability*, **40**, 239-250, (1993)
- 100 "Energetic ABA and (AB)<sub>n</sub> thermoplastic elastomers"  
B.P. Xu, Y.G. Lin, J.C.W. Chien, *J. Applied Polym. Sci.*, **46**, 1603-1611, (1992)
- 101 "New synthesis routes for energetic materials using dinitrogen pentoxide"  
R.W. Millar, M.E. Colclough, P. Golding, P.J. Honey, N.C. Paul, *Philosophical Transactions of The Royal Society of London Series, A-Physical Sci. and Eng.*, **339**, 1654, 305-319, (1992)
- 102 "Characterization of BAMO/NIMMO copolymers"  
E. Kimura, Y. Oyumi, H. Kawasaki, Y. Maeda, T. Anan, *Propellants explosives pyrotechnics*, **19**, 270-275, (1994)
- 103 "Synthesis of copolymers containing pseudohalide groups by cationic polymerization, 2a) Copolymerization of 3,3 -bis (azidomethyl)oxetane with substituted oxetanes containing azide groups"  
H. Cheradame, E. Gojon, *Makromol. Chem.*, **192**, 919-933, (1991)
- 104 "Triblock copolymers based on cyclic ethers: Preparation and properties of tetrahydrofuran and 3,3 -bis(azidomethyl) oxetane triblock copolymers"  
G.H. Hsiue, Y.L. Liu, Y.S. Chiu, *J. Polym Sci. -A: Polym. Chem*, **32**, 2155-2159, (1994)
- 105 "Synthesis of copolymers containing pseudohalide groups by cationic polymerization, 1) Homopolymerization of 3,3 -bis (azidomethyl)oxetane and its copolymerization with 3-chloromethyl-(2,5,8,-trioxadecyl)oxetane"  
H. Cheradame, J.P. Andreoloty, E. Rousset, *Makromol. Chem.*, **192**, 901-918, (1991)
- 106 "The low temperature polymerization of isobutene. Part VI, polymerization by titanium tetrachloride and water in methylene dichloride"  
R.H. Biddulph, P.H. Plesch, P.P Rutherford, *J. Chem. Soc.*, 275-286, (1965)
- 107 "The role of the termination bt the polymer chain in the cationic polymerization of oxetane and 3,3-dimethyloxetane"  
A. Bello,E. Perez, J.M. Gomez Fatou, *Makromol. Chem.*, **185**, 249-253, (1984)
- 108 "Copolymerization of oxetane with 3,3-dimethyloxetane"  
M. Bucquoye, E. Goethals, *European Polymer J.*, **14** , 323-328, (1978)

## APPENDIX 1

NMR spectra of the copolymers referring to the studies described in chapters 3 and 4

60341  
 60342  
 60343  
 60344  
 60345  
 60346  
 60347  
 60348  
 60349  
 60350  
 60351  
 60352  
 60353  
 60354  
 60355  
 60356  
 60357  
 60358  
 60359  
 60360  
 60361  
 60362  
 60363  
 60364  
 60365  
 60366  
 60367  
 60368  
 60369  
 60370  
 60371  
 60372  
 60373  
 60374  
 60375  
 60376  
 60377  
 60378  
 60379  
 60380  
 60381  
 60382  
 60383  
 60384  
 60385  
 60386  
 60387  
 60388  
 60389  
 60390  
 60391  
 60392  
 60393  
 60394  
 60395  
 60396  
 60397  
 60398  
 60399  
 60400  
 60401  
 60402  
 60403  
 60404  
 60405  
 60406  
 60407  
 60408  
 60409  
 60410  
 60411  
 60412  
 60413  
 60414  
 60415  
 60416  
 60417  
 60418  
 60419  
 60420  
 60421  
 60422  
 60423  
 60424  
 60425  
 60426  
 60427  
 60428  
 60429  
 60430  
 60431  
 60432  
 60433  
 60434  
 60435  
 60436  
 60437  
 60438  
 60439  
 60440  
 60441  
 60442  
 60443  
 60444  
 60445  
 60446  
 60447  
 60448  
 60449  
 60450  
 60451  
 60452  
 60453  
 60454  
 60455  
 60456  
 60457  
 60458  
 60459  
 60460  
 60461  
 60462  
 60463  
 60464  
 60465  
 60466  
 60467  
 60468  
 60469  
 60470  
 60471  
 60472  
 60473  
 60474  
 60475  
 60476  
 60477  
 60478  
 60479  
 60480  
 60481  
 60482  
 60483  
 60484  
 60485  
 60486  
 60487  
 60488  
 60489  
 60490  
 60491  
 60492  
 60493  
 60494  
 60495  
 60496  
 60497  
 60498  
 60499  
 60500  
 60501  
 60502  
 60503  
 60504  
 60505  
 60506  
 60507  
 60508  
 60509  
 60510  
 60511  
 60512  
 60513  
 60514  
 60515  
 60516  
 60517  
 60518  
 60519  
 60520  
 60521  
 60522  
 60523  
 60524  
 60525  
 60526  
 60527  
 60528  
 60529  
 60530  
 60531  
 60532  
 60533  
 60534  
 60535  
 60536  
 60537  
 60538  
 60539  
 60540  
 60541  
 60542  
 60543  
 60544  
 60545  
 60546  
 60547  
 60548  
 60549  
 60550  
 60551  
 60552  
 60553  
 60554  
 60555  
 60556  
 60557  
 60558  
 60559  
 60560  
 60561  
 60562  
 60563  
 60564  
 60565  
 60566  
 60567  
 60568  
 60569  
 60570  
 60571  
 60572  
 60573  
 60574  
 60575  
 60576  
 60577  
 60578  
 60579  
 60580  
 60581  
 60582  
 60583  
 60584  
 60585  
 60586  
 60587  
 60588  
 60589  
 60590  
 60591  
 60592  
 60593  
 60594  
 60595  
 60596  
 60597  
 60598  
 60599  
 60600  
 60601  
 60602  
 60603  
 60604  
 60605  
 60606  
 60607  
 60608  
 60609  
 60610  
 60611  
 60612  
 60613  
 60614  
 60615  
 60616  
 60617  
 60618  
 60619  
 60620  
 60621  
 60622  
 60623  
 60624  
 60625  
 60626  
 60627  
 60628  
 60629  
 60630  
 60631  
 60632  
 60633  
 60634  
 60635  
 60636  
 60637  
 60638  
 60639  
 60640  
 60641  
 60642  
 60643  
 60644  
 60645  
 60646  
 60647  
 60648  
 60649  
 60650  
 60651  
 60652  
 60653  
 60654  
 60655  
 60656  
 60657  
 60658  
 60659  
 60660  
 60661  
 60662  
 60663  
 60664  
 60665  
 60666  
 60667  
 60668  
 60669  
 60670  
 60671  
 60672  
 60673  
 60674  
 60675  
 60676  
 60677  
 60678  
 60679  
 60680  
 60681  
 60682  
 60683  
 60684  
 60685  
 60686  
 60687  
 60688  
 60689  
 60690  
 60691  
 60692  
 60693  
 60694  
 60695  
 60696  
 60697  
 60698  
 60699  
 60700  
 60701  
 60702  
 60703  
 60704  
 60705  
 60706  
 60707  
 60708  
 60709  
 60710  
 60711  
 60712  
 60713  
 60714  
 60715  
 60716  
 60717  
 60718  
 60719  
 60720  
 60721  
 60722  
 60723  
 60724  
 60725  
 60726  
 60727  
 60728  
 60729  
 60730  
 60731  
 60732  
 60733  
 60734  
 60735  
 60736  
 60737  
 60738  
 60739  
 60740  
 60741  
 60742  
 60743  
 60744  
 60745  
 60746  
 60747  
 60748  
 60749  
 60750  
 60751  
 60752  
 60753  
 60754  
 60755  
 60756  
 60757  
 60758  
 60759  
 60760  
 60761  
 60762  
 60763  
 60764  
 60765  
 60766  
 60767  
 60768  
 60769  
 60770  
 60771  
 60772  
 60773  
 60774  
 60775  
 60776  
 60777  
 60778  
 60779  
 60780  
 60781  
 60782  
 60783  
 60784  
 60785  
 60786  
 60787  
 60788  
 60789  
 60790  
 60791  
 60792  
 60793  
 60794  
 60795  
 60796  
 60797  
 60798  
 60799  
 60800  
 60801  
 60802  
 60803  
 60804  
 60805  
 60806  
 60807  
 60808  
 60809  
 60810  
 60811  
 60812  
 60813  
 60814  
 60815  
 60816  
 60817  
 60818  
 60819  
 60820  
 60821  
 60822  
 60823  
 60824  
 60825  
 60826  
 60827  
 60828  
 60829  
 60830  
 60831  
 60832  
 60833  
 60834  
 60835  
 60836  
 60837  
 60838  
 60839  
 60840  
 60841  
 60842  
 60843  
 60844  
 60845  
 60846  
 60847  
 60848  
 60849  
 60850  
 60851  
 60852  
 60853  
 60854  
 60855  
 60856  
 60857  
 60858  
 60859  
 60860  
 60861  
 60862  
 60863  
 60864  
 60865  
 60866  
 60867  
 60868  
 60869  
 60870  
 60871  
 60872  
 60873  
 60874  
 60875  
 60876  
 60877  
 60878  
 60879  
 60880  
 60881  
 60882  
 60883  
 60884  
 60885  
 60886  
 60887  
 60888  
 60889  
 60890  
 60891  
 60892  
 60893  
 60894  
 60895  
 60896  
 60897  
 60898  
 60899  
 60900  
 60901  
 60902  
 60903  
 60904  
 60905  
 60906  
 60907  
 60908  
 60909  
 60910  
 60911  
 60912  
 60913  
 60914  
 60915  
 60916  
 60917  
 60918  
 60919  
 60920  
 60921  
 60922  
 60923  
 60924  
 60925  
 60926  
 60927  
 60928  
 60929  
 60930  
 60931  
 60932  
 60933  
 60934  
 60935  
 60936  
 60937  
 60938  
 60939  
 60940  
 60941  
 60942  
 60943  
 60944  
 60945  
 60946  
 60947  
 60948  
 60949  
 60950  
 60951  
 60952  
 60953  
 60954  
 60955  
 60956  
 60957  
 60958  
 60959  
 60960  
 60961  
 60962  
 60963  
 60964  
 60965  
 60966  
 60967  
 60968  
 60969  
 60970  
 60971  
 60972  
 60973  
 60974  
 60975  
 60976  
 60977  
 60978  
 60979  
 60980  
 60981  
 60982  
 60983  
 60984  
 60985  
 60986  
 60987  
 60988  
 60989  
 60990  
 60991  
 60992  
 60993  
 60994  
 60995  
 60996  
 60997  
 60998  
 60999  
 61000

ARKWER  
 FID3  
 DATE 27-4-84  
 TIME 8:42  
 SF 300.137  
 SF 300.137  
 DI 4431.386  
 FI 522.69  
 UD 332.69  
 HZ/PI 1.03  
 PM 2.0  
 MD 1.000  
 QD 0.262  
 RG 16  
 TE 207  
 CW 3162.0  
 CG 63L PD  
 LB 0.0  
 CB 0.0  
 LC 0.0  
 FL 25.000  
 F2 981P  
 HZ/CH 71.160  
 PM/CH 1.237  
 SR 337.40

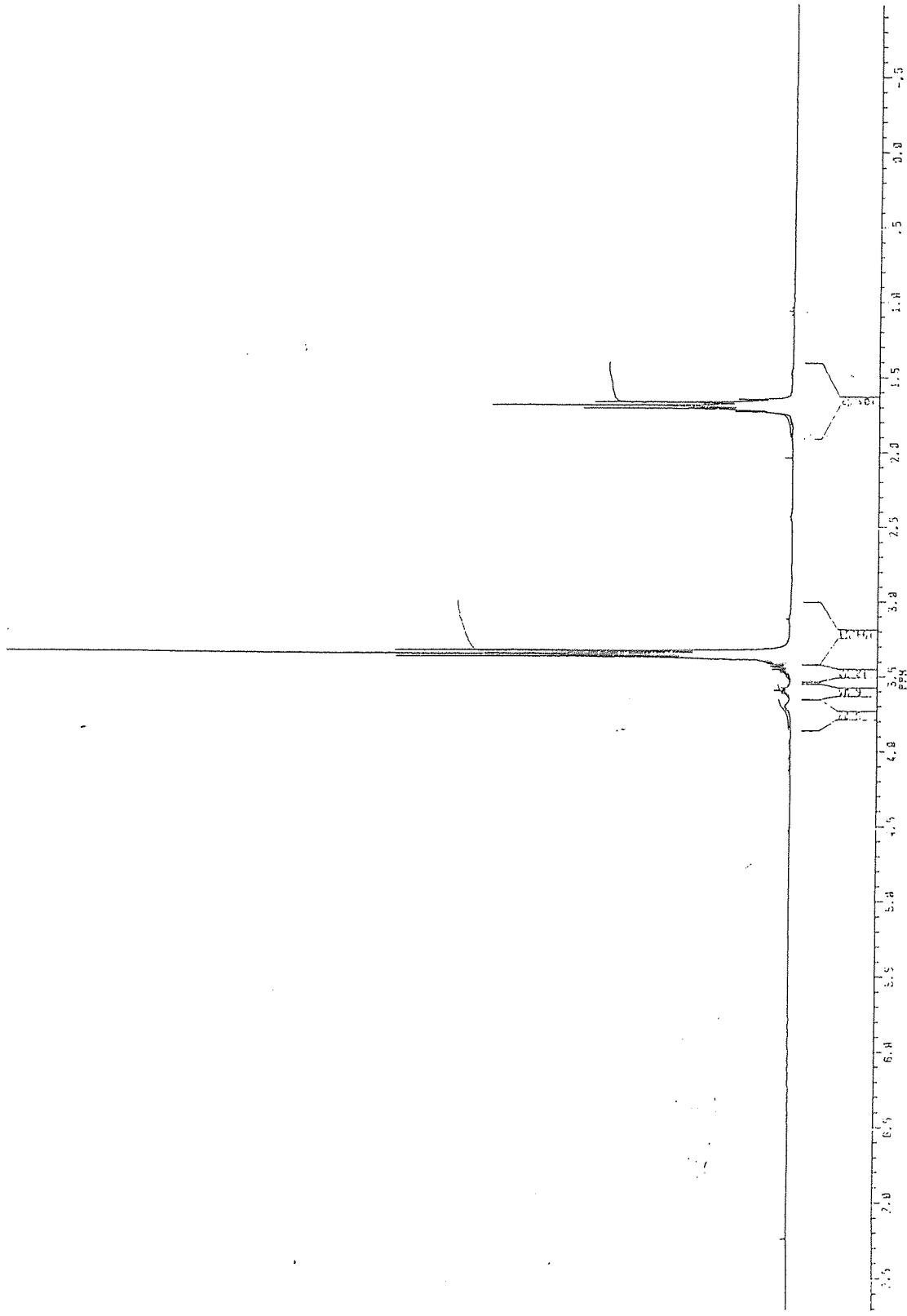


Figure 1.a. 1H NMR spectrum of polyoxetane



7.2236

4.2024

PRUNX

STOR004-9-91  
 DATE 71.1.23  
 TIME 11.13  
 RF 300.135  
 SF 300.135  
 SI 3252.611  
 TO 3255  
 SW 2202.723  
 HE/FI 1.155  
 PY 2.0  
 RO 1.233  
 AO 6.283  
 RG 1  
 NS 13  
 TE 287  
 FY 3400  
 DC 0.2  
 DP 63L 20  
 LB 0.0  
 CX 36.03  
 CY 22.23  
 F1 5.0081P  
 HZ/CX 71.985P  
 PPM/CX 71.337  
 IS 2  
 SR 5375.02

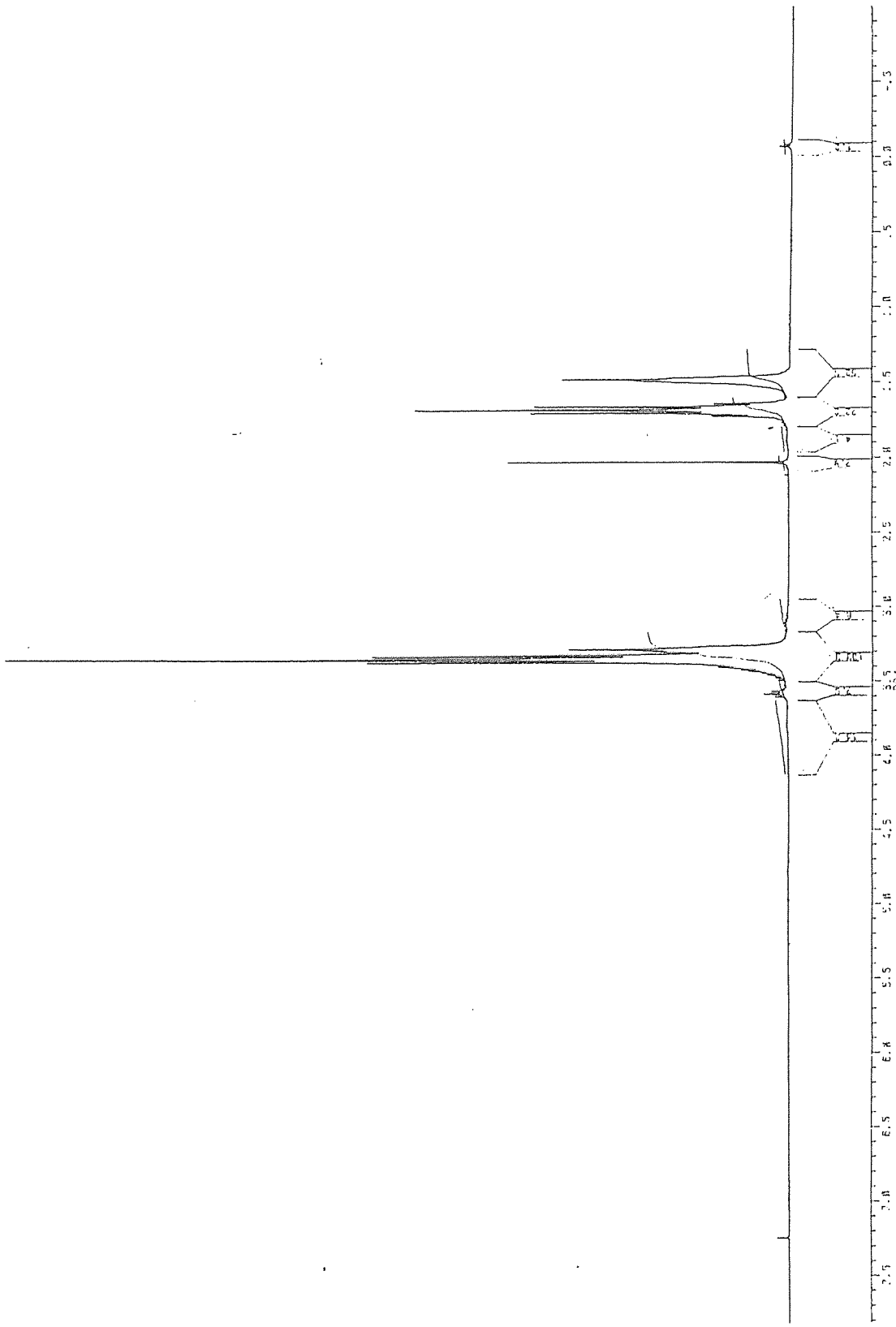


Figure 1.c. 1H NMR spectrum of copolymer OX:THF (feed 1:1)



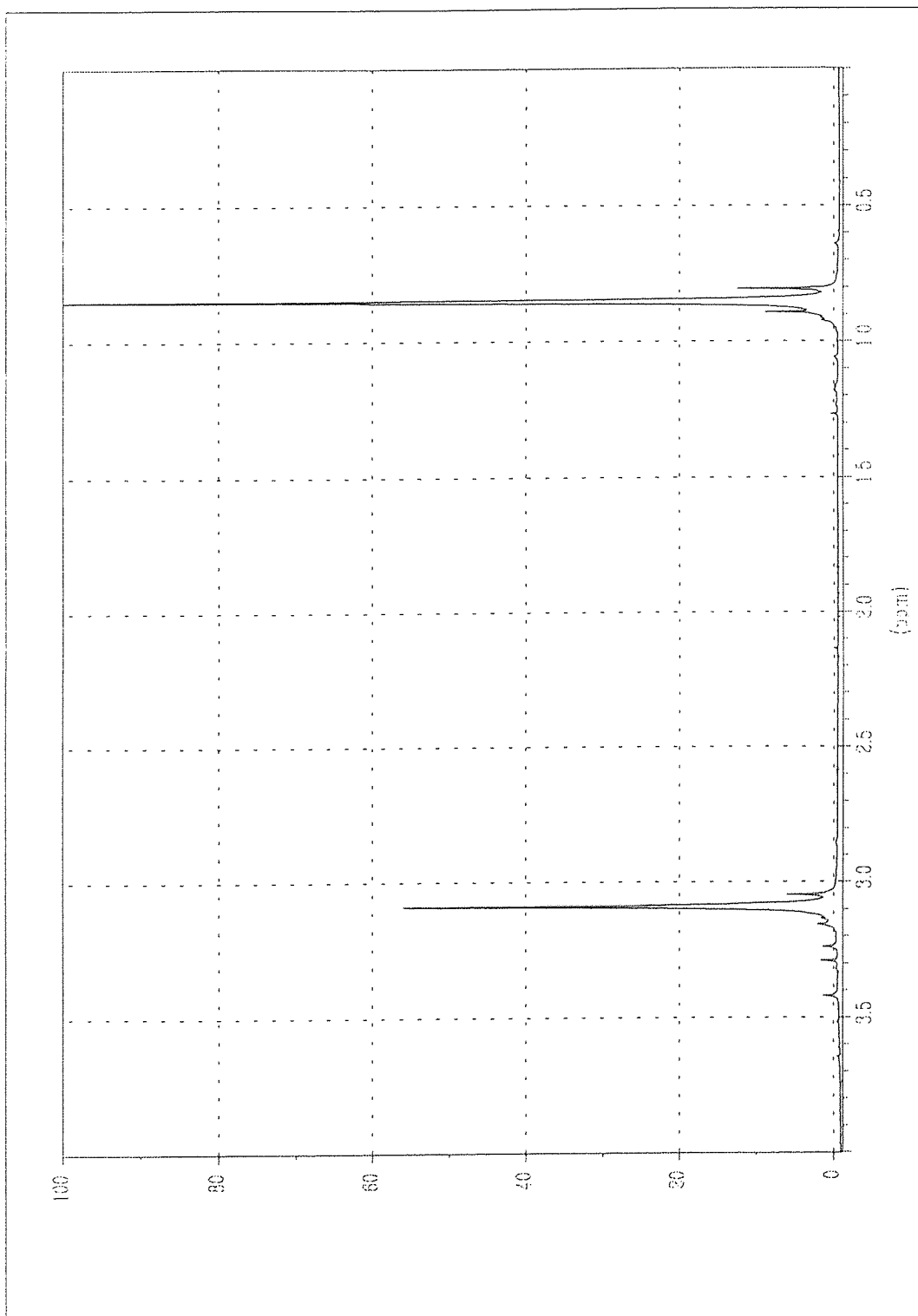


Figure 1.e.  $^1\text{H}$  NMR spectrum of polyDMOX





3.3 OX-OX 1 / F. GOURDRES/CELLS/15C PENDANT/CH3-CH2-CH2-CL/NCP

PCMOX

PCMOX  
AC PROD: CU  
DATE: 10-19-94  
TIME: 07:28

SF 75.450  
GR 36175.458  
SI 35703.463  
LO 32763  
S4 12857.145  
HZ/FI 1.838

PA 0.4  
RG 0.019  
RG 20  
MS 14992  
TE 5R3

FY 72400  
DZ 5183.388  
D0 144.00

LB 2.333  
CB 3.7  
CY 12.38  
F1 215.385P  
F2 -17.292P  
HZ/CH 463.396  
F3/CH 5.226

SR 18604.21  
D1 5.0000000  
P1 10.00  
P2 4.00  
D2 -0.017238  
P3 23.00  
S3 1.004318J  
RD 0.0

PM 0.0  
DE 37.59  
MS 14992  
PS 128.00

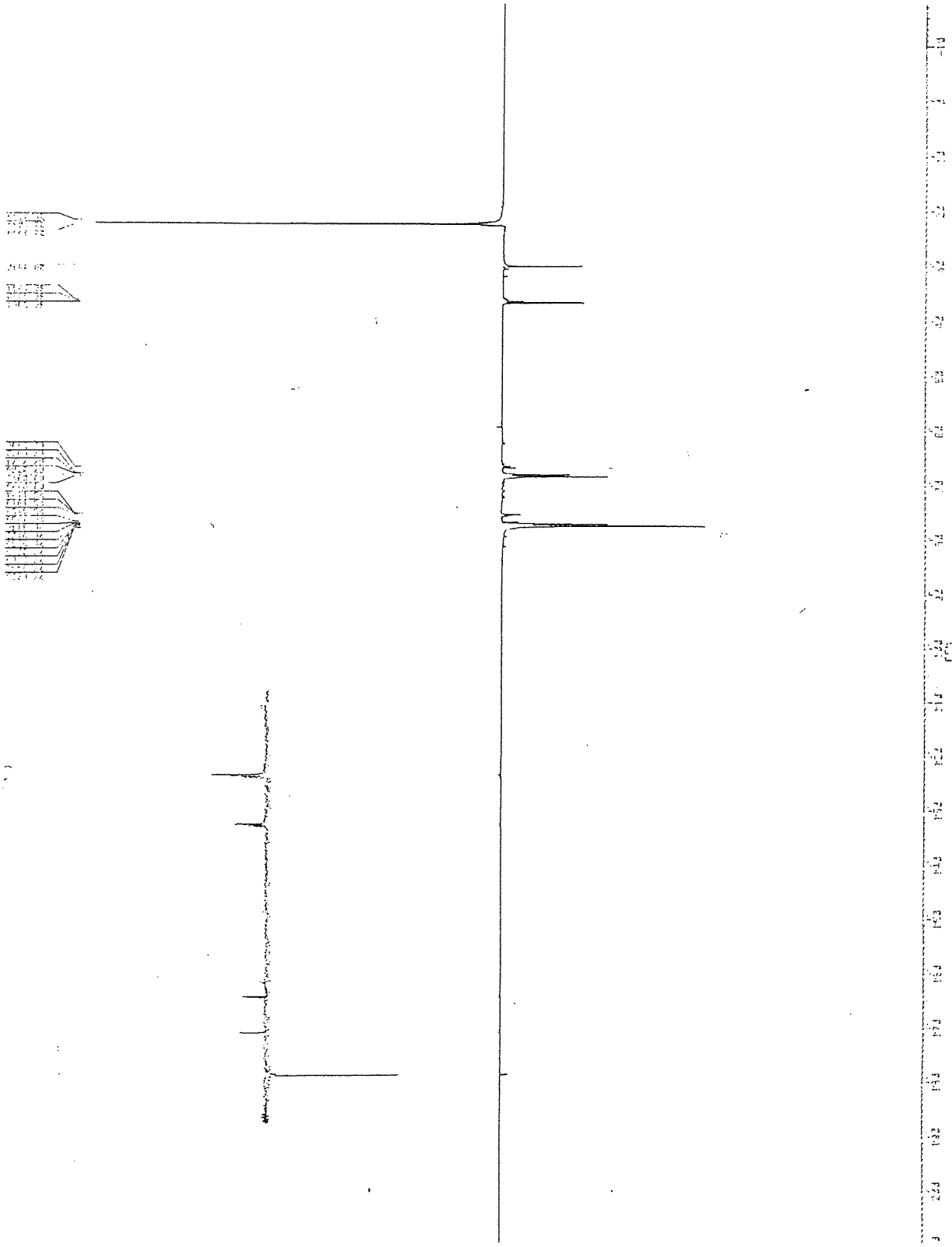


Figure 1.g. <sup>13</sup>C NMR spectrum of the copolymer OX:DMOX (feed ratio 1:1)

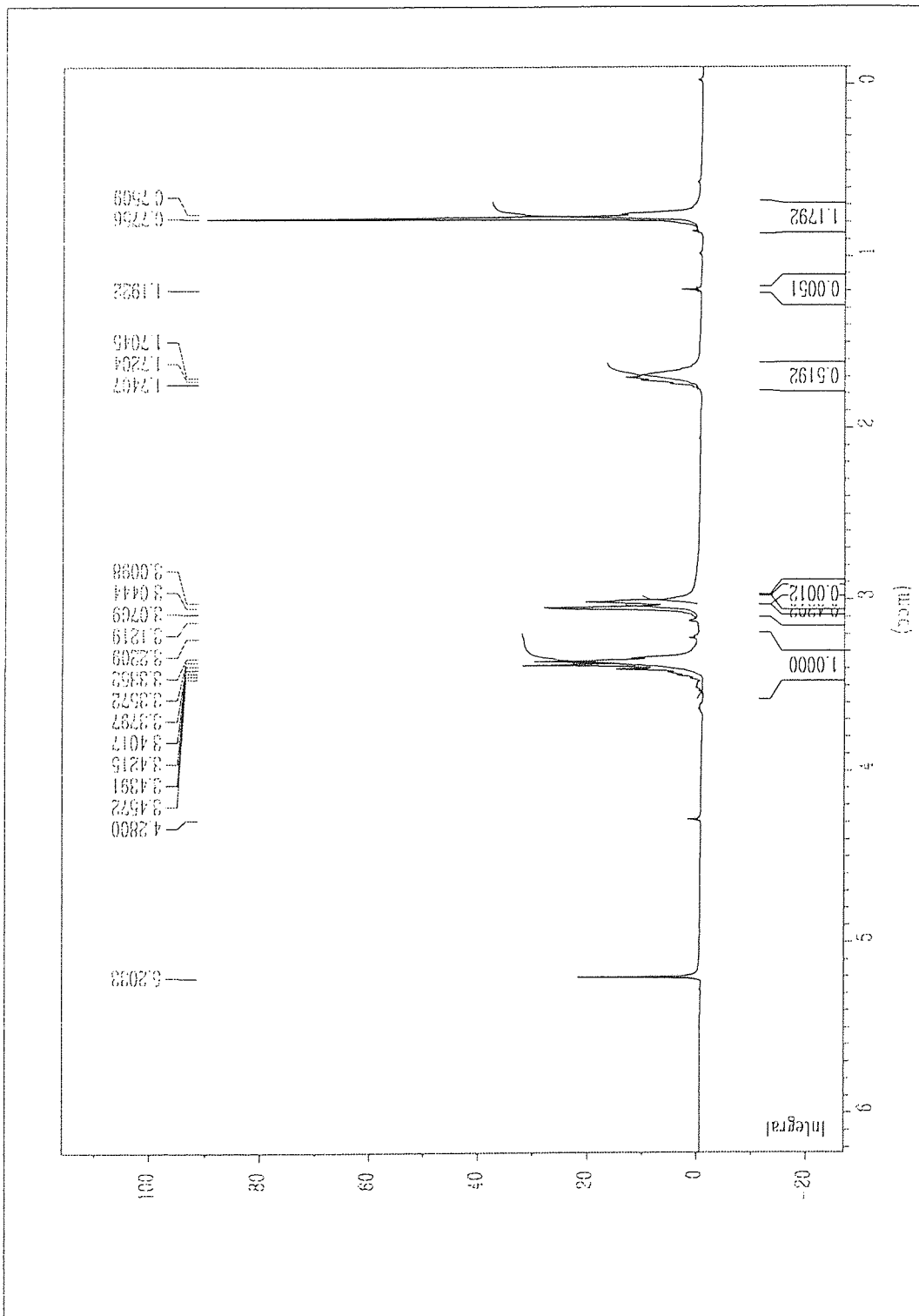


Figure 1.h.  $^1\text{H}$  NMR spectrum of the copolymer OX:DMOX (feed ratio 2:1)

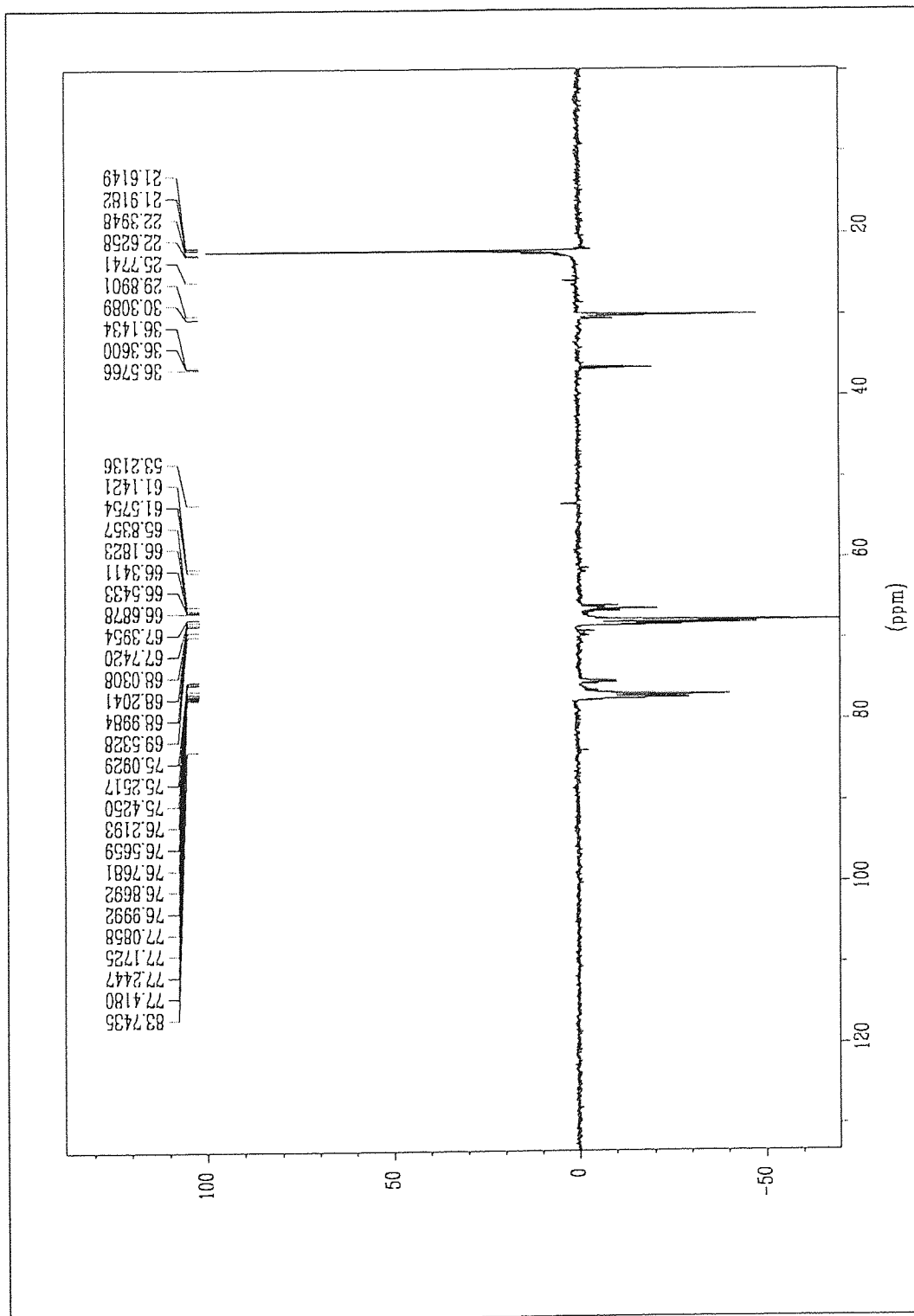


Figure 1.i.  $^{13}\text{C}$  NMR spectrum of the copolymer OX:DMOX (feed ratio 2:1)

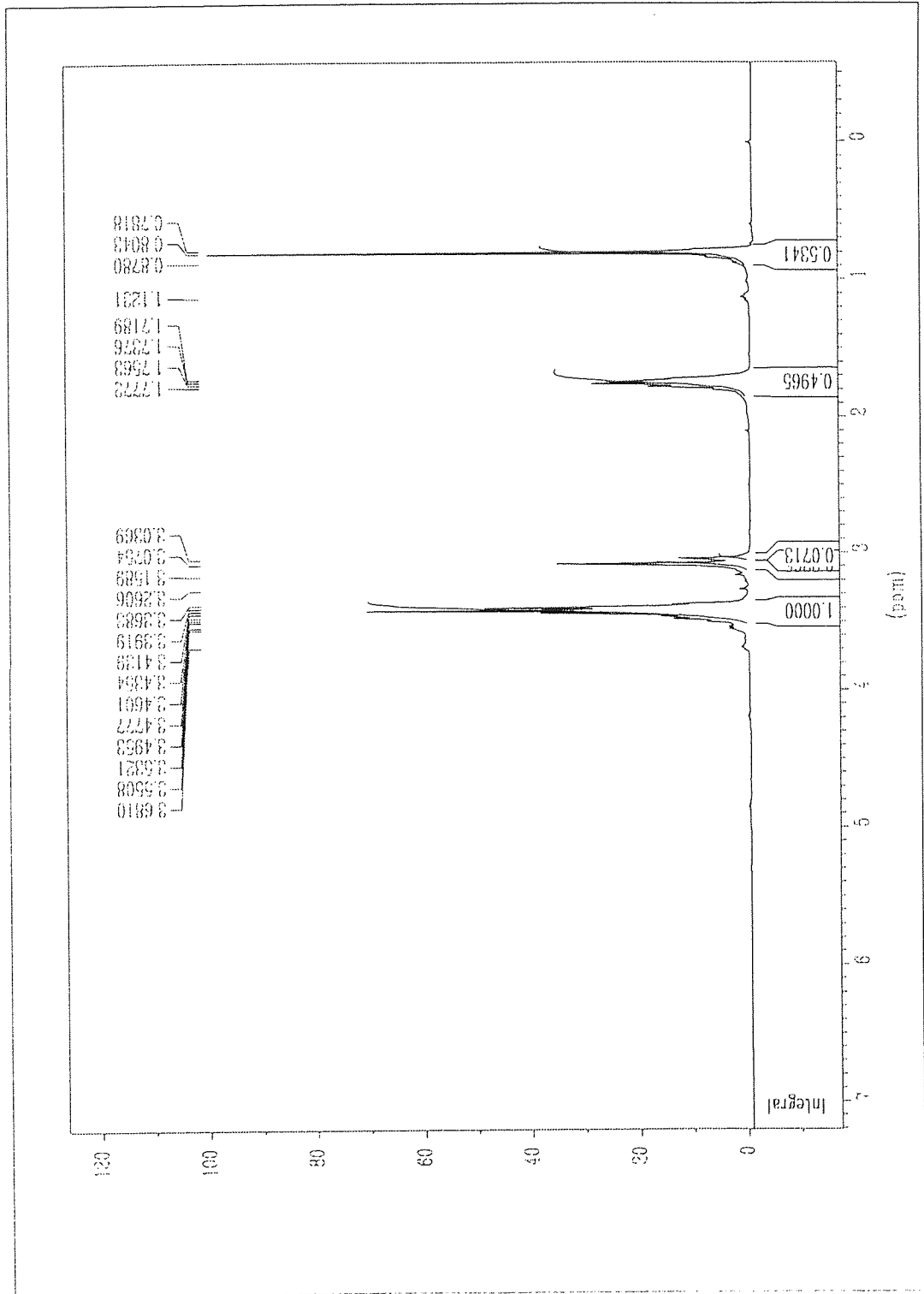


Figure I.j. <sup>1</sup>H NMR spectrum of the copolymer OX:DMOX (feed ratio 3:1)

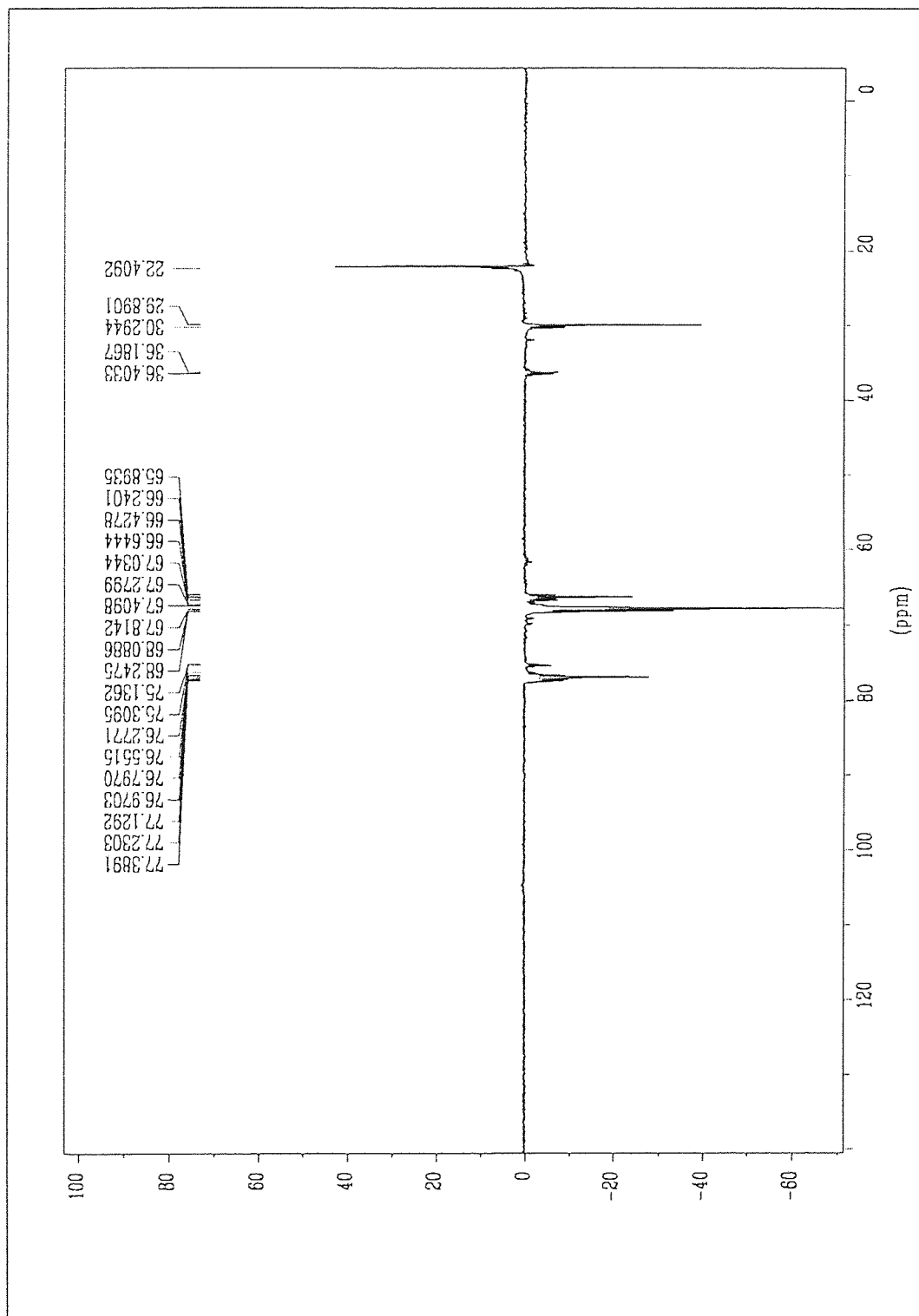


Figure 1.k.  $^{13}\text{C}$  NMR spectrum of the copolymer OX:DMOX (feed ratio 3:1)

## APPENDIX 2

Documents referring to the study described in section 3.2.3.

Figure 2.a COSY 2D NMR spectrum of polyDMOX

FG29 / F:\GUARDERES\CDCL3\COSY\MCP



FG.SMX  
 F1: PROJ:  
 FG29PROJ.001  
 F2: PROJ:  
 FG29PROJ.001  
 AU: PRDG:  
 COSY.AU  
 DATE: 15-2-95

SI2: 1024  
 SI1: 512  
 SW2: 1701.923  
 SW1: 600.962  
 NDB: -1

WDW2: S  
 WDW1: S  
 SSB2: 0  
 SSB1: 0  
 MC2: M  
 PL14: ROV:  
 F1: 4.002P  
 F2: .005P  
 AND COLUMN:  
 F1: 4.002P  
 F2: .005P  
 Q1: 4.000000  
 P1: 9.00  
 Q0: .0000330  
 P2: 9.00  
 R0: 0.0  
 PV: 0.0  
 DE: 522.00  
 NS: 8  
 DS: 4  
 NE: 256  
 IN: .0000320

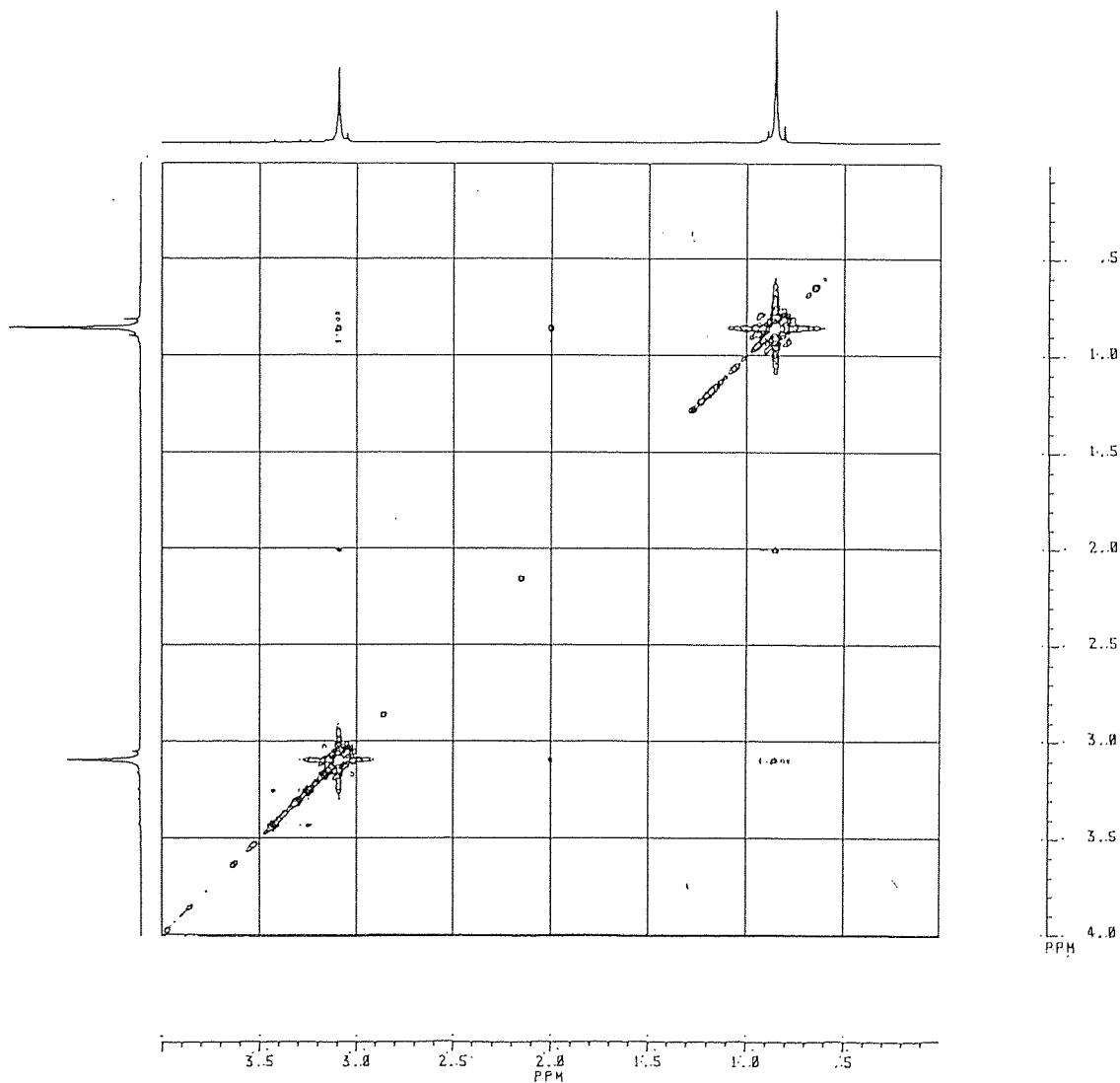
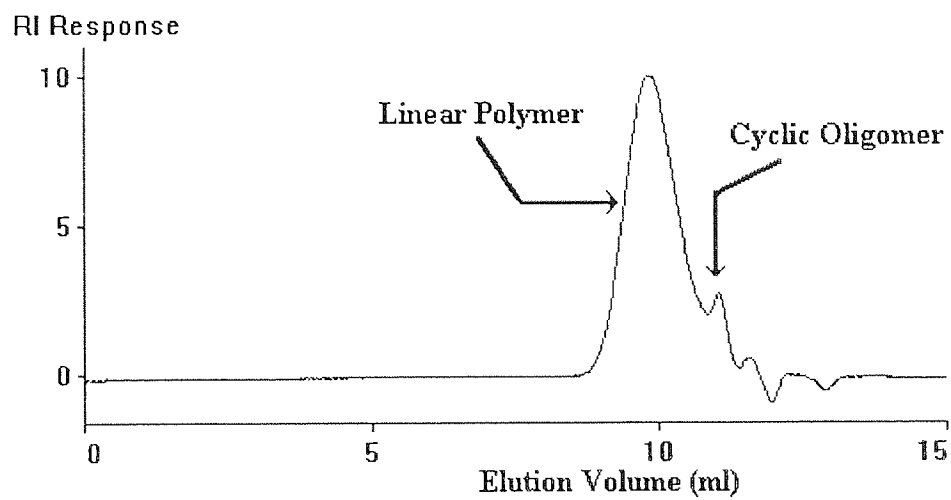




Figure 2.b GPC chromatogram of polyDMOX



### APPENDIX 3

GPC chromatograms of the polymers referring to the studies described in chapter 5

Figure 3.a GPC chromatogram of Polyoxetane with 18-crown-6

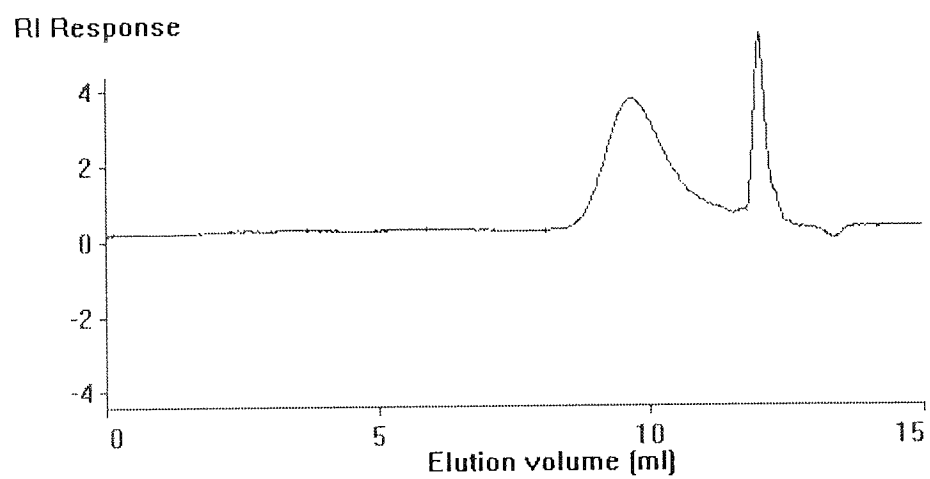


Figure 3.b GPC chromatogram of Polyoxetane with dibenzo-18-crown-6

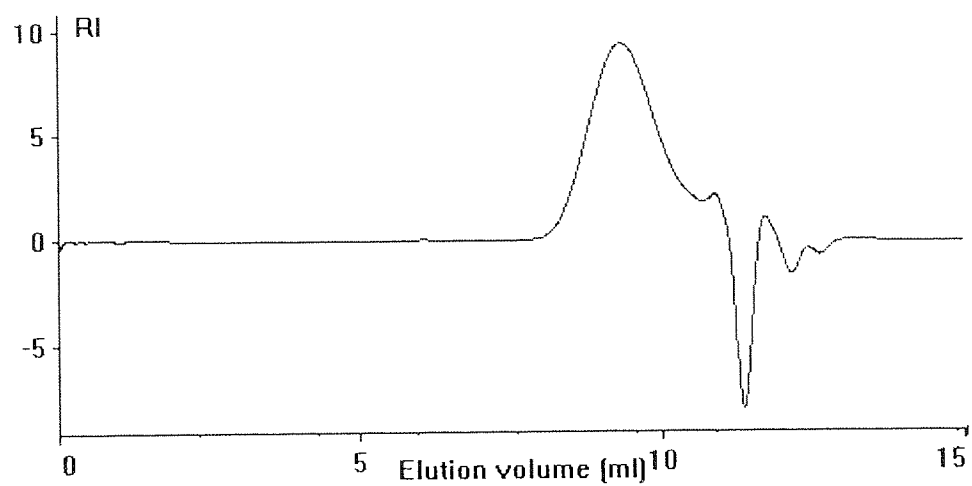


Figure 3.c GPC chromatogram of Polyoxetane with veratrole - MWD control

